Greece – China – Japan International Workshop

on

Recent Advances for Analyzing and Strengthening Resilience of Urban Areas Against Earthquake Disasters

June 28, 2019

Institute on Engineering Seismology and Earthquake Engineering (ITSAK-EPPO)

Thessaloniki, Greece

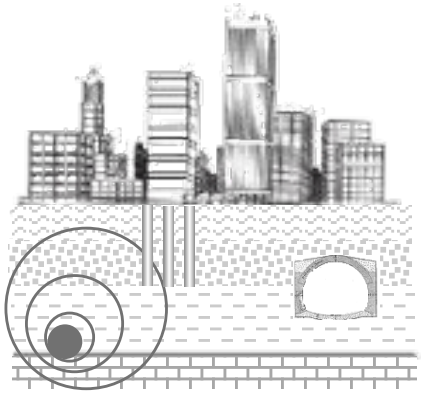

Under the auspices of
Earthquake Planning and Protection Organization (EPPO)

Ο.Α.Σ.Π.

Institute of Engineering Seismology and Earthquake Engineering (ITSAK-EPPO)
Dasylliou str, Eleones, 55535 Pylaia, Thessaloniki
Tel: +30 2310 476081-4 Fax: +30 2310 476085
E-mail: secretariat@itsak.gr Web: www.itsak.gr

Dear colleagues, participants of our joint Workshop in Thessaloniki,

We are very glad to host the international Workshop on "*Recent Advances for Analyzing and Strengthening the Resilience of Urban Areas against Earthquake Disasters*" in the ITSAK-EPPO premises in Thessaloniki. Such a Workshop, including scientists from China, Japan and Greece, countries exposed to high seismicity and devastating earthquakes could be a promising starting point towards seismic risk mitigation. The specific 'know-how' of each research team could contribute to an improved knowledge and understanding of the complex phenomenon of earthquakes and their impact on human and built environment. The in-depth discussion among participants during the Workshop, and the future follow up of a fruitful collaboration among our Research Centers, would undoubtedly bring us closer to potential solutions on how to protect our constructions against earthquake disaster and build future resilient cities in earthquake-prone regions.

Greece is the highest seismicity country in Europe. The first seismic code in Greece was put in force in 1959 and updated versions followed in 1984 and 2000. It was in 1978 for the first time that a modern Greek city, Thessaloniki, was hit by a strong earthquake, M6.5, which occurred in its vicinity. About twenty years later, in 1999, a moderate magnitude event, M5.9, severely hit Athens, the capital of Greece. Both earthquakes caused extended damage and socio-economic disorganization that took long time to recover. In addition, during the last twenty years, new infrastructure and critical lifelines were built around and within urban areas in Greece that have not been yet exposed to strong ground shaking. Although lessons learned from past earthquakes are necessary and precious for understanding the disaster-causing mechanism, it is well understood that we are far from achieving a reasonable understanding and effective preparation against future devastating events. It is mandatory to increase the seismic resilience of our cities, especially those lying nearby active seismic sources.

Finally, special thanks are due to all of our colleagues from China and Japan who kindly accepted to participate in this international Workshop and offer generously their scientific knowledge and experience to our country. We hope that this Workshop will play an important role on setting up a long-term research collaboration and exchanging of new ideas among the participants towards strengthening the seismic resilience of urban areas.

Sincerely yours,
On behalf of the research staff of ITSAK-EPPO

Nikos Theodoulidis
Research Director, Seismology PhD

中国地震局工程力学研究所
Institute of Engineering Mechanics, CEA

Dear respected participants,

I am very happy to join the international workshop on "*Recent Advances for Analysing and Strengthening the Resilience of Urban Areas against Earthquake Disasters*". It's great that researchers and professors from the institutes of different countries could meet face-to-face, conduct in-depth discussions and seek potential solutions on how to build future resilient cities in the earthquake-prone regions.

Nowadays cities tend to be more vulnerable due to their high and unplanned concentration of people, aging and overloaded buildings and infrastructures, and poor quality of materials. These cities may face very high disaster risk, and might not bear the consequences if a devastating earthquake occurred at the vicinity of the city. Although lessons learned from the previous earthquakes are necessary and very precious for the study of the disaster-causing mechanism, it is far from enough to achieve a reasonable understanding and preparation against future devastating earthquakes. For instance, the urban area of many Chinese cities has increased significantly in the past thirty years, and some of the eastern large cities have extended the downtown area by even over ten times. Located in the earthquake-prone area, I think, cities in Greece may have the special challenges and concerns, too. I hope the workshop will play an important role on initiating a long-term research collaboration and exchange of the new ideas between the participants.

Finally, special thanks to professors and staffs in ITSAK (the organizer of the workshop) and Dr. Konstantinos Skalomenos, who have been working hard to make the special international workshop possible.

Sincerely yours,
Xuchuan Lin, Ph.D.
Professor
Institute of Engineering Mechanics, China Earthquake Administration

About Institute of Engineering Mechanics (IEM)

Institute of Engineering Mechanics (IEM), China Earthquake Administration, formerly the Institute of Civil Engineering and Architecture, Chinese Academy of Sciences, was established in 1954. IEM is one of the national non-profit research institutes. Its main research fields are earthquake engineering and safety engineering. Currently, it has eight research directions, Strong Motion Seismology, Engineering Seismology, Structural Engineering, Geotechnical Engineering, Disaster Prevention for Urban and Engineering, Engineering Vibration Instrument, Infrastructure Earthquake Resistance Engineering, Information Technology and Engineering Material.

Disaster Prevention Research Institute (DPRI), Kyoto University
Section of Earthquake Resistant Structures
Division on Earthquake Hazards
Gokasho Uji, Kyoto 611-0011, Japan

Dear respected participants,

I would like to express my personal welcome to the International Workshop on "*Recent Advances for Analysing and Strengthening the Resilience of Urban Areas against Earthquake Disasters*" held at the Earthquake Planning and Protection Organization - Institute of Engineering Seismology and Earthquake Engineering (EPPO-ITSAK), Thessaloniki, Greece, on June 28th 2019. I am very excited to share new ideas during the Workshop and I look forward to an in-depth discussion.

I would like to thank all the invited speakers and participants for their active participation, all the members of the Organizing Committee and the administrative staff for their valuable help in all organizational aspects of the Workshop as well as our sponsor, the Earthquake Planning and Protection Organization (EPPO), for its generous financial support. All the above, contributed significantly to the success of the Workshop.

SPIRIT OF ADAPTATION

Success in global work depends on whether we work with a strong focus on adaptation, meaning an appreciation of one's counterpart's technology, development needs and culture. As far as our long-term sustainability is concerned, we must combine what exceptional each country offers (materials, elements, technology, education, facilities, experience and human resources) with the aim of designing and developing new and innovative advances in structural engineering.

In Japan, the number of new constructions is growing year by year as an effort of the country to reduce seismic losses. In Europe, and particularly in Greece, many old r/c and traditional brick structures exist in critical areas, which increases significantly the seismic risk. During the last years, both countries have dedicated efforts to improve the seismic performance of their construction traditions either by introducing new structural systems and technology (base-isolation, dampers, self-centering structures, structural health monitoring, early warning systems etc.) or by developing and implementing advanced technologies and novel materials to strengthen the existing structures (steel braces, high-performance concretes, fibre cements and mortars, composites etc.).

Greece is one of the most earthquake prone country in Europe, while Japan in Asia. We all, therefore, share the same passion and commitment to protect the human life as well as the integrity of our build environment and infrastructure against earthquake disasters. This workshop serves as a valuable opportunity to further our human network with experts in the field and identify the challenges in applying current technological advances and trends in critical engineering concepts in both regions.

Sincerely yours,

Konstantinos Skalomenos, Ph.D.
Specially Apptd. Assistant Professor
and Program Co-Coordinator

Greece – China – Japan International Workshop

Recent Advances for Analyzing and Strengthening Resilience of Urban Areas Against Earthquake Disasters

Friday, June 28th 2019	
9:00 – 9:30	Registration
9:30 – 10:00	Welcome messages Introduction to research activities of ITSAK (Dr. Ch. Papaioannou), IEM (Prof. X. Lin) and DPRI (Ass. Prof. K. Skalomenos) (5min each)
Session 1: Coordinated by Dr. K. Makra	
10:00 – 10:15	Professor Xuchuan LIN **Development of a simulation platform to model, assess and visualize the earthquake disasters in city level**
10:15 – 10:30	Research Director Nikos Theodoulidis **Contribution of accelerometric network in ShakeMaps and rapid earthquake damage assessment in Greece**
10:30 – 10:45	Research Director Vassilios Lekidis **Evaluation of economic loss for structures in the area struck by the 7/9/1999 Athens earthquake and comparison with actual repair costs**
10:45 – 11:00	Assistant Researcher Manos Rovithis **Airborne LIDAR and accelerometric data processing towards seismic risk assessment: An urban-scale approach including soil-structure interaction effects.**
11:00 – 11:30	Short Questions & Answers
11:30 – 12:00	*Coffee Break*
Session 2: Coordinated by Dr. B. Margaris	
12:00 – 12:15	Assistant Researcher Morfidis Konstantinos **Real time estimation of R/C buildings' seismic damage using Artificial Neural Networks and Pattern Recognition approach.**
12:15 – 12:30	Research Director Christos Karakostas **Seismobug© - A low-cost accelerograph for an enhanced seismic resilience of urban areas**
12:30 – 12:45	Assistant Professor Baijie ZHU. **Different levels seismic capacity identification method of reinforced concrete frame buildings**
12:45 – 13:00	Professor Zhe QU **A building-specific bi-directional dynamic loading protocol for experiments of non-structural components.**
13:00 – 13:30	Short Questions & Answers
13.30 – 14.30	*Light Lunch*

Session 3: Coordinated by Dr. K. Morfidis	
14:30 – 14:45	Senior Researcher Thomas Salonikios **Influence of the "Structural Flexibility" of Monuments at the Damage Distribution during Strong Earthquakes**
14:45 – 15:00	Professor Lingxin ZHANG **Mechanical behavior of assembled steel dampers with optimized shapes**
15:00 – 15:15	Assistant Professor Konstantinos Skalomenos **A multiphase yielding steel brace with tailored material properties**
15:15 – 15:30	Short Questions & Answers
15:30 – 16:30	Round table Discussion and Conclusions
16:30 – 17:00	Closing Remarks

Who is who

Christos Z. Karakostas
Research Director ITSAK-EPPO

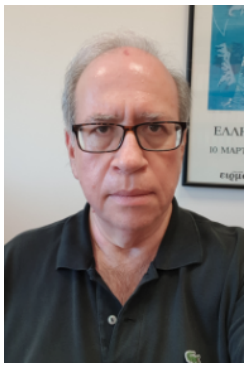

Doctorate in the field of Numerical Analysis of Structures using the Finite Element Method (Civil Engineering Dpt., Aristotle University of Thessaloniki, 1989). Consultant Engineer (1984-1995), specialized in the design of special Civil Engineering Structures. Researcher at EPPO-ITSAK since 1995. Research interests include: Assessment of seismic risk of urban areas and seismic evaluation of existing buildings; Instrumentation of structures and evaluation of their dynamic response; Experimental and analytical investigation of the dynamic behavior of structures, structural components, materials and non-structural components subjected to earthquake actions; New methods for seismic design and estimation of the seismic capacity of existing buildings; Development of Finite Elements for the dynamic analysis of shell structures; Development of Stochastic Boundary Elements for the estimation of the propagation of seismic waves in soils with random properties. Consultant in special seismic hazard/vulnerability studies performed at EPPO-ITSAK for important Civil Engineering structures (hospital buildings and dams) in Greece. Author/co-author of more than 130 papers published in International Scientific Journals or presented at International Conferences (more than 220 third-party citations). Scientific coordinator or participant in 34 Research Programmes funded by EPPO, the Greek Directory General for Research and Technology (GGET), and the European Union (coordinator in 5). Expert evaluator for research proposals for the European Union and GGET. Certified (2012) EU Civil Protection Technical Expert. An abridged Curriculum Vitae can be found at: http://www.itsak.gr/en/people/people/cv/9

Xuchuan Lin
Professor IEM

Dr. Xuchuan Lin is a Professor in Institute of Engineering Mechanics (IEM), China Earthquake Administration. He received M.E. and M.E. in civil engineering from Tsinghua University in 2007 and 2009, respectively. He received his Ph.D. from Kyoto University, Japan in 2012. After worked as postdoctoral fellow at Disaster Prevention Research Institute of Kyoto University and Earthquake Research Institute of the University of Tokyo. His research interests span urban earthquake disaster simulation and risk evaluation, untraditional seismic steel structure using high-strength steel and damage-control fuses, and collapse simulation of buildings subjected to very strong earthquakes. He developed a C++ code named YouSimulator, which provides automatic modeling, rapid parallel computing and 3D data visualization for city-scale physics-based earthquake disaster simulation.

Vassilios Lekidis
Research Director ITSAK-EPPO

Ph.D. in earthquake resistant structures (Finite Element Analysis) in 1994; Member of the board of Directors of ITSAK; Vice president of the general assembly of Technical Chamber of Greece; Member of Permanent Coordinating Committee for Earthquake Risk Reduction in the Balkan Region; Member of permanent Committee of New Greek Seismic Code (1987- 1996); Acting Director of ITSAK: 1986-1987, 1989-1991, 1999-2007. Member of Board of Directors of EGNATIA SA (construction of EGNATIA high-way road in Northern Greece). He is the author/co-author of more than 180 scientific publications in international journals and conference proceedings and more than 70 technical reports, 8 training books. Main Research projects:
(1) Lekidis, Talaslidis "Seismic behavior and vulnerability of buried lifelines.' Finite element methodology for static and dynamic analysis of pipelines." EPOCH -- TASK3. DECEMBER 1993 Lab. Of Dynamics and Applied Mechanics A.U.TH., 150,000€
(2) Theodulidis, Lekidis, Manos, "Euroseistest Volvi – Thessaloniki: A European Test Site for Engineering Seismology Earthquake Engineering and Seismology. ENVIRONMENT 1993-1995
(3) Lekidis, Papoulia, Koliopoulos, Sous "High Performance Fracture Approach to Fatigue Crack Analysis & Life Prediction (HiPER-CRACK)" Sener Ingenieria y Sistemas SA (Spain), Centro Ricerche FIAT (Italy), Universidad Pontificia Comillas (Spain), MSC Software GmbH (Germany), Samtech SA (Belgium), NCODE International Ltd. (UK) και VOLVO Aero Corporation (Sweden), April 2000, March 2003, 100,000€, Contract EC G5RD-CT-2000
(4) Lekidis, Antoine Armelle "Advanced Numerical Methods for Structures Submitted to Earthquakes, Including Cultural Heritage Structures" Improving Human Research Potential and the Socio-economic Knowledge Base, E.C. Marie-Curie programs, 45,000€.

Lingxin Zhang
Professor IEM

She is a Professor and Division Director in Institute of Engineering Mechanics (IEM), China Earthquake Administration. She received Ph.D. in earthquake engineering from IEM in 1996. Her research interests including a few topics, such as nonlinear dynamic response analysis of structures, seismic vulnerability and reliability analysis of structures, seismic behavior of structures, seismic capacity assessment of buildings, and earthquake secondary disaster simulation. She was awarded with the second prize of National Science Progress Award and the first prize of Scientific Progress at the Provincial and Ministerial Level (three times).

Konstantia A. Makra
Senior Researcher ITSAK-EPPO

Dr. Konstantia Makra is Senior Researcher in the Institute of Engineering Seismology and Earthquake Engineering (ITSAK) in Thessaloniki, Greece, since June 2002. She graduated in 1996 from the Department of Civil Engineering of the Aristotle University of Thessaloniki. She received her Ph.D. in 2000 from the same University. Her research lies in the field of Geotechnical Earthquake Engineering with specialization in soil dynamics, strong motion site characterization and soil categorization, empirical and theoretical studies on strong ground motion, site effects, seismic behavior and design of geotechnical structures and numerical and analytical methods in geotechncial earthquake engineering. She is the author or co-author of more than 80 scientific publications including 26 peer-reviewed journal papers and book chapters and more than 55 conference papers in National and International Conferences proceedings. She has participated in more than 30 National- and EU-funded research projects as a member of the research team and as principal investigator and scientific responsible. She has received more than 550 true citations in Referred Journals, Conferences and Dissertations.

Basil Margaris
Research Director ITSAK-EPPO

PRINCIPAL CONTRIBUTIONS TO ENGINEERING SEISMOLOGY

- Planning –Organization-Operation strong motion network
- Data processing of strong motion accelerograms
- Study of strong motion attenuation, duration and energy characteristics.
- Probabilistic – Deterministic Seismic Hazard Assessment.
- Strong Motion modeling-simulation.
- Strong Motion Aftershock activities in strong earthquakes in Greece.
- Microzation and Site Effects studies.

RESEARCH PROJECTS, PUBLICATIONS & SCIENTIFIC REPORTS:

- Scientist in charge in 10 research projects in engineering seismology & earthquake engineering (SRM-LIFE, EDE_2000, Thessaloniki Ring-Road, BackSea SciNetNatHaz, among others;) and participation in more than 55 research projects.
- More than 210 publications (47 peer-reviewed Inter. Journals, 18 peer-reviewed National Journals, 53 Proc. Inter. Conferences, 93 Other Publications).
- More than 25 technical reports in engineering seismology & earthquake engineering for seismic protection of Public Works and Lifelines (Person in charge in more than 10).

Konstantinos E. Morfidis
Assistant Researcher ITSAK-EPPO

Dr. Konstantinos Morfidis is Assistant Researcher in Institute of Engineering Seismology and Earthquake Engineering (ITSAK) in Thessaloniki, Greece, since October 2010. He graduated in 1994 from the Department of Civil Engineering of the Aristotle University of Thessaloniki. He received his Ph.D. in 2003 from the same University. He received his MSc in Information Systems from Hellenic Open University in 2015. He worked as designer and consultant in public and private civil engineering projects (1995-2010), and as consultant and programmer in Technical Software House (2003-2010). He is co-author in 7 scientific books and in more than 70 technical papers in peer-reviewed journals and conferences. His research experience includes 18 research projects funded by national and international organizations. His research interests are in the areas of statics and dynamics of structures, earthquake engineering, software development in the field of finite element method, modeling of engineering problems using artificial intelligence, and in the improvement of seismic codes in the field of the modeling and analysis of structures.

Thomas Salonikios
Senior Researcher ITSAK-EPPO

Earthquake Engineering with emphasis on:
<u>Experimental part</u>

- Experimental and/or analytical research on the response of Reinforced Concrete structural elements under seismic loading
- Experimental and/or analytical research of the response of repaired and/or strengthened R/C structural elements, by the use of steel, glass or carbon reinforced polymers.
- Experimental research of the response of jacketed or reinforced masonry walls.
- In situ instrumentation and measurement of the response of important structures (buildings, bridges) for the evaluation of their dynamic response.
- Evaluation, check and in-situ measurements of monumental and other cultural heritage buildings for the recognition of structural response and for structural upgrade.

<u>Analytical part</u>

- Analytical model composition of monumental brick or stone masonry buildings for the elastic or inelastic analysis under permanent and/or seismic loads.
- Modern inelastic methods for the seismic evaluation and the seismic design of important structures by the use of performance-based design, pushover and nonlinear dynamic techniques.

Author of publications to scientific Journals and Conferences after review. Reviewer for many international journals. Scientific coordinator to national and international research projects.

Baijie Zhu
Assistant Professor IEM

He is an Assistant Professor from 2018 in Institute of Engineering Mechanics (IEM), CEA. He received Ph.D. in Structural Engineering from IEM in 2018. His research fields include structural energy absorption technology, nonlinear dynamic response analysis of structures, and assessment of structural seismic capacity. During the doctoral period, he published more than ten papers. Currently he is working for two research projects: (1) energy dissipation coupling beam with two-stage yield mechanism and its energy absorbing effect on the core tube; (2) study on seismic resilience evaluation method of frame-shear wall structure based on total probability theorem.

Emmanouil Rovithis
Researcher ITSAK-EPPO

Dr. Emmanouil Rovithis is currently employed as a Researcher in the Institute of Engineering Seismology and Earthquake Engineering (ITSAK), Research Unit of Earthquake Planning and Protection Organization, in Thessaloniki, Greece. His main research fields of expertise include wave propagation in soil media, earthquake engineering, soil-structure interaction, seismic design and response of foundations, experimental and numerical modeling of structures and geotechnical systems and monitoring of structures and soil-structure interaction systems. He is the author or co-author of more than 60 scientific publications including 18 peer-reviewed journal papers, 3 book chapters and conference papers in National and International Conferences proceedings. He was nominated participant of Greece for the 21th EYGEC European Young Geotechnical Engineers Conference, Rotterdam, The Netherlands (2011). He has been appointed as a member of the organizing and/or scientific committees as well as special sessions chair of various International Conferences (4ICEGE 2007, EURODYN 2011, GEOMAPPLICA 2014, COMPDYN 2017, 16ECEE 2018, COMPDYN 2019). He has delivered more than 20 presentations in conferences and seminars. He is Reviewer of 18 international scientific journals including a Review Editor role in Frontiers in Earthquake Engineering. He has participated in 13 National- and EU-funded research projects as a member of the research team and has coordinated 3 as principal investigator and scientific responsible. In 2011 he was a visiting researcher at Institut Français des Sciences et Technologie des Transports, de l'Amménagement et des Réseaux, France (IFSTTAR) in the framework of DRESBUS II Transnational Access project of SERIES research program and recently at the Schofield Geotechnical Center of the University of Cambridge in the framework of the on-going COSMO Transnational Access project of SERA research program. He has received more than 270 true citations in Referred Journals, Conferences, Dissertations and Reports.

Zhe Qu
Professor IEM

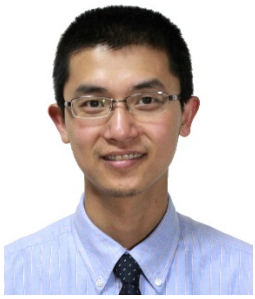

Zhe Qu is a Professor in Institute of Engineering Mechanics (IEM), China Earthquake Administration. He received his Ph.D. in Civil Engineering from Tsinghua University in 2010, where he also earned M.E. and B.E. degrees in Civil Engineering. After being a postdoctoral fellow in the Center for Urban Earthquake Engineering, Tokyo Institute of Technology, he joined the Institute of Engineering Mechanics in 2013 and was promoted to professor in 2017 in the same institute. He has experience of being visiting scholars in University of Edinburgh and UCLA. His research interest is in the reduction of functional loss of buildings under earthquakes and speeding their post-event recovery by controlling the seismic damage to both structural and non-structural components. His academic awards in recent years include the Outstanding Young Engineers' Contribution Award by IABSE in 2015, the 2nd-class National Award for Science and Technology Progress in China in 2016 and the AIJ Book Award by Architectural Institute of Japan in 2018.

Christos Papaioannou
Research Director ITSAK-EPPO

PRINCIPAL CONTRIBUTIONS TO SEISMOLOGICAL FIELDS: Seismic hazard assessment, attenuation of seismic intensities & peak ground parameters, application of macroseismic data for the calibration of earthquakes, stress pattern in the Aegean area, after-shocks, seismicity, tsunami & seismotectonic studies, long term earthquake prediction, statistical models in seismic hazard analysis, site effect studies in terms of strong, weak- motion and noise data.
Participation in aftershock studies of disastrous earthquakes in Greece, Cyprus and Turkey involving in data collection, installation and maintenance of temporally networks. Member of SSA (1979), EERI (1986-2014), AGU (1986), Hellenic Geophysical Union (1988). Member of the "ADRIA project" (GSHAP) and the SESAME project-working group for the Seismic Hazard Assessment of the Mediterranean region. Member of the Working Group for the compilation of the updated version of the official Seismic Hazard Map of Greece. Elected coordinator of the ''WG on SEISMIC HAZARD'' of the ESCommission (2000-2006). Elected member of the executive council of the European Mediterranean Seismological Center (1994-2004). Participation In more than 100 national and international congresses and conferences, In 8 of them as co-organizer of session.
Participation in 60 research projects and in 10 others as Responsible Scientist mainly for the seismic hazard assessment issues. 100 Publications in referee journals, proceedings of national and international congresses. Three atlases of macroseismic maps, one book. Participation (coordinator or principle researcher) in the compilation of scientific reports on earthquakes and their effects on

build environment.

Konstantinos A. Skalomenos
Assistant Professor DPRI

Dr. Konstantinos Skalomenos is working in the Disaster Prevention Research Institute at Kyoto University as Specially Apptd. Assistant Professor. He graduated in 2007 from the Department of Civil Engineering of the University of Patras, Greece. He received his M.Sc. in 2009 and Ph.D. in 2014 from the same University and he conducted two-year post-doctoral research at Kyoto University awarded by the Japan Society for the Promotion of Science (JSPS). Dr. Skalomenos will join this year the Dept. of Civil Engineering of the University of Birmingham, UK, as Assistant Professor. His professional experience includes roles as Design and Structural Research Engineer in seismic assessment and retrofit of old existing structures in 2013-2015 and as Construction Quality/Supervisor Engineer of the Hellenic Telecommunications Organization in 2008-2011. His research lies in the field of structural and earthquake engineering with specialization in steel and composite steel/concrete structures. His current research interests include analytical/numerical methods and model development for seismic analysis and experimentation of structures until collapse; conceptual development and experimental validation of new-type structural technologies using advanced materials; and design and implementation of minimum disturbance retrofitting schemes.

Nikos Theodoulidis
Research Director ITSAK-EPPO

PRINCIPAL CONTRIBUTIONS TO ENGINEERING SEISMOLOGY
Strong ground motion modeling.
Seismic hazard assessment.
Site effects estimation using earthquake and ambient noise.
Strong-motion and consequences of destructive earthquakes.
Planning and operation of accelerometric networks, data analyses.
RESEARCH PROJECTS, PUBLICATIONS & SCIENTIFIC REPORTS:

- Scientist in charge in 23 research projects in engineering seismology & earthquake engineering (international among others; EUROSEISTEST, EUROSEISMOD, EUROSEISRISK, SESAME, SYNARMA, NERIES-JRA4, NERA-JRA1) and participation in more than 70 research projects.
- More than 200 publications (75 peer-reviewed Inter. Journals, 13 peer-reviewed National Journals, 69 Proc. Inter. Conferences, 24 in Proc. National Conferences, 22 others).
- More than 60 technical reports in engineering seismology & earthquake engineering for seismic protection of Public Works and Lifelines.

PAPERS

(in order of appearance)

DEVELOPMENT OF A SIMULATION PLATFORM TO MODEL, ASSESS AND VISUALIZE THE EARTHQUAKE DISASTERS IN CITY LEVEL

Xuchuan Lin[1], Kexin Wang[2], Konstantinos Skalomenos[3], Lingxin Zhang[4], Dongping Li[5]

[1]Institute of Engineering Mechanics, China Earthquake Administration, China

Email: linxc03@gmail.com

[2]Institute of Engineering Mechanics, China Earthquake Administration, China

[3]Department of Civil Engineering, University of Birmingham, United Kingdom

[4]Institute of Engineering Mechanics, China Earthquake Administration, China

[5]Zhejiang Earthquake Agency, China

Keywords: *City-scale simulation tool, Automatic modeling, Building damage, Urban seismic resilience*

Abstract: *Cities tend to be more vulnerable due to the high and unplanned concentration of people, buildings and infrastructures. This study presents a simulation platform, called YouSimulator, for the automatic modeling, assessment and visualization of the seismic responses of urban areas. The proposed platform, which is primarily based on a C++ code, consists of four basic modules: (a) the automatic modeling module; (b) the response computing module; (c) the results analyses module; and (d) the 3-D visualization module. A high-performance algorithm is developed to realize the automatic physics-based modeling by utilizing the GIS database. The efficiency of the parallel computing can be maintained almost stable as the number of processes increases, by equivalently balancing the work load between different processes. Based on the computed damage states of each building, the global behavior of the cities and the demand of shelters in each local community are obtained. The nonlinear time history responses of about one million buildings in a Chinese large city can be achieved within 10 minutes by the scalable parallel computing. The proposed platform appears to be a promising tool for large-scale simulation and earthquake-resilience assessment of urban areas and cities.*

1 INTRODUCTION

The natural disasters, caused by earthquakes, typhoons, tsunamis and fires, have the potential to disrupt everyone's lifestyle by destroying access to basic services, energy, housing, transportation and more. Earthquakes have the potential even to exact a heavy toll from the communities to cities. Nowadays cities, particularly those located in the high-speed urbanization area, tend to be more vulnerable due to their high and unplanned concentration of people, aging and overloaded buildings and infrastructures, and poor quality of materials. The urban area of many Chinese cities has increased significantly in the past thirty years. For instance, the eastern city Hangzhou has extended its downtown area by tens of times, and has reached a population of over nine million. These cities may face very high disaster risk, and might not bear the consequences if a devastating earthquake occurred at the vicinity of the city.

City is such a large, complex and dynamic system that each city is unique and presents different seismic responses with others. Although lessons learned from the previous earthquakes are necessary and very precious for the study of the disaster-causing mechanism, it is far from enough to achieve a reasonable understanding and preparation against future devastating earthquakes. It seems impractical to carry out the city-scale destructive testing, while fortunately, there is always an option to perform the behavior of the cities to some extent by numerical analyses. Recently, the advancing technologies, such as the high-performance computing, Geographic Information System (GIS), big data and artificial intelligence (AI), provide a great potential to develop powerful numerical tools for the city-level detailed earthquake disaster simulations. A lot of research efforts have been made for the continuous improvement of the simulation methods. *Goto et al.* (*2004*) developed an earthquake disaster simulation systems based on GIS by integrating the models of the ground responses, building collapse, road blockage and fire spread [1]. *Hori et al.* (*2006*) proposed the integrated earthquake simulation (IES) [2] based on the full computation of the earthquake hazards and disasters. *Sahin et al.* (*2016*) built a Turkey version of IES [3], which was built on the MATLAB environment. *Lu et al.* (*2017*) presented a solution for earthquake disaster simulation of urban areas using nonlinear multiple degree-of-freedom (MDOF) model and time-history analysis [4].

As part of the above efforts, a simulation platform called YouSimulator was developed in this study to model, assess and visualize the seismic behavior of the cities by making full use of the automatic physics-based nonlinear modeling and modern scalable simulation techniques. The basic modules of YouSimulator were made in 2016 and became available online in 2018 (see http://yousimulator.net/homePage.html, in Chinese). The platform is primarily based on the C++ code, which makes the program portable for different computer operation systems. In this study, the framework, basic modules and performance of YouSimulator V1.0 are introduced, and its typical applications to achieve the detailed seismic responses of the Chinese large cities are presented.

2 SIMULATION PLATFORM

The Version 1.0 of YouSimulator was primarily focused on the automatic modeling and nonlinear time history analyses for a large area of buildings subjected to earthquakes. Figure 1 shows the basic modules and workflow of the proposed platform. The platform consists of four basic modules, the automatic modeling module, the response computing module, results analyses module and the 3-D visualization module. Each of the modules works independently. The communication between the modules is basically based on the data files.

3 APPLICATIONS

The simulation platform has been utilized preliminarily in different ways and for various objectives, such as the rapid damage evaluation for the earthquake emergency response, earthquake disaster scenario simulation, shelter planning for the new downtown and the simulation of city restoration after earthquakes. The performance of the proposed simulation platform is evaluated by simulating the large cities in China, such as Beijing, Hangzhou and Tianjin. The nonlinear time history responses of about one million buildings in Hangzhou were presented. Figure 2 shows the displacement responses of a millions of buildings in and around the Hangzhou. The computing time can be significantly reduced to less than 10 minutes by making full use of the scalable parallel computing and the super computer.

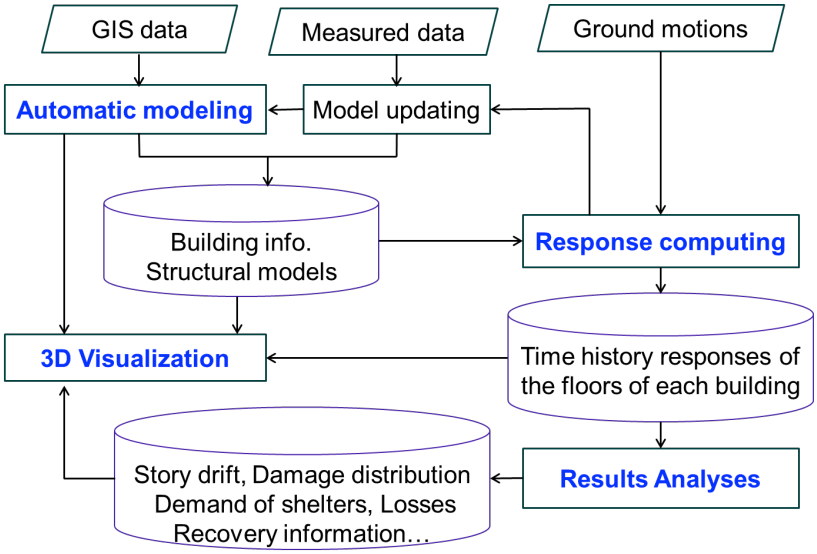

Figure 1. Basic modules and workflow of YouSimulator V1.0

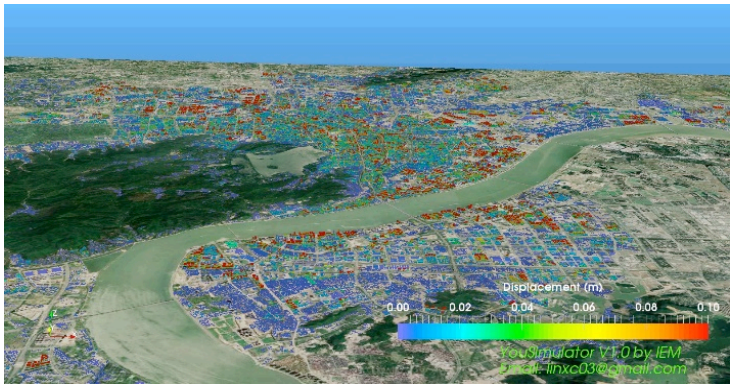

(a)

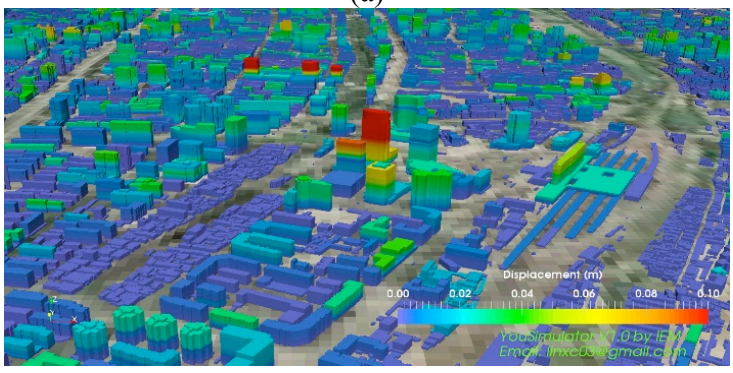

(b)

Figure 2. Displacement responses: (a) global view; (b) local enlarged view

With the proposed platform, the incremental dynamic analyses can also be applied a region by continuously increasing the scale of the input ground motion. The ultimate capacity and the fragility curve of any specified region can be obtained. As an example, the damage distributions of the buildings at different earthquake intensities are shown in Figure 3. The tool can also estimate the floor area of buildings under certain degree of damage for each of the communities, as shown in Figure 4, so the demand of shelters can be estimated.

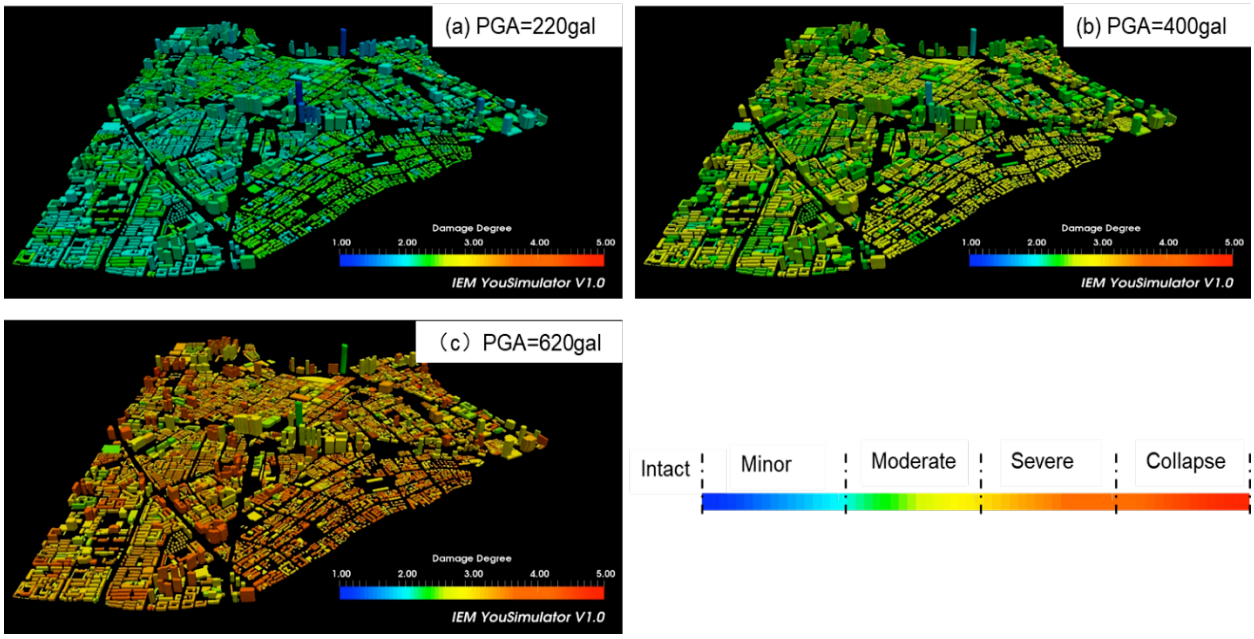

Figure 3. Building damage distribution of a district subjected to different scales of ground motions

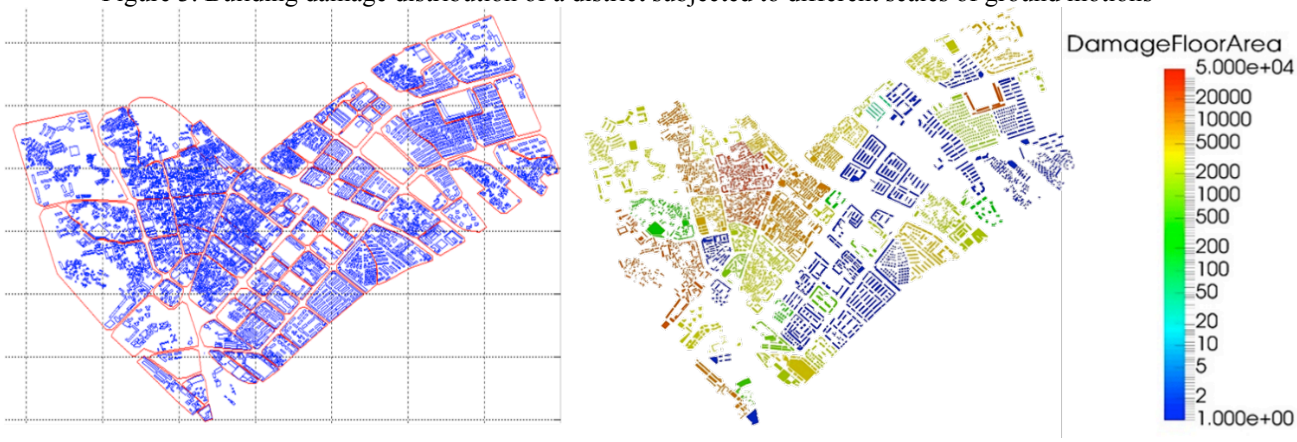

(a) (b)

Figure 4. Demand analysis for mid-to-long term shelters: (a) Communities; (b) The damaged floor area that may induces the demand for mid-to-long term shelters

4 CONCLUSIONS

A code is made to realize a simulation platform YouSimulator, which can be implemented to model, assess and visualize the seismic behavior of urban areas against earthquakes. In the Version 1.0 of YouSimulator, the automatic physics-based modeling of buildings is proposed by using the GIS data. The performance of the proposed platform is examined by simulating the Chinese large cities, and the nonlinear time history responses of about one million buildings can be computed within 10 minutes with developed scalable parallel computing and the super computer. The simulation platform has been utilized for various objectives, such as rapid damage evaluation for the earthquake emergency response, earthquake disaster scenario simulation, shelter planning for the new downtown, simulation of city restoration after earthquakes. The platform appears to be a promising tool for large-scale simulations and earthquake-resilience assessment of urban areas and cities.

ACKNOWLEDGEMENT

The research is supported by the National Key R&D Program of China (Grant No. 2017YFC1500605 & 2018YFC1504401) and Scientific Research Fund of Institute of Engineering Mechanics (IEM), China Earthquake Administration (Grant No. 2017QJGJ01 & 2017QJGJ04).

REFERENCES

[1] Goto, Y., Takeuchi, I., Kakumoto, S., Integrated earthquake disaster simulation systems for the highly-networked information society, 13th World Conference on Earthquake Engineering, Paper No. 2793, 2004, August 1-6, Vancouver, B.C., Canada.

[2] Hori, M., Ichimura, T., Oguni K. Development of integrated earthquake simulation for estimation of strong ground motion, structural responses and human actions in urban areas, Asian Journal of Civil Engineering (Building and Housing), 2006, 7(4), pp.381-392.

[3] Sahin, A., Sisman, R., Askan, A., Hori, M., Development of integrated earthquake simulation system for Istanbul, Earth, Planets and Space, 2016, 68(115), pp.1-21.

[4] Lu, X.Z., Guan, H., Earthquake Disaster Simulation of Civil Infrastructures: From Tall Buildings to Urban Areas, Singapore: Springer, 2017. DOI: 10.1007/978-981-10-3087-1.

CONTRIBUTION OF ACCELEROMETRIC NETWORK IN SHAKEMAPS AND RAPID EARTHQUAKE DAMAGE ASSESSMENT IN GREECE

Theodoulidis N., Konstantinidou K., Margaris B., Morfidis K., Papaioannou C.

Institute of Engineering Sismology & Earthquake Engineering (ITSAK-EPPO)
Terma Dasylliou, 55535 Pylea, Thessaloniki
e-mail: ntheo@itsak.gr

Keywords: accelerometric network, shakemaps, neural networks, rapid damage assessment

1. INTRODUCTION

During the last decades following the occurrence of damaging earthquakes and associated extensive life and property losses, the availability of earthquake ground motion data distribution in almost real time after strong earthquakes, has been considered of vital importance. Such data, together with information related to the building stock environment, can be used for the first estimation of spatial distribution of earthquake losses in order to plan an efficient emergency response. This was the experience gained after past devastating earthquakes in densely populated urban centers (among others; 1994 Northridge; 1995 Kobe; 1999 sequences of Kocaeli-Düzce, Athens; 2009 L'Aquila; 2011 Van-Erciş, 2017 Amatrice) which clearly showed that substantial social and economic losses can be expected. Previous studies indicate that inadequate emergency response can increase the number of casualties by a maximum factor of 10, highlighting a critical necessity for research on rapid earthquake damage and loss estimation. The reduction of casualties in urban areas immediately following an earthquake can be improved if the location and severity of high degree damage can be rapidly assessed using information from rapid response systems.

One of the earliest examples of the use of shakemaps for emergency management and response was the M7.1 Hector Mine earthquake of October 16, 1999. Given all these pieces of information and considering results of recent research work as the pioneering works of Böse (2006) and NRC (2006), one can consider the management of earthquake risks as a process that involves pre-, co- and post-seismic phases. These encompass the compilation of real time ground motion estimation maps and rapid response systems immediately after the earthquake to provide assessment of the distribution of ground shaking intensity and information on the structural damage, casualties and economic losses. This rapid information on the consequences of the earthquake can serve to direct the search and rescue teams to the areas most needed and assist civil protection authorities in the emergency action. The need for a rapid loss estimate after an earthquake has been recognized and requested by governments and international agencies. Bird and Bommer(2004) have shown that 88% of damage in recent earthquakes has been caused by ground shaking, rather than secondary effects (e.g. ground failures, tsunamis etc.). Consequently, spatial distribution of vibratory effects of earthquakes is of prime importance in rapid loss assessment. In Greece, the ShakeMap software (ShakeMap hereafter) distributed by the USGS has been used since 2012 by the ITSAK (http://www.itsak.gr) to provide region-wide maps of the spatial variability of ground motions following any earthquake with M≥4.0.

In this work, a methodology utilizing the USGS ShakeMap, accelerometric stations and the Artificial Neural Network theory is proposed, to rapidly estimate the degree of expected seismic

damage in three simple levels; Light, Moderate and Heavy damage. In parallel, effects of seismic source representation, namely, point source and finite fault, as well as inclusion of a local soil condition model are examined, as case study in Cephalonia (Paliki). As expected, the use of finite fault and local soil condition model provide the most reliable results compared with the observed damage. However, this may have significant implications in the near field rapid damage assessment since shakemaps calculation is mostly based on the automatic earthquake epicenter location without any provision of the causative finite fault.

2. ACCELEROMETRIC NETWORK

After the destructive earthquake, in Thessaloniki, northern Greece (Jun. 20, 1978, **M**6.5), the Greek Ministry of Public Works established the Institute of Earthquake Engineering and Engineering Seismology-ITSAK, with main research activities in engineering seismology, soil dynamics and earthquake engineering. In order to serve these activities, ITSAK undertook the installation, maintenance and operation of a permanent strong motion network in Greece. The deployment of ITSAK accelerographic network in Greece was accomplished after an analytical study, which took into account all available seismological, seismotectonic and seismic hazard assessment results (Theodoulidis et al. 1986). By 90's ITSAK strong motion network has been expanded to over 65 installations Greece, covering free-field and in basements of mainly low rise buildings, various site conditions and tectonic environments,whileNOA-IG, based on the State financial support, expanded its network reaching a number of 45 permanently installed instruments of SMA-1 type. Due to the rapid evolution of digital technology, installation of digital instruments of low resolution (12-bit) started by mid 90s (A-800/A-900 of Geotech), while the analog units of ITSAK and NOA-IG have been replaced by common digital accelerographs with an "almost" 11-bit A/D converter (QDR of Kinemetrics) by 2001 and after the September 7, 1999 M5.9 Athens earthquake. The dynamic range of those instruments can not be considered as better than the analog ones, however the main advantage of these accelerographs is the elimination of digitization processing errors and remote data accessibility through modem. The data analysis and processing of the aforementioned digital recordings can be carried out by computer software provided by Kinemetrics Ltd. At that time, the first Greek unified accelerographic relational database was developed, including records from the two networks, which were selected under specific criteria, processed uniformly and after careful metadata selection resulted to the new Greek Ground Motion predictive Equations GMPE's (Theodoulidis et al. 2004; Skarlatoudis et al. 2003a). In 2007–2008, the Regional Authority of Central Macedonia, Greece, funded the purchase and installation of 32 high resolution recorders (GSR-24), all equipped by Guralp CMG-5T sensors, covering the largest settlements of Central Macedonia and the city of Thessaloniki itself. This network is remotely maintained via dial-up and Internet connections procedure by the EPPO-ITSAK. Since 2008, the Greek strong motion network consisted totally from digital instruments (A-800/A-900, QDR, ETNA, K2, CMG-5TD, GSR-24). At that time a national project led to a tremendous increase of quantity and quality of the national strong motion instruments, namely the purchase of 120 CMG-5TD-EAM units by the two Institutes and their installation at permanent sites. The up to date deployment of the free-field strong motion stations in Greece is shown in Fig. 1.

For each accelerometric station all available site metadata are provided for its documentation (Fig. 2). Duringthe last 35 years more than 5000 acceleration time histories have been recorded by the national accelerometric network for earthquakes with $M \geq 4.0$ and distances $1km \leq R \leq 1000km$ (Fig. 3).

Figure 1. ITSAK-EPPO Accelerometric network of free-field stations in Greece.

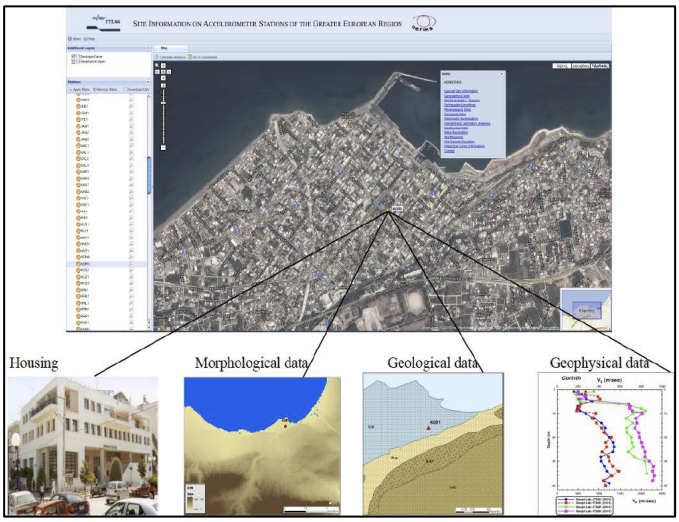

Figure 2. Site metadata for accelerometric stations in Greece (example for Korinthos station).

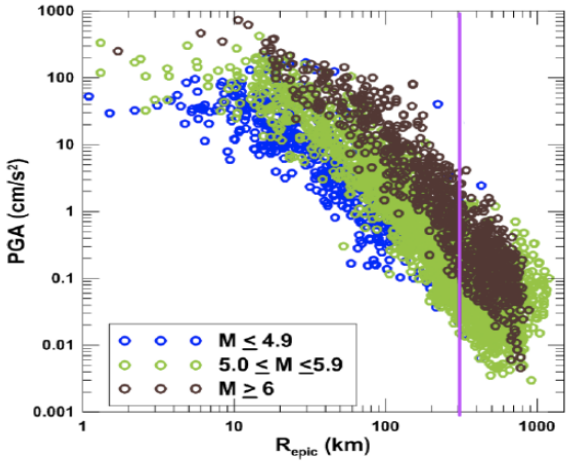

Figure 3. Distribution of PGA with distance of the accelerometric network in Greece (Scordilis et al. 2018).

2. SHAKEMAPS & DAMAGE ASSESSMENT METHODOLOGY

The methodology applied in this work is based on the USGS ShakeMap software (Wald et al. 1999; https://earthquake.usgs.gov/data/ShakeMap/) and on the Artificial Neural Network (ANN) theory (e.g. Haykin, 2009). The ITSAK-EPPO broadband accelerometric network transmits data to ITSAK-EPPO data center, through Internet, in real-time continuous streams. When an earthquake occurs, above a certain magnitude (M≥4.0), an alert is sent by the seismological station of the Aristotle University of Thessaloniki with the earthquake automatic solution including its origin time, epicenter coordinates, depth and magnitude. This information is used to automatically extract the acceleration time histories for all accelerometric stations with the help of a custom made Perl script. Offset correction and a low pass filter of 20Hz is applied to all time histories. After the acceleration time histories are selected, the PGA, PGV, PSA(T=0.3, 1, 3sec) and Macroseismic Intensity are calculated to produce the input for the ShakeMap.

ShakeMap software is configured according to the regional characteristics of the area of interest as they resulted from previous studies, i.e. local site conditions (geology, topography, V_{S30}), Ground Motion Prediction Equations (Skarlatoudis et al., 2003, 2004, 2007; Theodoulidis and Papazachos, 1992; Boore and Atkinson 2008), as well as Instrumental Macroseismic Relations (Theodoulidis, 1991). Regarding the V_{S30} values, their estimation is based on the slope of 3 arc-sec and geologic age on 30 arc-sec DEM, utilizing the respective relations proposed by Stewart et al. (2014). An example of Shakemap is shown in Fig. 4 based on point source and finite fault model for the Feb. 3, 2014, Cephalonia event (M6.0) (Theodoulidis et al. 2019).

A Multilayer Feed-forward Perceptron (MFP) Artificial Neural Network (ANN) is utilized for the rapid estimation of the seismic damage level of Reinforced Concrete (R/C) buildings. The problem was formulated in terms of "Pattern Recognition" (PR) problems (Theodoridis and Koutroumbas, 2008). The solution of the PR problem can lead to the classification of buildings in pre-defined seismic damage classes. This functionality is required for a rapid estimation of the seismic damage level within few minutes after a seismic event, since in this critical time period the accurate calculation of the seismic damage level of a large group of buildings is impossible. Additionally, the output of the ShakeMap software (e.g. maps with spatial distribution of PGA, PGV etc) is the appropriate input to the PR problem. The required input data parameters for the ANNs are classified to the following categories:

1. The ground motion parameters (seismic parameters), used for the evaluation of the impact of seismic motions on structures. In this study, the seismic parameters PGA and PGV (and their ratio PGV/PGA), which are automatically calculated by the ShakeMap software, were utilized.

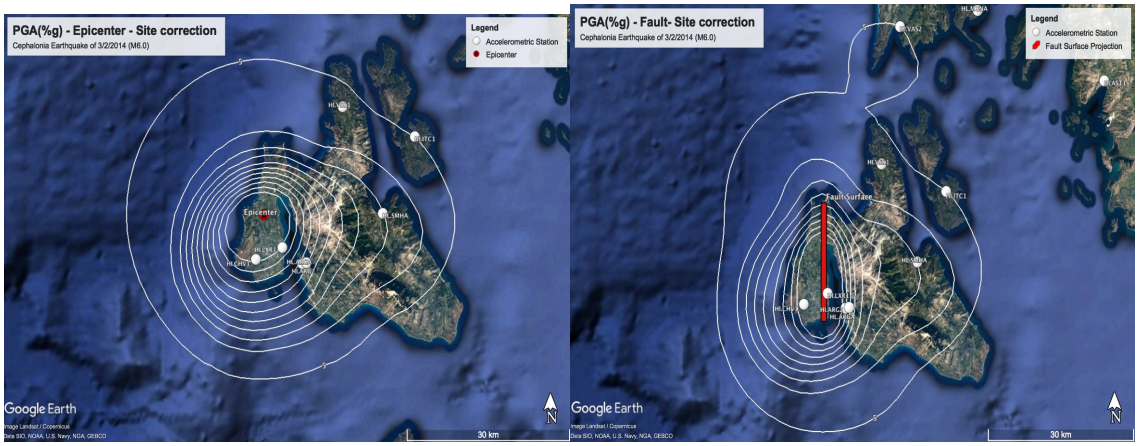

Figure 4. ShakeMap PGA distribution for point source(left) and finite fault model(right) scenarios.

2. The structural parameters, used for the description of the seismic response (performance) of buildings. In this study, 4 structural parameters were selected. These parameters are widely utilized in well-known methods for the seismic vulnerability assessment of existing R/C buildings (e.g. Kappos et al., 2006). These parameters are the total height of buildings H_{tot}, the structural eccentricity e_o of storeys, and the ratio of the seismic base shear that is received by R/C walls (if they exist) along two perpendicular directions (axes x and y): n_{vx} and n_{vy}. In addition, the existence of masonry infill was taken into account. This consideration was made in the generation of the data set which is required for the training of ANNs.
3. The parameters describing the local soil conditions in the studied region. These parameters quantify the influence of soil on the seismic response of buildings (Soil-Structure interaction effects). In the framework of the present study, the parameters of this category were neglected. The reason for this decision is the fact that the utilized ANNs' training data set is comprised of samples which are extracted from the analytical solution (using non-linear time history analyses) of R/C buildings which were considered to be fully fixed to the ground.

The output of ANNs is the classification of selected types of R/C buildings, defined on the basis of the selected structural parameters in three damage classes (Light – Moderate – Heavy), which are compatible to the well-known R/C buildings' rapid seismic vulnerability approach "Green – Yellow – Red". In the framework of this approach the R/C buildings are characterized as:

- "Green" if they are safe to occupy instantly but possibly not fully operational until Light repair is made.
- "Yellow" if they are safe during event but not fully functional until significant repair is made.
- "Red" if they suffer heavy damages or they are on verge of collapse.

It must be noted that for the classification to three damage classes, the Maximum Inter-storey Drift Ratio (MIDR) was utilized. The MIDR damage index is widely used in studies which concern seismic vulnerability assessment of structures (e.g. Morfidis and Kostinakis, 2018, Theodoulidis et al. 2019).

Figure 5a briefly illustrates the parameters which were selected for the configuration of the utilized ANNs (i.e. the input and output parameters, the number of hidden layers, the number of neurons in each hidden layer and the neurons' activation functions). In Figure 5 the correlation between the MIDR values and the three damage classes (Light-Moderate-Heavy) is also presented (Figure 5b), relating the ANNs' predictions with the actual damage patterns which are observed through the in-situ inspections of structural engineers after a strong seismic event.

4. RESULTS AND DISCUSSION

The aforementioned methodology applied for the Feb. 2, 2014 Cephalonia earthquake (M6.0), taking into account four different seismic scenarios (Table 1).

Scenario	Description	PGA (cm/sec^2)	PGV (cm/sec)	PGV/PGA (sec)
SC1	Epicenter, no site correction	539	63	0.117
SC2	Epicenter, site correction	539	56	0.104
SC3	Fault, no site correction	441	54	0.122
SC4	Fault, site correction	441	49	0.111

Table 1. ShakeMap estimated average PGA, PGV values due to earthquake of Feb. 3, 2014 (M6.0), for the area of Paliki.

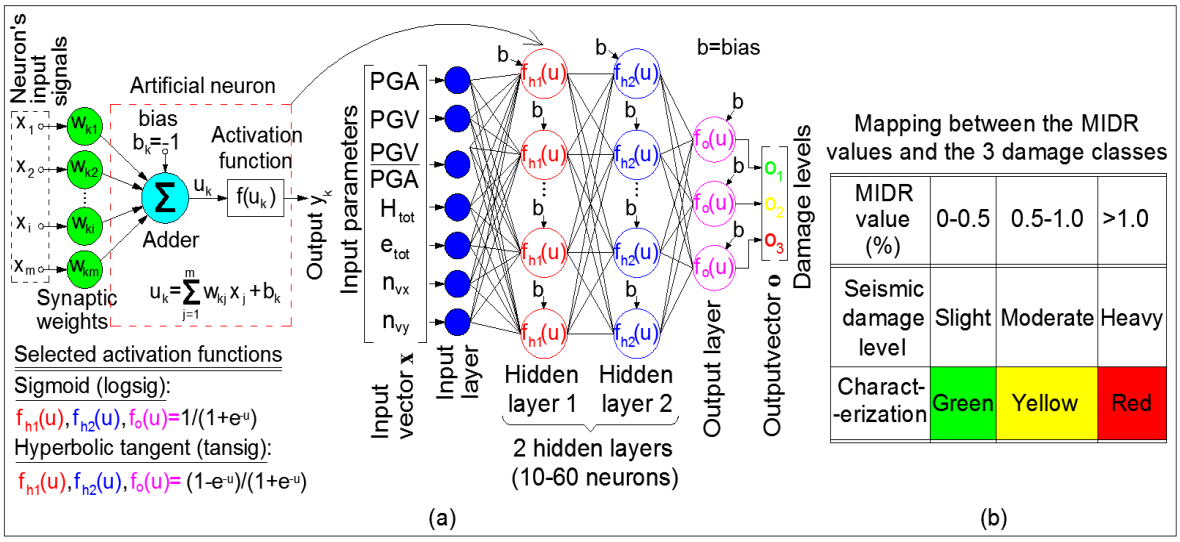

Figure 5. The configuration parameters of the utilized MFP networks and the correlation between the Damage Index (MIDR) values and the three damage classes (from Theodoulidis et al. 2019).

The resulted classifications of the selected R/C buildings into three pre-defined damage classes (Light="Green" – Moderate="Yellow" – Heavy="Red") which were extracted by the optimum configured network for four scenarios, are presented in Table 2. The implementation of the proposed methodology in near-real time is of paramount importance for seismic risk reduction, provided that ground motion estimation is of satisfactory reliability. Contribution of accelerometric network recordings as well as site correction factors are of high importance to realistic estimation of ground shaking in the vicinity of the causative fault. The testing results obtained in this work concern to the classification of R/C buildings of a stricken region in Paliki peninsula (Cephalonia, Greece) to three pre-defined seismic damage classes which were classified on the basis of the well-known R/C buildings' rapid seismic vulnerability approach "Light, Moderate and Heavy Damage".

	Description of the bearing system	Damage state			
		SC1	SC2	SC3	SC4
1	Low rise frame system (1 storey)	Heavy	Heavy	Moderate	Moderate
2	Low rise frame-equivalent dual system (1 storey)	Heavy	Heavy	Light	Light
3	Low rise frame-equivalent dual system (2 storeys)	Heavy	Heavy	Moderate	Moderate
4	Medium rise frame-equivalent dual system (3storeys)	Heavy	Heavy	Moderate	Moderate
5	Low rise wall-equivalent dual system (2 storeys)	Moderate	Moderate	Light	Light
6	Medium rise wall-equivalent dual system (3 storeys)	Heavy	Heavy	Moderate	Moderate
7	Medium rise wall system (3 storeys)	Moderate	Moderate	Moderate	Light

Table 2. Classification of the selected R/C buildings to the 3 damage classes in cases the four scenarios.

As expected, the use of finite fault and local soil condition model provided the most reliable results qualitatively compared with the observed damage in the Paliki peninsula. However, causative seismic fault cannot be easily pre-defined. Such a constrain may have significant implications in the near-field rapid damage assessment when using ShakeMap results based only on the automatic earthquake epicenter location without any provision of the causative finite fault. As a consequence, correlation of automatic earthquake epicenter location with source parameters of the causative finite fault in near-real time, is of great importance in future steps to improve the

proposed methodology. In addition, a reliable soil condition model for the examined area is of great significance since it drastically affects the ground motion amplification and affects the lateral variability of strong ground motion. Thus, the proposed methodology can be used as a decision tool after a disastrous earthquake, only if such limitations and requirements are taken into consideration in future development of rapid earthquake damage assessment systems.

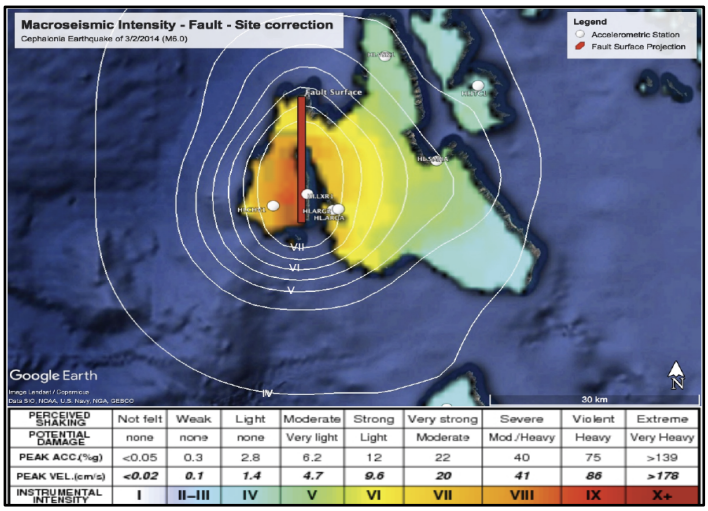

PERCEIVED SHAKING	Not felt	Weak	Light	Moderate	Strong	Very strong	Severe	Violent	Extreme
POTENTIAL DAMAGE	none	none	none	Very light	Light	Moderate	Mod./Heavy	Heavy	Very Heavy
PEAK ACC.(%g)	<0.05	0.3	2.8	6.2	12	22	40	75	>139
PEAK VEL.(cm/s)	*<0.02*	*0.1*	*1.4*	*4.7*	*9.6*	*20*	*41*	*86*	*>178*
INSTRUMENTAL INTENSITY	I	II–III	IV	V	VI	VII	VIII	IX	X+

Figure 6. Shakemaps Macroseismic Intensity distribution for the finite fault scenario showing the increased expected damage in the Paliki western Cephalonia area (Theodoulidis et al. 2019).

REFERENCES

Bird J.F. & J.J. Bommer (2004). Earthquake losses due to ground failure. Eng Geology 75:47–79

Boncori J. P. M., I. Papoutsis, G. Pezzo, Cr. Tolomei, S. Atzori, A. Ganas, V. Karastathis, St. Salvi, Ch. Kontoes, and A. Antonioli (2015). The February 2014 Cephalonia Earthquake (Greece): 3D Deformation Field and Source Modeling from Multiple SAR Techniques, Seism. Res. Lett., 86, 124-137 doi: 10.1785/0220140126.

Boore D. and Atkinson G. (2008). Ground motion prediction equations for the averagehorizontal component of PGA, PGV, and 5% damped PSA at spectral periods between 0.01s and 10.0 s, Earthquake Spectra 24 , 99– 138.

Böse M. (2006). Earthquake Early Warning for Istanbul using Artificial Neural Networks. PhD. Diss. Thesis, Fakultät für Physik der Universität (TH) Karlsruhe, 180pp.

Haykin S. (2009). Neural networks and learning machines. 3rd ed. Prentice Hall.

Kappos AJ, Panagopoulos G, Panagiotopoulos C, Penelis G. (2006). A hybrid method for the vulnerability assessment of R/C and URM buildings. Bull Earthquake Eng; 4(4):391–413.

Morfidis, K., Kostinakis, K., (2018). Approaches to the rapid seismic damage prediction of r/c buildings using artificial neural networks. Eng Struct 165, 120-141.

National Research Council (NRC) (2006). Improved seismic monitoring - Improved decision-making. Assessing the value of reduced uncertainty. The National Academic Press, Washington DC, ISBN 0-309-55178-1, 197 pp.

Papazachos, B. C. and C.B. Papazachou (2003). The Earthquakes of Greece, Ziti Publications, Thessaloniki, 273 pp.

Scordilis E., Theodoulidis N., Kalogeras I., Margaris B., Klimis N., Skarlatoudis A., Stewart J., Boore D., Seyhan E., Savvaidis A., Mylonakis G., Pelekis P. (2018). Strong Motion Database for Crustal Earthquakes in Greece and Surrounding Area, Proc. 16th European Conference on Earthquake Engineering (16ECEE), Thessaloniki, Greece, June 18-21, 2018, Paper No. 12077.

Skarlatoudis, A.A., C.B. Papazachos, B.N. Margaris, N. Theodulidis, Ch. Papaioannou, I. Kalogeras, E.M. Scordilis and V. Karakostas (2003): Empirical peak ground motion predictive relations for shallow earthquakes in Greece. Bull. Seism. Soc. Am., 93: 2591-2603

Skarlatoudis A., N. Theodoulidis, Ch. Papaioannou and Z. Roumelioti (2004). The dependence of the peak horizontal acceleration on magnitude, distance and site effects from small magnitude earthquakes in Greece. Proc. 13th WCEE, CD-Paper No. 1857.

Skarlatoudis, A. A., C. B. Papazachos, B. N. Margaris, N. Theodoulidis, Ch. Papaioannou, I. Kalogeras, E. M. Scordilis, and V. Karakostas (2007). Erratum to Empirical Peak Ground-Motion Predictive Relations for Shallow Earthquakes in Greece. Bull. Seim. Soc. Am., 97, 2219–2221.

Sokos E., A. Kiratzi, F. Gallovič, J. Zahradník, A. Serpetsidaki, V. Plicka, J. Janský, J. Kostelecký and G.-A. Tselentis (2015). Rupture process of the 2014 Cephalonia, Greece, earthquake doublet (Mw6) as inferred from regional and local seismic data. Tectonophysics, 656, 131-141 http://dx.doi.org/10.1016/j.tecto.2015.06.01.

Stewart J.P., Klimis N., Savvaidis A., Theodoulidis N., Zargli E., Athanasopoulos G., Pelekis P., Mylonakis G., and Margaris B. (2014). Compilation of a local Vs profile database and its application for inference of VS30 from geologic and terrain-based proxies, Bull. Seism. Soc. Am., Bull. Seism. Soc. Am., 104 (6): 2827-2841.

Theodoridis S, and Koutroumbas K.(2008). Pattern Recognition. 4th ed. Elsevier.

Theodoulidis N, Margaris B, Papastamatiou D (1986) Planning of strong motion network. Report ITSAK, Report: 86-04 (in Greek).

Theodoulidis N. (1991). Contribution to strong ground motion study in the area of Greece. PhD Thesis, Aristotle Univ. Thessaloniki, 500p (in greek).

Theodoulidis N. and B. Papazachos (1990). Strong motion from intermediate depth subduction earthquakes and its comparison with that of shallow earthquakes in Greece. Proc. XXII Gen. Ass. ESC, Barcelona, II, 857-864.

Theodoulidis, N. and B. Papazachos (1992). Dependence of strong ground motion on magnitude-distance, site geology and macroseismic intensity for shallow earthquakes in Greece: I, Peak horizontal acceleration, velocity and displacement" Soil Dyn. Earth. Eng., 11, 387-402.

Theodoulidis N, Kalogeras I, Papazachos C, Karastathis V, Margaris B, Papaioannou Ch, Skarlatoudis A(2004) HEAD 1.0: a unified hellenic accelerogram database. Seism Res Lett 75:36–45.

Theodoulidis, N., C. Karakostas, V. Lekidis, K. Makra, B. Margaris, K. Morfidis, Ch. Papaioannou, E. Rovithis, T. Salonikios and A. Savvaidis (2015):The Cephalonia, Greece, January 26(M6.1) and February 3, 2014 (M6.0) Earthquakes: Near-Fault Ground Motion & Effects on Soil & Structures. Bull. Earthq. Engin. 14, 1–38.

Theodoulidis N., Morfidis K., Konstantinidou K., Margaris B, Papaioannou C. (2019). Shake-Map and Rapid Earthquake Damage Assessment in Greece, Proc. ICONHIC2019, Chania, Crete.

Wald, D. J., V. Quitoriano, T. H. Heaton, H. Kanamori, C. W. Scrivner, and C. B. Worden (1999). TriNet "ShakeMap": Rapid generation of peak ground motion and intensity maps for earthquakes in southern California, Earthq. Spectra, 15, 537–555.

Wald, D. J., C. Br. Worden, V. Quitoriano and J.G. Worden (2002). ShakeMap: its role in pre-earthquake planning and post-earthquake response and information. Proc. SMIP02, 20 pp.

Wald, D. J., C. B. Worden, V. Quitoriano, and K. L. Pankow (2006). ShakeMap manual, Advanced National Seismic System, 156 pp.

EVALUATION OF ECONOMIC LOSS FOR STRUCTURES IN THE AREA STRUCK BY THE 7/9/1999 ATHENS EARTHQUAKE AND COMPARISON WITH ACTUAL REPAIR COSTS

V.A. Lekidis[1], Ch.Z. Karakostas[1], I.I. Sous[2], A. Anastasiadis[3], A. Kappos[4], G. Panagopoulos[5]

[1] Research Director, Earthquake Planning and Protection Organization (EPPO-ITSAK)
Terma Dasylliou, 55535, Thessaloniki, Greece
email: lekidis@itsak.gr, christos@itsak.gr

[2]Associate Professor, Department Civil Engineering and Surveying Engineering & Geomatics, TEI of Central Macedonia, Terma Magnisias, 62124, Serres, Greece

[3]Associate Professor, Department of Civil Engineering, Aristotle University of Thessaloniki
Aristotle University campus, 54124, Thessaloniki, Greece
email: anas@civil.auth.gr

[4]Professor, Department of Civil Engineering, Aristotle University of Thessaloniki
Aristotle University campus, 54124, Thessaloniki, Greece
email: ajkap@civil.auth.gr

[5]Lecturer, Department Civil Engineering and Surveying Engineering & Geomatics, TEI of Central Macedonia, Terma Magnisias, 62124, Serres, Greece
email: panagop@teiser.gr

Keywords: seismic risk scenarios, loss assessment, vulnerability of buildings, fragility curves, damage probability matrices.

Abstract. *Reliable loss assessment (in monetary terms) for buildings struck by an earthquake is an essential factor in the development of seismic risk scenarios for a given urban area. The evaluation of the seismic risk for a certain region depends both on the seismic hazard and the vulnerability of the building stock in the area. For the evaluation of building vulnerability, a hybrid methodology was recently proposed for the estimation of vulnerability (fragility) curves and the corresponding damage probability matrices. The methodology is applied here to the municipality of Ano Liosia, in the meisoseismal area of the Athens, Greece earthquake of 7/9/1999, for both reinforced concrete (R/C) and unreinforced masonry (URM) buildings. An in-situ survey of 150 building blocks was performed, and data regarding the structural type, actual earthquake damage and corresponding repair costs were collected. The actual repair cost for the area, was compared with the economic loss estimation obtained using the hybrid methodology and various estimates of the seismic action in the area considered. The analytical economic loss assessment was found to agree, to a satisfactory degree, with the actual repair costs, for certain seismic hazard scenarios.*

1. INTRODUCTION

The present work aims towards a reliable, technically sound, estimation of seismic risk scenarios in the meisoseimal region of the 07/09/1999 Athens earthquake. The seismic risk depends both on the seismic hazard as well as the vulnerability of the building stock in the region. Using both deterministic and stochastic approaches, referring at outcropping bedrock soil conditions, the simulation of near-field strong ground motion is achieved using gathered geotechnical and geophysical data. Five suites of motion were derived, which were then utilized to evaluate the response of both reinforced concrete (R/C) and unreinforced masonry (URM) buildings. Using a methodology proposed by Kappos et al. [1], which correlates the structural damage index with the repair cost, and using a more refined set of collapse criteria, a number of inelastic time-history analyses of typical R/C buildings allowed the prediction of economic loss in the study area.

The actual repair cost was derived through data collected in the municipality of Ano Liosia, within the meisoseimal area of the 7/9/1999 earthquake ([2], [3]). A thorough in situ survey of structures in a representative sample of 150 building blocks (corresponding to approximately 10% of the total building stock) was performed. The total "actual cost" as well as the "actual cost" for each damage category was estimated. A suitable grouping of the actual data was performed, for it to be directly comparable to the results of the predicted economic loss.

Predicted and actual costs are compared for the entire area, as well as separately for each geological and geophysical zone. The analytical economic loss assessment was found to agree, to a satisfactory degree, with the actual repair costs, for certain seismic hazard scenarios.

The proposed methodology can be easily adapted for application in other urban areas, and is expected to contribute towards the development of rational earthquake risk mitigation efforts for major Greek urban areas, as well as in prioritisation policies for strengthening of buildings.

2. BUILDING STOCK, GROUPING AND "ACTUAL COST" ESTIMATION

The actual repair cost was derived through data collected by the research team in the municipality of Ano Liosia, within the meisoseimal area of the 7/9/1999 earthquake. The collected database, from the survey of 150 building blocks (corresponding to approximately 10% of the total building stock) contained a full set of data regarding the building block number, the number of the building in the block, the building address, year of construction, information regarding construction permit (or its absence), use of the building, total area, total height, total volume, and number of storeys. Also, data regarding structural characteristics of the building were included, such as presence or not of basement, soft storey/pilotis (discontinuity of brick infills at the ground storey), type of construction (R/C, URM, etc.). Finally information regarding the damage level determined by inspection was included. Damage classification was based on the "green-yellow-red" tagging scheme, with the following meaning:

- "Green": Original seismic capacity has not been decreased, the building is immediately usable, and entry is unlimited,
- "Yellow": Building with decreased seismic capacity that should be repaired. Usage is permitted only for limited time,
- "Red": Buildings in this category are unsafe and entry is prohibited; decision for demolition will be made on the basis of subsequent, more thorough, inspection.

Using the mean repair cost per square meter for each damage category, provided by the Department for Seismic Retrofit (TAS) in the meisoseismal areas of Ano Liosia and Menidi, an estimation of the total "actual cost" was performed. The accuracy of these mean repair costs was tested by cross checking with corresponding values provided by other Departments for Seismic Retrofit in the metropolitan area of Athens. The "actual cost" used for each damage category, as

well as the total "actual cost", are shown in table 1. The geological and geophysical zones in Ano Liosia are presented in Figure 1 together with the building blocks, building damage classification (green-yellow-red tags) and "actual cost" distribution.

Damage category	no. of buildings	Area (m^2)	Repair cost	Total cost (€)
Green	407	33.258,00	35,5 €/m^2	1.180.659
Yellow	351	47.535,00	92,4 €/m^2	4.392.234
Red	230	15.433,75	361,1 €/m^2	5.573.127
TOTAL	988	96.226,75	-	**11.146.020**

Table 1: "Actual cost" estimation

For the analytical estimation of the retrofit cost, suitable grouping of the building database was performed, for it to become comparable with the results of analytical models described below. Firstly, buildings were grouped, depending on construction year, in two categories: a) buildings designed and built before 1996, according to older seismic codes (issued in 1959 and 1984) and b) buildings designed and built, according to modern seismic codes (issued in 1996 and 2000).

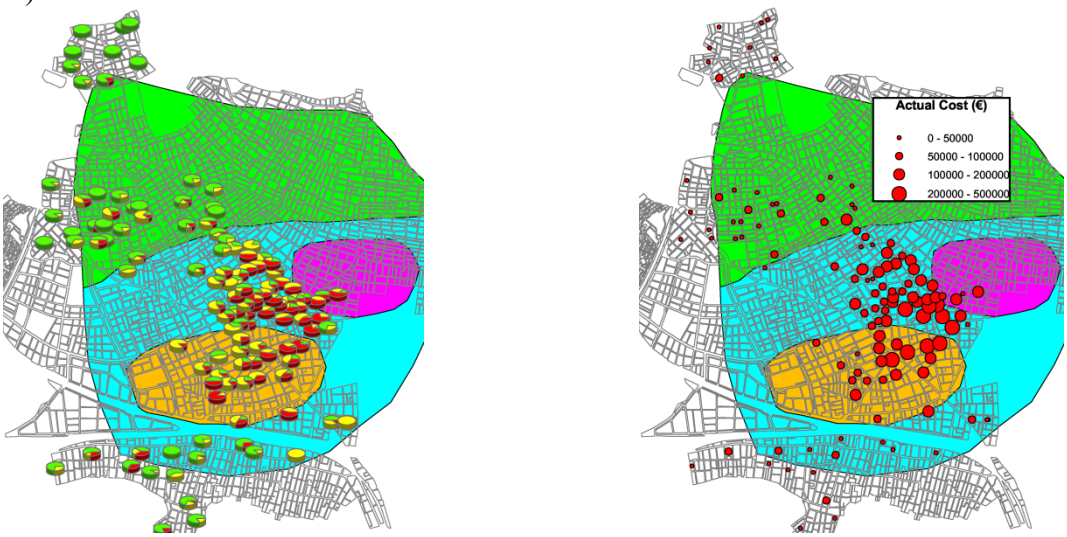

Figure 1: Geological zones in the Municipality of Ano Liosia with building damage classification (left) and actual cost distribution (right)

All R/C buildings of the 1st group were assumed to have space frame structural systems without shear walls, while buildings of the 2nd group were assumed to have space frame structural systems with shear walls (dual system); this assumption was verified by in-situ inspections. Then, classification was further refined, leading finally to the following groups:

<u>Buildings designed and built before 1996</u> (frame structural system)

- One- and two- storey R/C buildings with brick infills and without "soft" ground storey (pilotis). Total area of the sample: 52.775 m^2.
- One and two storey R/C buildings with brick infills and with "soft" ground floor (pilotis). Total area of the sample: 4.657 m^2.
- Three- and four- storey R/C buildings with brick infills and without "soft" ground storey (pilotis). Total area of the sample: 5.562 m^2.

- One- and two- storey unreinforced masonry buildings without "soft" ground storey (pilotis). Total area of the sample: 26.512 m^2.
- One- storey stone built structures. Total area of the sample: 345 m^2.

Buildings designed and built in or after 1996 (dual structural system)

- One- and two- storey R/C buildings with brick infills and without "soft" ground storey (pilotis). Total area of the sample: 2.565 m^2.
- One and two storey R/C buildings with bricks infill and with "soft" ground storey (pilotis). Total area of the sample: 1.711 m^2.
- Three- and four- storey R/C buildings with bricks infill and without "soft" ground storey (pilotis). Total area of the sample: 1.327 m^2.
- Three- and four- storey R/C buildings with bricks infill and with open "soft" ground storey (pilotis). Total area of the sample: 191 m^2.

One- and two- storey buildings were assumed to correspond to low-height (2-storey) analytical models, while three and four- storey building were assumed to correspond to medium-height (4-storey) analytical models (see section 3.2). High (9-storey) analytical models could not be addressed here, since no buildings of such height existed in the area under consideration. All masonry structures in the area had a single storey and were assigned to the one-storey stone analytical model. Distribution of the two main R/C groups and the unreinforced masonry (URM) buildings, in the studied region, is presented in Figure 2, together with the area per building type.

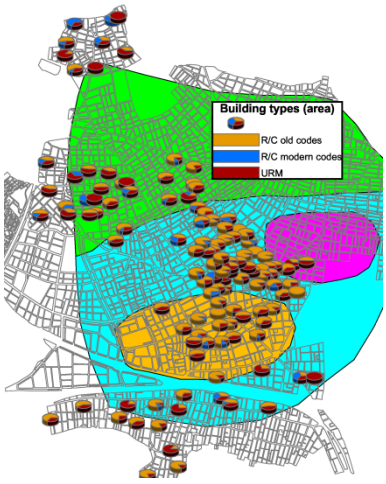

Figure 2: Area (m^2) / building type

3. VULNERABILITY ASSESSMENT

Five suites of motions were used to evaluate the response of typical R/C buildings. Based on the procedure proposed by Kappos et al. [1] that correlates the structural damage index with the repair cost and using a more refined set of collapse criteria, a number of inelastic time-history analyses of typical R/C buildings allowed the prediction of economic loss in the study area.

Referring to the height of the buildings, 2-storey, 4-storey, and 9-storey R/C buildings were analysed. Regarding the structural system, both frames and dual (frame+shear wall) systems were addressed. Each of the above buildings was assumed to have three different configurations, namely bare, infilled and pilotis (soft ground storey) type. Two seismic code levels were considered: low (early seismic codes) and high (modern seismic codes); the specific codes applied for designing the structures were the 1959 and the 2000 Greek Codes (the latter is similar to the 1995 code). This classification resulted in a total of 36 R/C types, not all of which were

present in the study area (the actual building stock was not clearly known at the time the analyses were performed). To keep the cost of analysis within reasonable limits, all buildings were analysed as 2D structures.

Using the DRAIN2000 code, R/C members were modelled using lumped plasticity beam-column elements, while infill walls were modelled using shear panel isoparametric elements developed in previous studies [1], [5]. From each analysis, the cost of repair (which is less than or equal to the replacement cost) is estimated for the building type analysed, using the models for member damage indices proposed by Kappos et al. [1]. The total loss for the entire building is derived from empirical equations (calibrated against damage cost data from Greece)

$$G = G_c + G_p = 0.25D_c + 0.08D_p \ (\leq 5 \text{ storeys}) \quad (1)$$

$$G = G_c + G_p = 0.30D_c + 0.08D_p \ (6 - 10 \text{ storeys}) \quad (2)$$

where D_c and D_p are the global damage indices (≤ 1) for the R/C members and the masonry infills of the building, respectively. Due to the fact that the cost of the R/C structural system and the infills totals less than 40% of the cost of a (new) building, the above relationships give values up to 38% for the loss index G, wherein replacement cost refers to the entire building. In the absence of a more exact model, situations leading to the need for replacement (rather than repair/strengthening) of the building are identified using failure criteria for members and/or storeys, as follows:

- In R/C *frame* structures, failure is assumed to occur (hence G=1) whenever either 50% or more of the columns in a storey 'fail' (i.e. their plastic rotation capacity is less than the corresponding demand calculated from the inelastic analysis), or the interstorey drift exceeds a value of 4% at any storey.
- In R/C *dual* structures, failure is assumed to occur whenever either 50% or more of the columns in a storey 'fail', or the walls (which carry most of the lateral load) in a storey fail, or the interstorey drift exceeds a value of 2% at any storey (drifts at failure are much lower in systems with R/C walls).

This is a new, more refined, set of failure criteria (compared to those used in previous studies by the authors of [1], [5] and they resulted after carrying out a large number of (time history) analyses; a more detailed discussion of these criteria and their limitations can be found in [4].

Typical analysis results are presented in figures 4 and 5 where it is clear that the set of stochastic motions results in significantly higher values of calculated loss compared to the set of recorded motions for which no collapse was predicted for all building types (note the different scale in the figures). The effect of seismic design is found to be very significant especially for the more severe motion sets (all 'collapses' were predicted for low code building types).

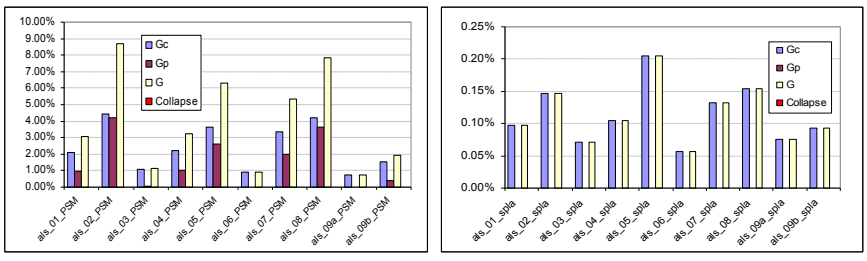

Figure 3: 2 storey dual infilled building/new code– PSM, spla series

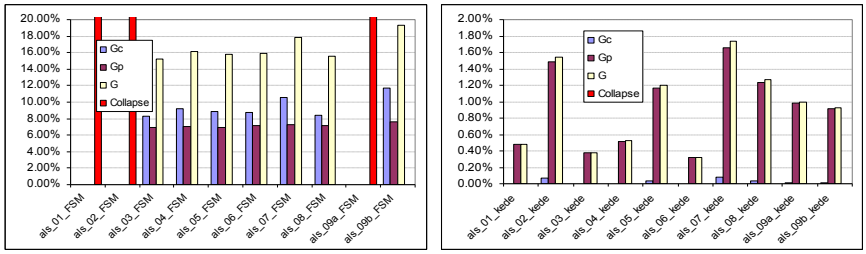

Figure 4: 4 storey frame infilled building/old code – FSM, kede series

4. COMPARISON OF ACTUAL AND PREDICTED COST

The prediction of economic loss seems to be quite good when the stochastic motion sets (FSM and PSM) are used (see table 2). In this case the difference between the actual cost for the entire Ano Liosia area is less than 5%, while for the average of the two sets it is almost zero (0.6%). On the other hand, the sets derived from the (far-field) recorded motions underestimate significantly the economic loss, predicting almost 90% less than the actual damage. A closer examination reveals that the accuracy of the stochastic motion based predictions (for the entire area) deteriorates when each zone is examined separately (table 2 and fig. 7); nevertheless the results are still quite satisfactory (especially for the PSM set), bearing in mind all the uncertainties involved in the evaluation.

Zones	"Actual"	FSM series	PSM series	mean value of stochastic motion set	mean value of recorded motion set	mean value, all sets
ALL	11357	11875	10981	11428	1450	5986
B	926	1935	1524	1729	279	1121
C	6751	3870	5006	4438	743	2428
D1	394	490	524	507	69	258
D2	3287	5579	3928	4754	359	2178

Table 2: Cost prediction for each zone (in €1000)

As expected, the age (and hence the seismic design level) and the structural system significantly affect the vulnerability of the structures (fig. 8). The URM buildings are the most vulnerable (actual cost: 208€/m^2), while for the R/C buildings age is the most crucial parameter (buildings designed according to modern seismic codes are only slightly damaged). Once again the stochastic input motions give satisfactory estimations for all building typologies, while the recorded motions underestimate significantly the economic loss, and it is interesting to note that the latter is more the case for R/C rather than for URM.

5. CONCLUSIONS

Regarding the verification of the vulnerability assessment models, the key finding of the present study was that the main factor contributing to the discrepancies between actual and predicted cost of damage was the set of ground motions used. It was found that the prediction was overall very good when the stochastic motion sets were used for the vulnerability analysis (discrepancies did exist in some of the zones in the area studied), but results based on the motions derived on the basis of the actual records in the far field, significantly underestimated damage and loss. Hence, it was clear that there was no real point in trying to calibrate the vulnerability models on the basis of these results; this clearly hints to the importance of

accurately knowing the ground motion in areas struck by earthquakes causing damage to the building stock.

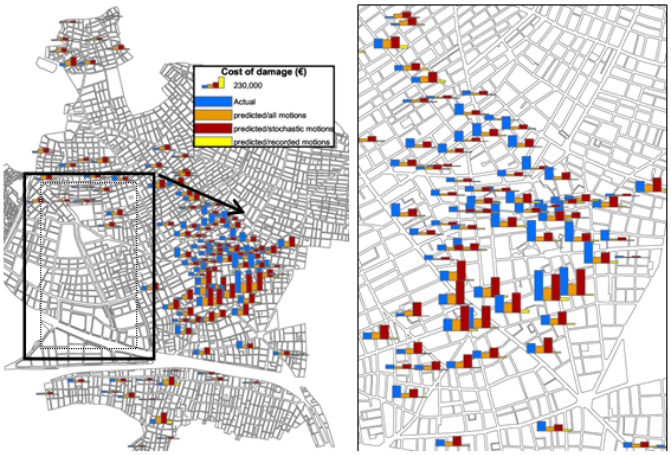

Figure 5: Actual and estimated economic loss in the study area

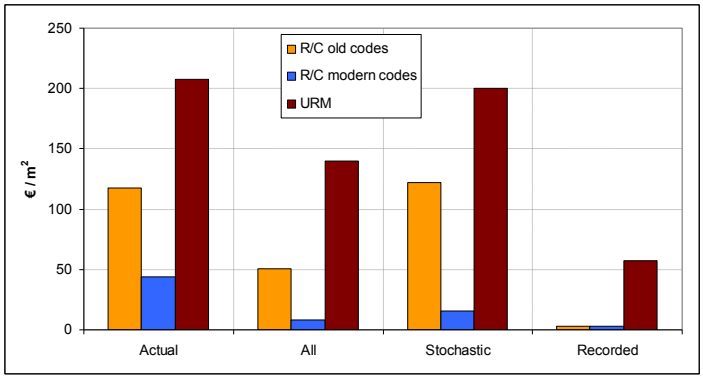

Figure 6: Cost/m^2 for different building typologies/seismic design

REFERENCES

[1] Kappos, A.J., Stylianidis, K.C., and Pitilakis, K., Development of seismic risk scenarios based on a hybrid method of vulnerability assessment. *Natural Hazards*, 17(2): 177-192, 1998.

[2] P. Dimitriou, C. Karakostas and V. Lekidis "The Athens (Greece) Earthquake of 7 September 1999: The Event, its Effects and the Response" Proceedings of 2nd Euroconference on Global Change and Catastrophe Risk Management : Earthquake Risks in Europe, IIASA, Laxenburg, Austria, July 6-9, 2000 (on web site: http://www.iiasa.ac.at/Research/RMP/july2000/).

[3] V. Lekidis and C. Karakostas "The Athens (Greece) Earthquake of September 7, 1999: Seismological data and structural response". Proceed. of the 2nd Panhellenic Conference on Earthquake Engineering and Engineering Seismology, Thessaloniki, November 2001, vol. B' pp. 143-152 (in Greek).

[4] Kappos, A.J., Panagiotopoulos, C., and Panagopoulos, G. "Derivation of fragility curves using inelastic time-history analysis and damage statistics", *ICCES'04* (Madeira, Portugal), CD ROM Proceedings, pp. 665-672, 2004.

[5] Kappos, A., Pitilakis, K., Morfidis, K. and Hatzinikolaou, N., Vulnerability and risk study of Volos (Greece) metropolitan area. *CD ROM Proceed. 12th ECEE* (London, UK), Paper 074, 2002.

AIRBORNE LIDAR AND ACCELEROMETRIC DATA PROCESSING TOWARDS SEISMIC RISK ASSESSMENT: AN URBAN-SCALE APPROACH INCLUDING SOIL-STRUCTURE INTERACTION EFFECTS

Emmanouil Rovithis[1], Konstantia Makra[1], Emmanouil Kirtas[2], Christos Karakostas[1] & Vasileios Lekidis[1].

[1] Institute of Engineering Seismology and Earthquake Engineering (EPPO-ITSAK)
Terma Dasylliou, 55535, Thessaloniki, Greece
e-mail: rovithis@itsak.gr, makra@itsak.gr, christos@itsak.gr, lekidis@itsak.gr

[2] Surveying Engineering & Geomatics Department
Technological Educational Institute of Central Macedonia, 62124 Serres, Greece
e-mail: kirtas@teiser.gr

Keywords: urban mapping, LiDAR, building stock, soil-structure interaction, seismic loading of structures.

Abstract. *We present a methodology for a large-scale assessment of soil-structure interaction (SSI) effects on the vibrational characteristics and the seismic loading of structures in a real urban fabric by combining airborne monitoring techniques, field surveys and simple calculations in the realm of structural and geotechnical dynamics. The methodology is applied in the residential area of Kalochori, located west of Thessaloniki, as part of a broader instrumented urban site, including a dense network of 7 accelerometric stations. The examined case study showed that SSI may be significant even for a low-amplitude motion and may lead to higher seismic forces compared to the fixed-base case, depending on the dynamic characteristics of the structures, the soil conditions and the shape of the response spectrum. The above may be of importance in microzonation and seismic vulnerability studies at urban-scale where a building-by-building assessment is not feasible and SSI effects are too important to be ignored. Future developments and application towards seismic risk assessment of an urban area monitored by different monitoring schemes are discussed.*

1. INTRODUCTION

Seismic risk and vulnerability of urban sites constitute an inherently spatial problem, leading to an emerging need for integrated and highly accurate monitoring schemes, continuous data acquisition and well-designed dissemination solutions. On the other hand, despite the well-known effect of soil-structure interaction (SSI) in controlling the dynamic characteristics of the structure and the effective seismic motion imposed at the foundation, especially for stiff structures founded on soft soil, earthquake damage and loss scenarios for an urban area are commonly addressed by assuming fixed-base structures, without taking into account the compliance of the foundation soil.

The purpose of this paper is twofold: (a) to present an efficient combination of data from airborne LiDAR missions and in-situ inspections, towards the identification of building stock characteristics in urban areas and (b) to propose a LiDAR-aided procedure for the assessment of soil-structure interaction effects on the vibrational characteristics and the seismic loading of

structures at urban scale. A multi-parametric work-flow is presented where data from a LiDAR-based three-dimensional city model are enriched with field data from representative building blocks, followed by code-defined calculations of structural dynamic characteristics for both fixed- and flexible-base conditions. Soil response analyses based on geophysical field tests or available geotechnical data are employed to compute the free-field seismic motion at the ground surface under specific earthquake scenarios with varying return periods. Spatially distributed ratios of the flexible- over the fixed-base period of the identified structures and the corresponding spectral accelerations are mapped in GIS environment, as an index of SSI effects over an entire urban area [1]. The proposed procedure is implemented in the test site of the recently completed research project INDES-MUSA (www.indes-musa.gr, [2-3]), referring to the residential area of Kalochori which is located west of Thessaloniki in Greece. Besides the above residential site, the broader urban area of Kalochori includes also an industrial urban unit and a tanks zone, which coexist in a relatively small area of approximately 13 km^2. This broader area has also been instrumented with a dense accelerometric network [4], as detailed in the ensuing. Thus, the selected test site may serve future applications towards seismic risk assessment by means of different monitoring schemes.

2. OUTLINE OF THE URBAN-SCALE APPROACH AND RESULTS

The procedure followed to obtain the spatial variation of the structural dynamic characteristics and the corresponding seismic loading imposed on the structures of a building stock for fixed- and flexible-base conditions under a prescribed seismic scenario is outlined in Figure 1. Each step of the proposed work-flow and representative results obtained for the residential area of Kalochori are described in the ensuing.

Stage 1: Compilation of the building stock inventory from LiDAR and field data

The starting point of the proposed workflow is a 3D city model of the urban area obtained from processed LiDAR data. The latter refers to the height H, the perimeter Π and the plan area A of each LiDAR record with known geo-coordinates (x, y) (Figure 2). The LiDAR data is verified by in-situ inspections in properly selected city blocks in order to: (i) filter out LiDAR recordings that refer to secondary manmade constructions (ii) collect data on structural materials and typologies which is not feasible by the LiDAR scenes and (iii) correlate buildings height with the number of storeys (N) by implementing a typical value for the storey height. Thus, the LiDAR data offer a promising solution for detailed building stock inventories with accurate 3D geometrical features of structures if complemented by in-situ verification of the LiDAR data at carefully selected city blocks.

Stage 2: Estimation of the fundamental period (T_{fixed}) of structures under fixed-base conditions

The geometrical and structural features of the building stock compiled in *Stage 1* are implemented to derive the fundamental natural period (T_{fixed}) of each structure under fixed-base conditions by means of simplified code-defined (NEHRP 1997; CEN 2003) relationships between structural height and fundamental period.

Stage 3: Soil response analysis under selected input motions and estimation of the flexible-base (T_{ssi}) periods of structures

In the case of the Kalochori urban area, a 1D shear wave propagation velocity (V_s) model was derived by means of the Microtremor Array Measurements method. Soil response analyses under selected seismic hazard scenarios are performed to obtain the free-field response at ground surface in the form of elastic response spectra and derive a weighted average value of the effective shear modulus (G_{avg}) being compatible to the shear strains (γ) generated during

earthquake shaking. The above results derived for the examined test site under are shown in Figure 3 for three different seismic scenarios (i.e. SC1 with peak rock acceleration (PGA_r) at 0.10g corresponding to a mean return period (T_m) of 100 years, SC2 with PGA_r=0.15g and T_m = 475 years, and SC3 with PGA_r=0.20g and T_m = 1000 years).

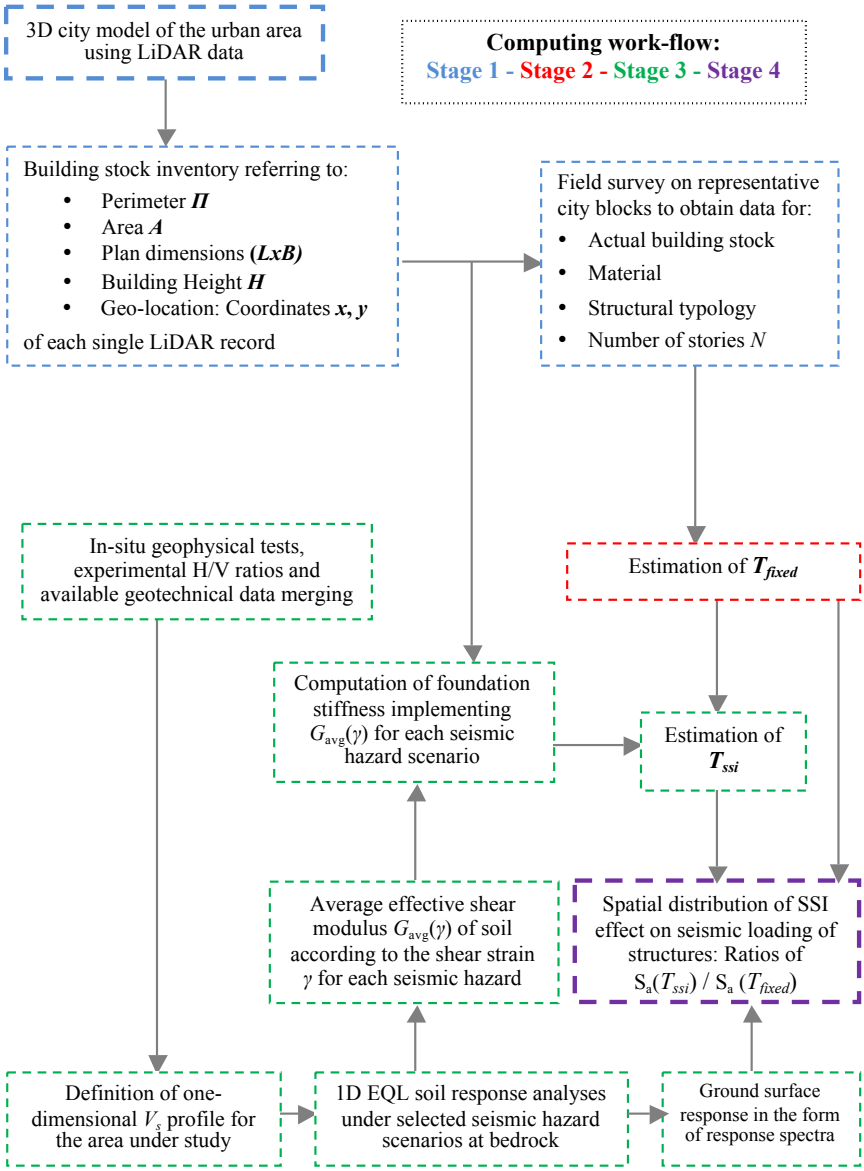

Figure 1. Proposed methodology for the assessment of soil-structure interaction (SSI) effects on the vibrational characteristics and the seismic loading of structures in an urban area.

The replacement oscillator with allowable translational and rocking base motion is introduced to compute the effective SSI period (T_{ssi}) of each single structure. For this reason, analytical expressions reported in the literature for the foundation stiffness are adopted by implementing the LiDAR-detected plan dimensions of the foundation area for each identified building and the abovementioned G_{avg} of the foundation soil. In this manner, strain-compatible values of the foundation stiffness are derived, allowing the dependence of T_{ssi} on the intensity of the input motion. Spatially distributed ratios of T_{ssi}/T_{fixed} are then employed as an index of the period elongation effect due to SSI at urban scale (Figure 4-left). The application of the proposed

procedure at the urban fabric of the Kalochori residential area showed moderate to strong SSI effects on the period elongation of structures even for a low-amplitude seismic motion.

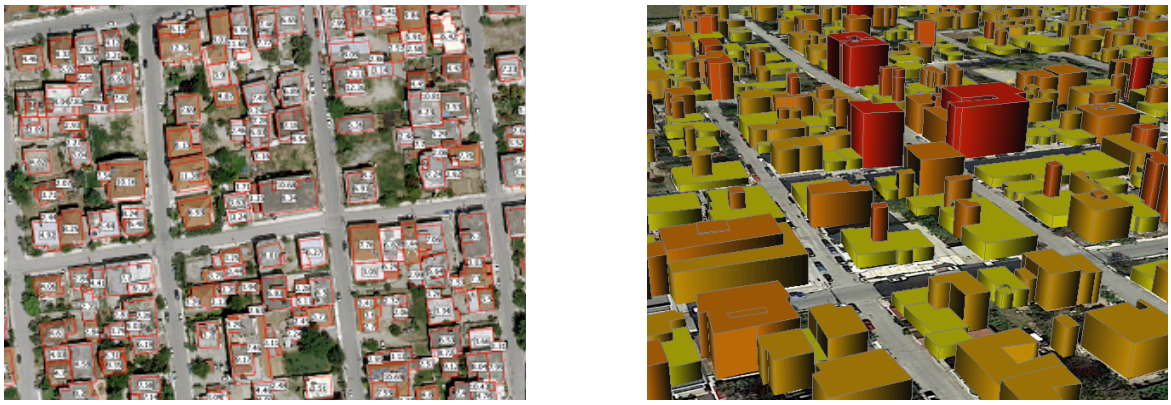

Figure 2. The descriptive height information of the polygons (left) and the corresponding buildings colored by the polygon height (right)

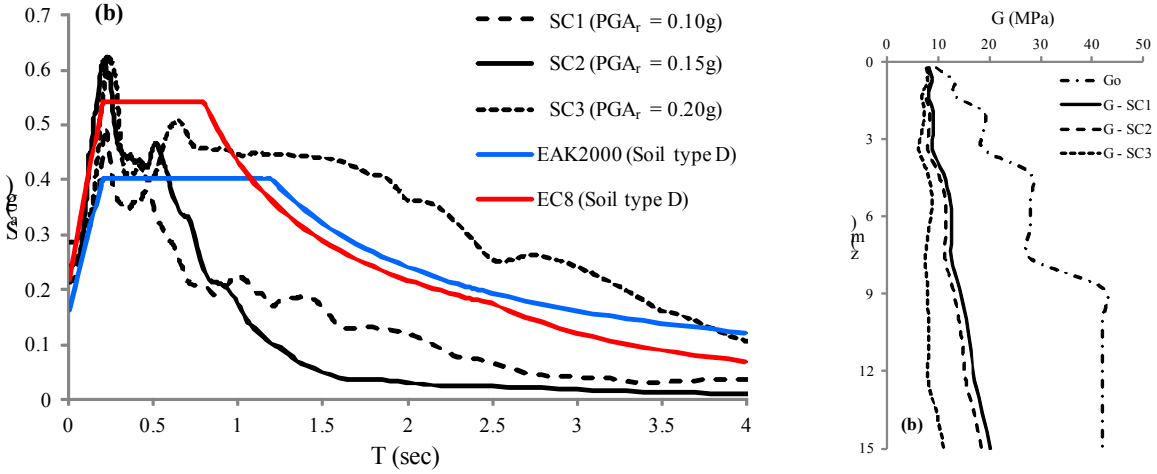

Figure 3. Mean elastic response spectra computed at the ground surface of the Kalochori residential area (left) and mean shear modulus (G) of soil computed from soil response analysis under the prescribed seismic scenarios SC1 (PGA$_r$ = 0.10g), SC2 (PGA$_r$ = 0.15g) and SC3 (PGA$_r$ = 0.20g).

Stage 4: Spatial distribution of SSI effect on the seismic loading of structures

Upon implementing the elastic response spectra at ground surface from site response analysis, the spatial distribution of the spectral accelerations $S_a(T_{fixed})$ are derived, referring to the fixed-base natural period of each single structure. Similar results are obtained for the effective period (T_{ssi}) under flexible-base conditions of each structure. Of course, proper treatment of the free-field response spectrum is required to account for additional damping mechanisms due to SSI and obtain the corresponding spectral acceleration $S_a(T_{ssi})$. Ratios of $S_a(T_{ssi})$ over $S_a(T_{fixed})$ are then computed in a spatial context as a preliminary index of SSI effects on the seismic loading of structures at urban scale. It is worth mentioning that, contrary to the usual belief of an always beneficial role of SSI on the seismic loading of structures, spectral acceleration ratios of flexible- over fixed-base response in the urban area of Kalochori revealed that SSI may lead to higher seismic forces compared to the fixed-base case (Figure 4-right). The above may be of importance in the estimation of the actual seismic loading imposed on a building stock depending on the structural, seismic and soil conditions of the urban area under consideration, especially for seismic motions that are rich in low frequencies.

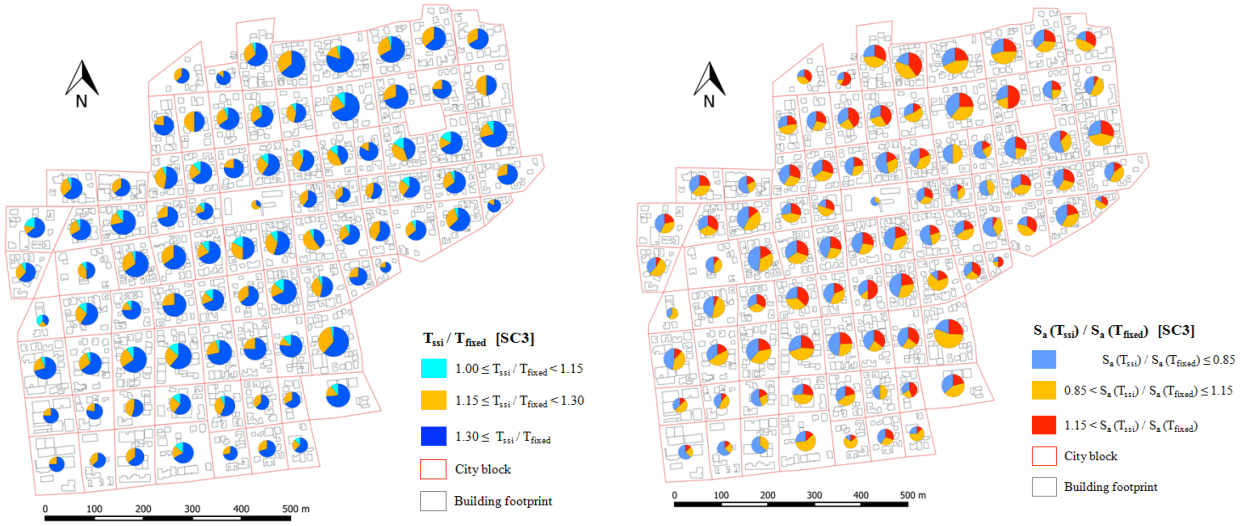

Figure 4. Spatial distribution of T_{ssi}/T_{fixed} ratios (left) and $S_a(T_{ssi})/S_a(T_{fixed})$ ratios (right) computed in the residential area of Kalochori for the seismic scenario SC3 (PGA_r = 0.20g, T_m = 1000 years).

3. THE KALOCHORI ACCELEROMETRIC NETWORK

As mentioned above, besides the airborne LiDAR scanning, the broader urban area of Kalochori has been instrumented with a dense accelerometric network since 2014 (Figure 5). More specifically, the Kalochori Acellerometric Network is composed of three ground stations installed in each distinct urban zone (i.e. residential, industrial and tanks zone), three stations on top of a selected structure within each urban zone and one free-field station away from the built environment [4]. Some main features of the KAN stations are summarized in Table 1. The stations are documented with installation and operating features, available characteristics of the housing structures and geotechnical data. A set of 78 earthquakes has been recorded by KAN between 01/16/2014 and 12/31/2016, allowing investigation of local site effects on seismic motion, variation of ground surface motion within different urban environments [5] and evaluation of dynamic response features of the instrumented structures [6]. KAN stations monographs, processed acceleration recordings and metadata of the recorded earthquakes are available online through a Web-GIS platform ((http://apollo.itsak.gr/apollo-portal/ApolloPro.aspx). The DOI linked to the complete set of KAN data is 10.6084/m9.figshare.5044804.

4. FUTURE APPLICATIONS

The proposed urban scale assessment of SSI effects may be adopted in different urban environments with structural typologies not deviating substantially from those conforming to seismic design codes. The available LiDAR data can also serve as reference for future applications on urban change detections and land-use design for urban extensions [7]. Further applications in the future may involve seismic vulnerability studies at local or urban level when a building-by-building assessment is not feasible and structural, soil and seismic conditions necessitate consideration of soil-structure interaction and microzonation studies at local or urban level to support seismic risk prevention and mitigation strategies In this regard, real earthquake recordings from the Kalochori Accelerometric Network may contribute to the above research topics under realistic seismic scenarios for the area at hand. In this regard, real earthquake recordings from the Kalochori Accelerometric Network [4], which is installed in the broader urban area of Kalochori since 2014, may contribute to the above research topics under realistic seismic scenarios for the area at hand.

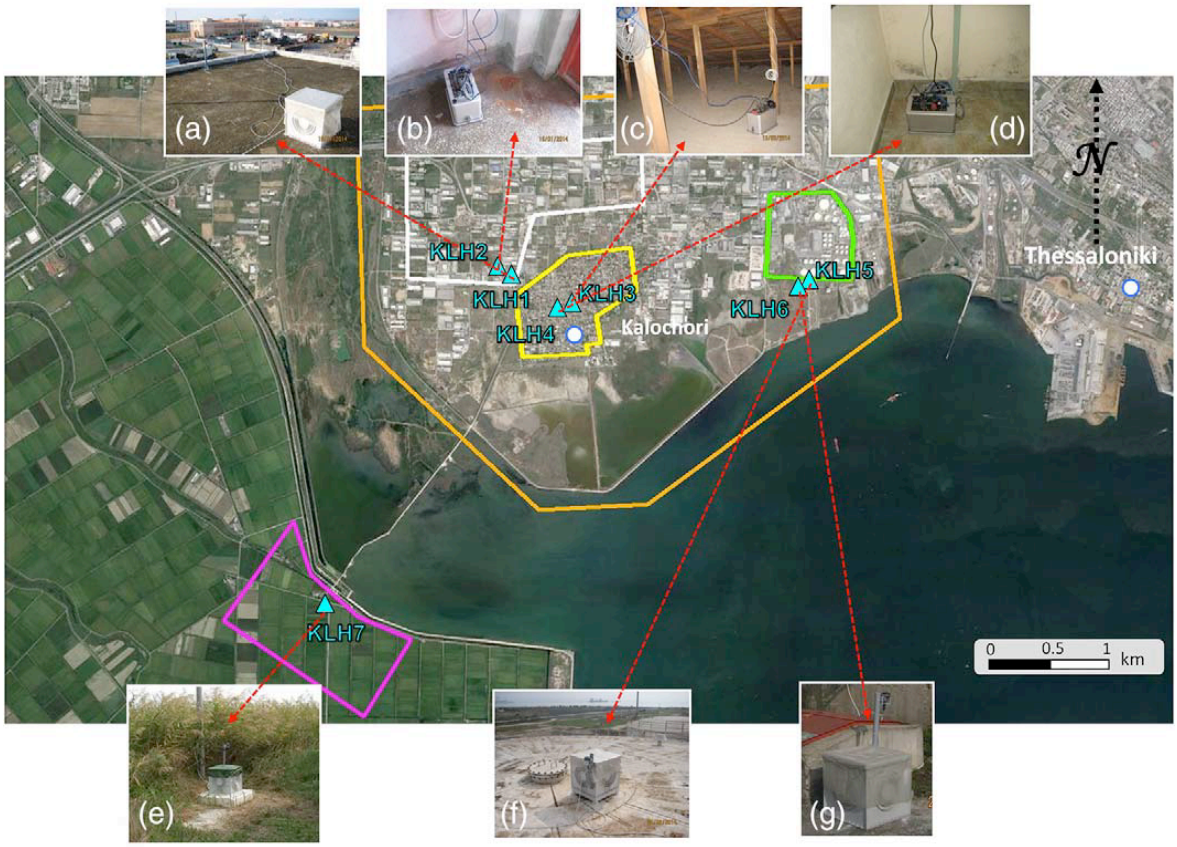

Figure 5. Definition of three urban and a free-field zone in the broader area of Kalochori (Google Earth™ image) and locations of the Kalochori Accelerometric Network stations: (a) KLH1 and (b) KLH2 stations in the industrial zone (white polygon), (c) KLH3 and (d) KLH4 stations in the residential zone (yellow polygon), (e) KLH7 station in the free-field zone (magenta polygon), (f) KLH5 and (g) KLH6 stations in the tanks zone (green polygon).

Table 1. Main features of the Kalochori Accelerometric Network

Station code	**Coordinates**	**Zone**	**Type of station****	**Distance between S and UF stations**	**Short description of installation**	**Date of Installation**	**$V_{s,30}$ (m/sec)**	**Soil type according to EC8**
KLH1*	40.6428N 22.8485E	Industrial	*S*	20m	RC building of industrial type	16/01/2014	180	D
KLH2	40.6427N 22.8484E		*UF*		Small warehouse	16/01/2014		
KLH3*	40.6419N 22.8569E	Residential	*S*	100m	2storey stone masonry structure	13/03/2014	163	D
KLH4	40.6418N 22.8586E		*UF*		Small warehouse	22/01/2014		
KLH5	40.6430N 22.8799E	Tanks	*S*	25m	Steel water tank	20/02/2014	153	D
KLH6	40.6428N 22.8798E		*UF*		Open ground	20/02/2014		
KLH7	40.6178N 22.8322E	Free-field	*FF*	-	Open ground	15/09/2014	148	D

*Collocated with GNSS base reference station
**_S_: "Structural" station, _UF_: "Urban reference" station, _FF_: "Free-field" station

REFERENCES

[1] Rovithis, Emm., Kirtas, Emm., Bliziotis, D., Maltezos, E., Pitilakis, D., Makra, K., Savvaidis, A., Karakostas Ch. and Lekidis, V., 2017. A LiDAR-aided urban-scale assessment of soil-structure interaction effects: The case of Kalochori residential area (N. Greece), *Bulletin of Earthquake Engineering*, 15(11), 4821 - 4850.

[2] Rovithis Emm, Charalampopoulou B, Ganas A, Savvaidis A, Makra K, Konstantinidou K, Kirtas Emm, Karakostas Ch, Lekidis V, Pitilakis D, Loupasakis C, Tsimi Ch and Manesis Ch., 2014. INDES-MUSA Project - Integrated monitoring of subsiding coastal areas prone to large earthquakes: the case of Kalochori in Greece. In Proceedings of the 2nd European Conference on Earthquake Engineering and Seismology, Istanbul, 24-29 August, paper No. 2739.

[3] Charalampopoulou B, Manesis Ch, Tsivikis K, Savvaidis A, Makra K, Ganas A, Rovithis Emm. (2014) 3D city model using LiDAR & digital color imagery in Kalochori region. In Proceedings of the 1st International Geomatics Application Conference (GEOMAPPLICA), Skiathos, September 08-10, pp 36-43.

[4] Rovithis, E., K. Makra, E. Kirtas, Ch. Manesis, D. Bliziotis & K. Konstantinidou, 2018. Field monitoring of strong ground motion in urban areas: the Kalochori Accelerometric Network (KAN), database and Web-GIS portal. *Earthquake Spectra*, Volume 34, No. 2, pages 471–501

[5] Makra, K., A. Savvaidis, E. Rovithis, 2018. Site Response Characteristics Of A Deep Sedimentary Basin. The Case Of Kalochori, N. Greece. Proc 16th European Conference on Earthquake Engineering (16ECEE), Thessaloniki, Greece, June 18-21, 2018, Paper No 1322.

[6] Kirtas, E., E. Rovithis, K. Makra, I. Papaevangelou, 2018. Dynamic response characteristics of an instrumented steel water tank in Kalochori, N. Greece. Proc. 16th European Conference on Earthquake Engineering (16ECEE), Thessaloniki, Greece, June 18-21, 2018, Paper No 1167.

[7] Maltezos E, Ioannidis C (2015) Automatic detection of building points from LIDAR and dense image matching point clouds. In: ISPRS Annals of the Photogrammetry, Remote Sensing and Spatial Information Sciences, La Grande Motte, France, Vol. II-3/W5, pp 33-40.

REAL TIME ESTIMATION OF R/C BUILDINGS' SEISMIC DAMAGE USING ARTIFICIAL NEURAL NETWORKS AND PATTERN RECOGNITION APPROACH

Konstantinos E. Morfidis[1] and Konstantinos G. Kostinakis[2]

[1]Assistant Researcher, Earthquake Planning and Protection Organization (EPPO-ITSAK)
Terma Dasylliou, 55535, Thessaloniki, Greece
e-mail: konmorf@gmail.com

[2]Assistant Professor, Department of Civil Engineering, Aristotle University of Thessaloniki
Aristotle University campus, 54124, Thessaloniki, Greece
e-mail: kkostina@civil.auth.gr

Keywords: Seismic damage prediction, Artificial Neural Networks, Pattern Recognition, R/C buildings, Seismic vulnerability assessment.

Abstract. *The investigation of the ability of Artificial Neural Networks (ANN) to reliably predict the r/c buildings' seismic damage state is subject of this study. In this investigation, the problem was formulated and solved as a pattern recognition problem using Multilayer Feedforward Perceptron networks. For the creation of the ANNs' training data set, 30 r/c buildings with different structural characteristics, which were subjected to 65 actual ground motions, were selected. These buildings were subjected to Nonlinear Time History Analyses. These analyses led to the calculation of the buildings' damage indices expressed in terms of the Maximum Interstorey Drift Ratio. In order to investigate the generalization ability of the trained networks, testing scenarios were considered. In these scenarios, the ANNs' seismic damage predictions were evaluated for buildings subjected to earthquakes, neither of which are included to the training data set. The most significant conclusion of the investigation is that the ANNs can reliably approach the seismic damage state of r/c buildings in real time after an earthquake.*

1. INTRODUCTION

The assessment of seismic damage level in case of r/c structures is at the core of the civil engineering research globally, since a large number of strong earthquakes that happened in the past have caused extensive structural damages and human losses. As a consequence, numerous researchers have published studies dealing with the methods that can be used in order to estimate the seismic vulnerability of existing buildings. The research studies can be classified into two general categories: a) studies dealing with the development of methods that can estimate the seismic performance of individual buildings and b) studies dealing with the development of methods that can rapidly assess the seismic vulnerability of groups of buildings with common structural characteristics. The research studies belonging to the first category resulted in analytical methodologies of assessment which are based on linear and nonlinear methods that have been adopted by modern seismic codes. Respectively, the researches belonging to the second category led to the development of methodologies that can accomplish the approximate assessment of the seismic vulnerability of buildings' groups with common structural characteristics (e.g. [1]). These methods can be used in order to estimate the buildings' seismic

vulnerability in a very short time comparing with the methods of the first category, with the price of losing accuracy. However, the merit of these approximate methods is important, since the use of them can lead to rapid and reliable decisions about the need for further investigation of buildings' seismic performance. In the context of the direct (though approximate) assessment of the seismic vulnerability of buildings' groups with common structural characteristics, in the past 25 years many research studies have been conducted aiming to utilize the capacities of artificial intelligence, such as the Artificial Neural Networks (ANNs). Although the ANNs have been developed on an idea that dates back to the 1940s, the first thorough investigation dealing with the use of them for the direct (in real time) estimation of the level of structural seismic damage was published in 1994 [2]. Since then, this approach has been the subject of numerous research studies (e.g. [3]), which led to highly important results.

The aim of the present study is to further investigate the ability of ANNs to reliably predict the seismic damage level of r/c buildings. More specifically, the problem is formed and solved as a pattern recognition problem which can be solved reliably using ANNs. For the needs of the investigation, the training of the ANNs was achieved with the aid of a data set created using results from Nonlinear Time History Analyses (NTHA) of 30 r/c buildings with different heights, structural systems and structural eccentricities, subjected to 65 actual ground motions. The Maximum Interstorey Drift Ratio (MIDR), (e.g. [4]) was used as the damage index. As a consequence, 1950 values of MIDR resulted from the analyses conducted. These values were categorized into three general damage levels, into which the investigated buildings were classified with the aid of the ANNs. Moreover, the influence of the number of hidden layers, the number of neurons in the hidden layers, as well as the activation functions of neurons was also examined. The prediction ability of the trained ANNs was checked through the prediction they made in the case of future earthquakes and it was demonstrated that they can extract especially reliable (though approximate) results.

2. THE ARTIFICIAL NEURAL NETWORKS (ANN)

It is well-known that the ANNs are complex computational structures which are able to solve problems using the general rules of the human brain functions (e.g. memory, training etc.). Thus, the use of ANNs makes it feasible to approximate the solution of problems such as pattern recognition, classification and function approximation, with the aid of computers utilizing algorithms based on a different philosophy than the conventional ones.

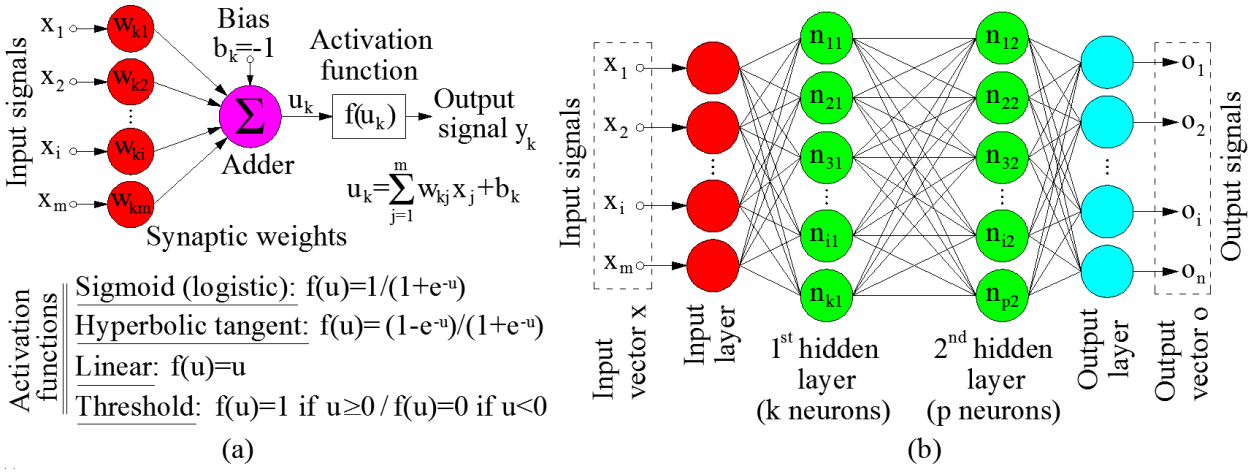

Figure 1: The model of the artificial neuron (a), and the typical form of a MFP (b).

Various types of ANNs have been proposed (e.g. [5]). However, in the present study, Multilayer Feedforward Perceptron (MFP) networks were utilized. Fig. 1(a) presents the model of the function of a typical artificial neuron which receives the input signals through its synapses (connecting links) and transforms them to an output signal through the use of an adder and the use of an activation function. More details are available in specialized references (e.g. [5]). The function of ANNs is based on the combined action of interconnected artificial neurons (Fig. 1(b)). Due to the fact that the function of ANNs is based on the general rules of the human brain functions such as the memory and the training, the necessary procedure for the successful solution of problems by them is the training. The training of an ANN consists of the detection of values of the synaptic weights of neurons which produce the minimum output error. This detection is achieved through the use of training algorithms (e.g. [5]). A trained ANN includes the optimum vector of synaptic weights which incorporate the "knowledge" acquired from the used training data set. Thus, a trained ANN is capable of extracting predictions about the solution of problems with input data that are not included in the training data set (generalization ability). The generalization ability can be constantly improved through the re-training of ANNs using wider training data sets.

3. MODELING OF THE PATTERN RECOGNITION PROBLEM USING ANNs

Figure 2 briefly presents the steps for the formulation of the pattern recognition problem in terms compatible to ANNs' function, and the choices for the basic parameters (e.g. [6]).

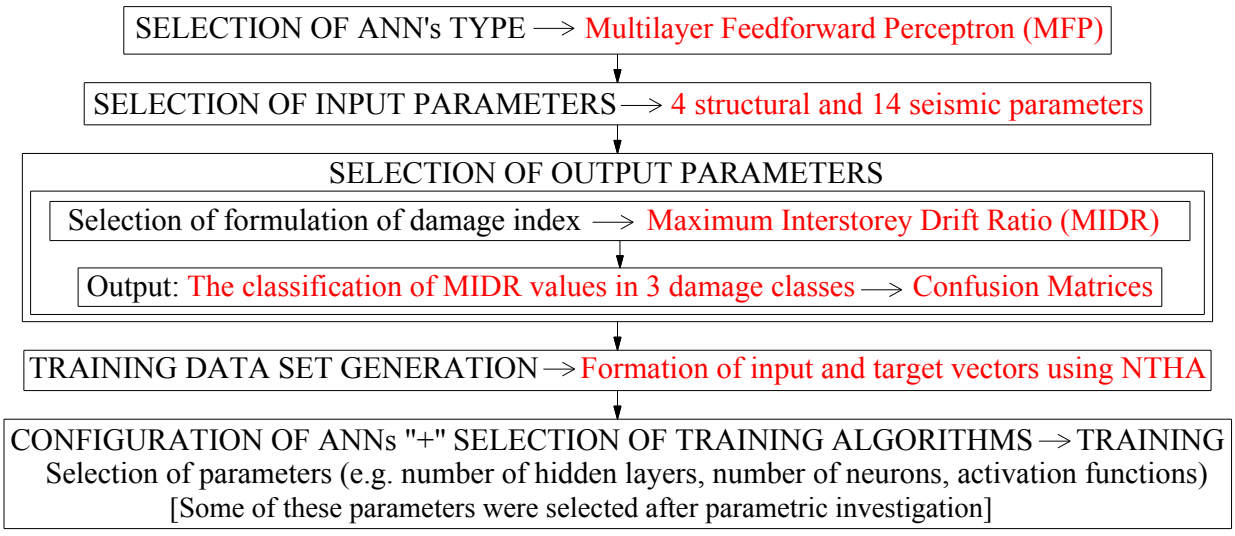

Figure 2: Procedure for the formulation of the problem in terms compatible to the structure of ANNs.

As regards the 4 structural input parameters the total height of buildings H_{tot}, the structural eccentricity e_o (the distance between the mass center and the stiffness center of storeys), and the ratio of the base shear that is received by r/c walls (if they exist) along two perpendicular directions: n_{vx} and n_{vy} were selected. The corresponding 14 input seismic parameters are presented in Table 1 [7]. Thus, in the present study, the input vectors **x** (18x1) have the form which is given by the Eq. (1):

$$\mathbf{x} = \left[\mathbf{x}_{seism} \mid \mathbf{x}_{struct}\right]^T$$
$$\mathbf{x}_{seism} = \left[PGA \mid PGV \mid PGD \mid I_a \mid SED \mid CAV \mid ASI \mid HI \mid EPA \mid PGV/PGA \mid PP \mid TUD \mid TBD \mid TSD\right]^T \quad (1)$$
$$\mathbf{x}_{struct} = \left[H_{tot} \mid e_0 \mid n_{vx} \mid n_{vy}\right]^T$$

1	Peak Ground Acceleration: **PGA**	8	Housner Intensity: **HI**
2	Peak Ground Velocity: **PGV**	9	Arias Intensity: $\mathbf{I_a}$
3	Peak Ground Displacement: **PGD**	10	V_{max}/A_{max} (**PGV/ PGA**)
4	Effective Peak Acceleration: **EPA**	11	Predominant Period: **PP**
5	Specific Energy Density: **SED**	12	Uniform Duration: **UD**
6	Acceleration Spectrum Intensity: **ASI**	13	Bracketed Duration: **BD**
7	Cumulative Absolute Velocity: **CAV**	14	Significant Duration: **SD**

Table 1: The selected seismic (ground motion) parameters.

The formulation of the PR problem requires the definition of classes into which a r/c building can be classified on the basis of its seismic damage level. To this end, in the present study three damage states were defined using specific limit values of MIDR. These damage states are presented in the Table 2. The number of the damage classes (three) was selected in order to be compatible to the commonly used rationale of seismic damage classification in slight (green), moderate (yellow) and heavy (red) damage states which are utilized in the case of r/c buildings' rapid seismic assessment after strong events. The choice of the limit MIDR values of the three damage classes was based on the fusion of the two lower as well as the two higher damage classes of a well-known MIDR-based damage classification of r/c buildings.

MIDR (%)	0.0-0.50	0.50-1.00	>1.00
Degree of damage	Slight **(S)** (No damages or slight damages)	Moderate **(M)** (Significant but repairable damages)	Heavy **(H)** (non-repairable damages)

Table 2: Relation between MIDR and damage state.

Thus, the output vectors as well as the target vectors must have dimension (3x1). In other words, the number of outputs of ANNs in the present case is three. The general form of the output vectors is given (using an example) in Figure 3.

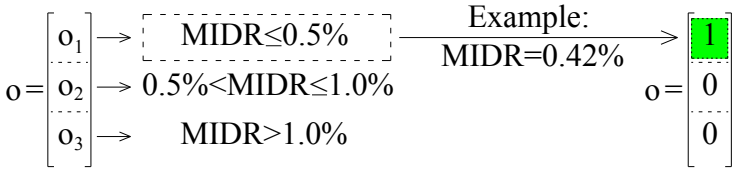

Figure 3: General form of output vectors **o**

As it emerges from Figure 3, each element of a vector **o** represents one of the three classes/damage states of Table 2 and attains value equal to 1 if the corresponding MIDR belongs to the interval of values which define the specific damage state. Otherwise, it attains value equal to 0.

Since the training data set is created (using the results of the NTHA), the last step of the problem's formulation according to Figure 2 is the selection of the utilized ANNs' configuration

and their training procedure. As regards the configuration of networks in the present study the optimum combination of the following parameters was investigated: (a) the number of hidden layers, (b) the number of neurons in each hidden layer and (c) the activation functions of neurons. The choice of the other parameters which influence the MFP networks' function are summarized in Table 3.

Number of hidden layers	1 or 2
Number of neurons in hidden layer(s)	10÷60
Activation functions in hidden layer(s) and output layer	logsig or tansig
Performance parameters	Confusion Matrix (CM), (see e.g. [8])
Partition ratios of randomly composed data sub-sets	Training/testing/validation: 70%/15%/15%
Normalization functions of input values	in the range [-1,1]
Training algorithm	Resilient Backpropagation (RP)

Table 3: Configuration parameters of MFP networks

4. PARAMETRIC INVESTIGATION OF THE OPTIMUM ANNS' CONFIGURATIONS

Eight different types of networks with one hidden layer and sixteen different types of networks with two hidden layers were formed (Table 3). More specifically a total of 204 MFP networks with one hidden layer and 20808 MFP networks with two hidden layers were configured. In Figure 4 the CMs of the classifications made by the best trained ANNs with one and two hidden layers for the 293(=1950x0.15) samples of the testing sub-set are illustrated. In the blue colored cells of these matrices the "Overall Accuracy" (OA) index values which represent the total percentage of the correct networks' classifications are also presented.

(a)

True class \ *ANNs' classification*	S	M	H	Recall%
S	**82**	*3*	0	96.5%
M	*3*	**46**	9	79.3%
H	0	5	**145**	96.7%
Precision%	96.5%	85.2%	94.2%	***93.2%***

(b)

True class \ *ANNs' classification*	S	M	H	Recall%
S	**92**	*6*	0	93.9%
M	*2*	**48**	*1*	94.1%
H	0	*8*	**136**	94.4%
Precision%	97.9%	77.4%	99.3%	***94.2%***

Figure 4: CMs of the MFP networks with (a) one hidden layer and (b) with two hidden layers

The conclusions which arise from Figure 4 are the following:

- The MFP networks export generally reliable classifications for the r/c buildings' damage state. More specifically, the optimum values of the OA parameter are significantly high: OA=93.2% (i.e 93.2% of the tested samples were classified in the correct damage category) for the network with one hidden layer and OA=94.2% for the network with two hidden layers.
- All classifications which are presented in Figure 4 are in the correct classes (bold characters) or in classes adjacent to them (italics). Thus, no classifications in categories which are not adjacent to the correct category are exported. This means that the general conclusions which are extracted from the study of the CMs are reliable and give instantly a correct approach of the real seismic damage's level.
- The use of two hidden layers increases the effectiveness of networks but not significantly.

In Table 4 the configuration parameters of the MFP network which export the optimum results are summarized. This network is utilized for the assessment of ANNs' generalization ability (Section 5).

Number of hidden layers	2
Number of neurons in hidden layer(s)	1st: 44 / 2nd: 50
Activation functions in hidden layer(s) and output layer	1st: tansig / 2nd: logsig / output: tansig

Table 4: Configuration parameters of the optimum MFP network

5. TESTING OF GENERALIZATION ABILITY OF THE OPTIMUM CONFIGURED ANN

In the current section the prediction ability of network presented in Table 4 is investigated through the predictions of the seismic damage level for a set of samples which are not included to the training data-set. To this end, three new testing r/c buildings were selected. Moreover, 15 new testing seismic excitations were chosen. Then, following the same procedure as the one which was conducted for the generation of the training data set, a new testing data set was generated. This data set consists of 45(=3x15) samples. As in case of the training data set, the target vectors which was formed are compatible to the formulation of the PR problem (Figure 3). The input vectors of the new testing data set were introduced to the most efficient network of Table 4 in order to predict the seismic damage state for the 45 testing samples. Figure 5 illustrates these predictions.

		ANNs' classification			
		S	**M**	**H**	**Recall%**
True class	**S**	**19**	*2*	0	90.5%
	M	*2*	**4**	*2*	50.0%
	H	0	0	**16**	100.0%
	Precision%	90.5%	66.7%	88.9%	***86.7%***

Figure 5: CM of the new testing samples' damage state classifications made by the most efficient network

The main conclusion which is extracted from Figure 5 is the high quality of classifications of the examined network (OA=86.7%). More specifically, besides the high value of the OA index the percentages of correct classifications to individual classes are also acceptable. Furthermore, it must be stressed that none of the examined samples is classified to classes not adjacent to the correct ones.

6. CONCLUSIONS

The aim of the present study is the investigation of the Artificial Neural Networks' (ANN) ability for rapid and reliable estimation of seismic damage state of numerous r/c buildings. For this purpose, Multilayer Feedforward Perceptron (MFP) networks were used. The examined problem was formulated and solved as a pattern recognition problem. The influence of the networks' configuration parameters on the reliability of their predictions was also examined. This investigation led to the best configured network on the basis of the optimization of their predictions. The generalization ability of this network was examined using seismic scenarios.

The main conclusion of the above described investigation procedure is that the MFP networks export generally significantly reliable predictions for the r/c buildings' damage state when the problem is formulated as PR problem. Thus, the methods which are based on Artificial Intelligence (as the ANNs) are very promising methods for rapid and reliable estimation of numerous r/c buildings' seismic damage. Consequently, used in the first critical moments after a

strong seismic event the ANNs are capable to extract in near-real time an estimation for the damage lever of existing r/c building stock in urban areas. To this end, the algorithms that simulate the function of properly trained ANNs can be integrated to software systems which are connected with accelerometric networks. Thus, receiving the recorded accelerogram immediately after a strong seismic event the system which contains trained ANNs can automatically produce maps of the spatial variability of buildings' seismic damage level in the stricken area. These maps can be extremely valuable to the authorities (i.e. civil protection agencies) in order to make decisions about the priorities which must be given as regards the management of the available human and equipment resources.

REFERENCES

[8] A.J. Kappos, G. Panagopoulos, Ch. Panagiotopoulos, Gr. Penelis, A Hybrid Method for the vulnerability assessment of R/C and URM buildings. *Bulletin of Earthquake Engineering*, **4(4)**, 391-413, 2006.

[9] J.E. Stephens, R.D. VanLuchene, Integrated Assessment of Seismic Damage in Structures. *Microcomput Civ Eng*, **9**, 119-128, 1994.

[10] S.J.S. Jegadesh, S. Jayalekshmi, A review on artificial neural network concepts in structural engineering applications. *Int J Appl Civ Env Eng*, **1(4)**, 6–11, 2015.

[11] F. Naeim, *The seismic design handbook*, *2nd edition. Kluwer Academic*, Boston, 2011.

[12] S. Haykin, *Neural Networks and Learning Machines*, *3rd Edition, Prentice Hall*, 2009.

[13] K. Morfidis, K. Kostinakis, Approaches to the rapid seismic damage prediction of r/c buildings using artificial neural networks, *Engineering Structures*, **165**, 120-141, 2018.

[14] S.L. Kramer, *Geotechnical Earthquake Engineering, Prentice-Hall*, 1996.

[15] S. Theodoridis, K. Koutroumbas, *Pattern Recognition, 4th edition, Elsevier*, 2008.

SEISMOBUG©: A LOW COST ACCELEROGRAPH FOR AN ENHANCED SEISMIC RESILIENCE OF URBAN AREAS

Christos Z. Karakostas[1] **and Vassilios K. Papanikolaou**[2]

[1] Institute of Engineering Seismology & Earthquake Engineering (ITSAK-EPPO)
christos@itsak.gr

[2] Civil Engineering Dpt., Aristotle University of Thessaloniki
billy@civil.auth.gr

Keywords: Low-cost accelerograph; MEMS; Strong motion dense network; PGA distribution; Seismic hazard; Resiliency of urban areas.

Abstract. *This paper proposes the dense instrumentation of areas of interest (typically urban ones) with low-cost accelerographs based on MEMS sensor technology that were designed and manufactured in-house, together with custom software for wireless device configuration, data retrieval and processing. In this way the actual variation of earthquake motion in the area is obtained, without recourse to less accurate and more expensive theoretical approaches (such as microzonation studies). The implementation of such a dense network in the Greek city of Lefkas and the results for some recorded events are presented.*

1 INTRODUCTION

For a site-specific seismic hazard assessment in an urban area, and hence for a reliable estimation of the seismic risk on a local level the traditional seismic zonation adopted in Seismic Codes, may be inadequate. This need led to the development of microzonation studies, which however typically require a large number of data on the soil profile and geology, in order to produce hazard maps whose level of reliability inevitably heavily depends on the quantity and quality of the original field measurements. As an alternative to these implicit theoretical approaches, a complementary explicit approach herein proposed is the use of low-cost devices that allow the deployment of dense networks which will record the actual spatial distribution of the earthquake excitations. Towards this aim, the research team designed and produced autonomous accelerographs based on the micro-electro-mechanical sensor (MEMS) technology. The developed sensors cost an order of magnitude less than high-accuracy commercial accelerographs, they are however capable of accurately capturing at least light intensity earthquake events, which are of interest for the estimation of seismic risk of the structures in a study area. An extra advantage of the low cost of the devices is the elimination of need for specialized repair facilities and personnel, since it is more economically feasible to just replace a defective unit with a new one. After proper quality and accuracy tests performed at the ITSAK-EPPO laboratory, an ultra-dense urban network of 21 devices was installed in 2013 in the broader urban area of Lefkas city, Greece. The results of some recorded seismic events by the network are herein presented.

2 DEVELOPMENT OF THE LOW-COST MEMS ACCELEROGRAPH

The in-house designed and manufactured prototype device *SeismoBug*© (www.seismobug.com, Figure 1a) was developed between 2012 and 2013 at the Institute of Engineering Seismology & Earthquake Engineering (EPPO-ITSAK), within a post-doctorate research grant by the Greek

Secretariat of Research and Technology (GSRT). It is an autonomous triaxial accelerograph based on the MEMS sensor technology. The device can operate totally unattended on external power supply with battery backup, featuring automatic event triggering and non-volatile local storage. For the testing, the devices were mounted collinearly (successively along each of their axes) to a high accuracy and high cost commercial accelerometer (*Güralp*© Systems CMG-5TDE), on a uniaxial seismic table. The results were overall very satisfactory, especially for at least light intensity levels of excitation (e.g. Figure 1b, where the two devices yield practically identical results). In general the device was shown to be able to adequately record excitations higher than approximately 2 mg, satisfactory for civil engineering purposes. More details on the hardware features of the device and the validation procedure can be found in [1].

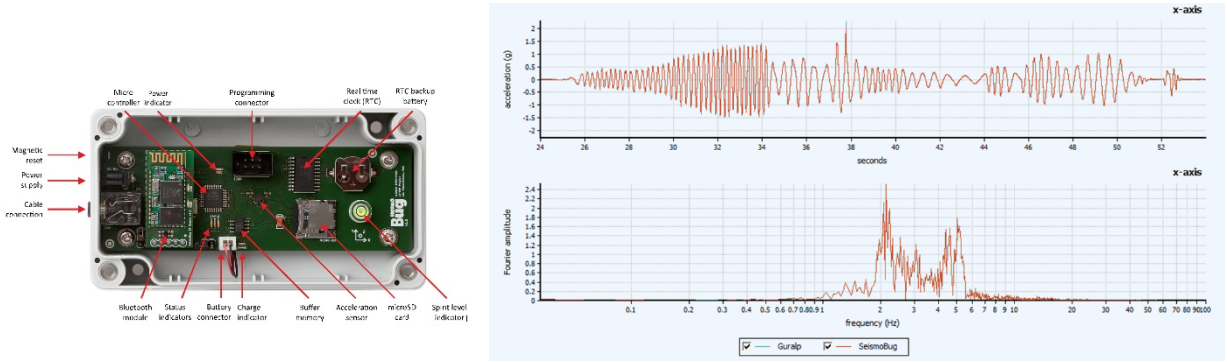

(a) (b)

Figure 1. The developed MEMS accelerograph (a) main components
(b) Arbitrary excitation comparison (SeismoBug vs Güralp) in time and frequency domain (from [3])

A software suite comprising of three different custom-made programs was developed for data retrieval, processing and management. The software *SeismoBug*© *Monitor* allows device configuration and data retrieval via a Bluetooth connection to a host computer (Figure 2a). For fast viewing and postprocessing of the data volume collected from all installed devices, the *SeismoBug*© *Browser* software was developed (Figure 2b). Finally, for the compilation of ground motion variability maps after a successful recording of an earthquake, the collected records from the grid of installed devices are corrected/filtered and forwarded to the GIS-type *SeismoBug*© *Manager* software (Figure 2c). More details on the developed software capabilities can be found in [2, 3].

3 IMPLEMENTATION AT THE ULTRA-DENSE NETWORK IN LEFKAS

A total number of 21 *Seismobug*© sensors were installed in the high-seismicity wider urban area of the city of Lefkas (Lefkada), in the northeastern part of the namesake Ionian Sea island. The main criteria used for the selection of installation locations were (a) the regularity of the network grid in the broader city area, which should become denser towards the more highly populated city center, (b) the implementation of free-field conditions at the selected locations, if possible and (c) the availability of uninterrupted power supply. These conditions were mostly met by installing most of the devices inside feeder pillars (steel enclosures) that provide electric power to street lights or in waterproof electrical junction boxes on the ground (Figure 3c). Seven

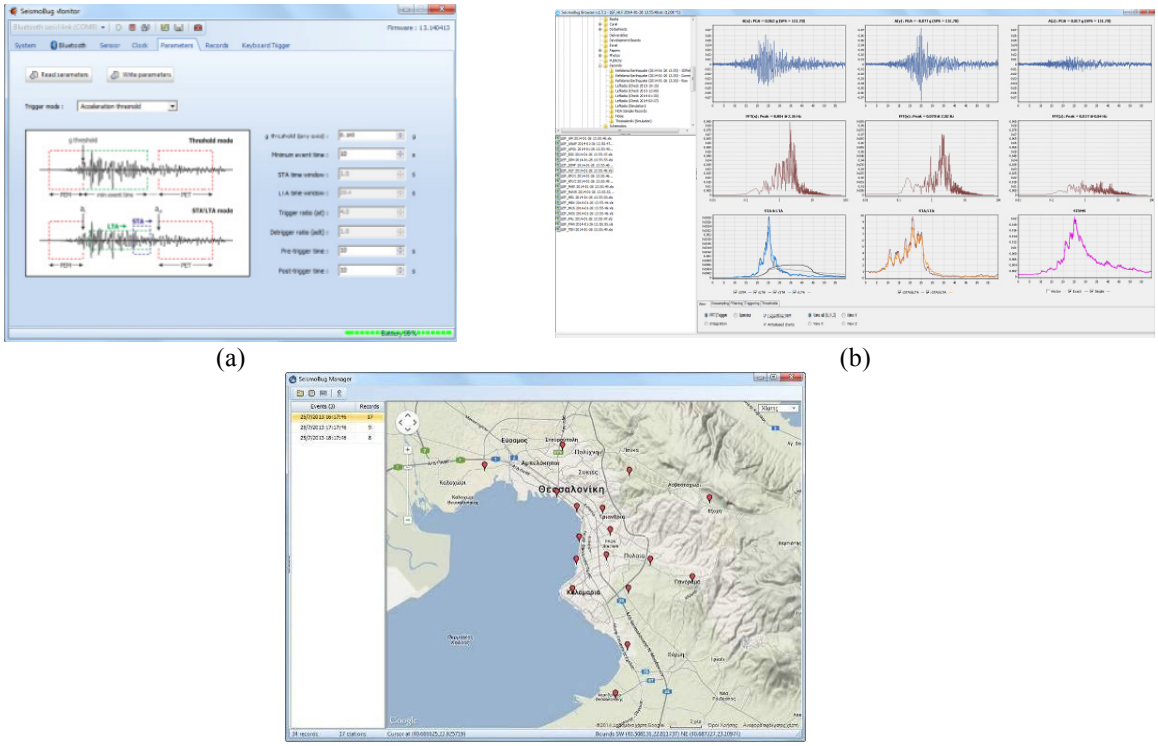

Figure 2. The custom-made software suite (a) *SeismoBug*© *Monitor* (b) *SeismoBug*© *Browser* and *(c) SeismoBug*© *Manager* (from [3])

devices were installed inside buildings, mainly due to unavailability of suitable free-field conditions (five of them on ground level, two at the existing basement level). One unit (station LEF_DIM) was purposefully placed next to a high-accuracy (by *Guralp*©) one (station LEF2, belonging to the National Strong Motion Network operated by EPPO-ITSAK) at the basement of the Prefecture building of Lefkas (Figure 3d). At a distance of about 70 m from the Prefecture building, a similar pair of *SeismoBug*© (station LEF_DIMF) and *Guralp*© (station LEF3) accelerographs were installed in free-field conditions in order to assess the effect of the Prefecture building's response to the recordings at its base. As can be seen from Figure 3b, the installed network forms an ultra-dense grid with the distance between adjacent sensors ranging from a maximum of approximately 1200 m to a minimum of less than 100 m. More detailed information on the deployment of the network can be found in [4].

4 SELECTED RESULTS FROM THE ULTRA-DENSE NETWORK IN LEFKAS

Since its installation in August 2013, the Lefkas network has been operating with minimal fails, mainly due to external factors (e.g. power outage), and has been since approximately 50 earthquakes in the broader area. More details on the collected data and on the obtained results for three selected major earthquake events (26/1/2014 M6.1, 17/11/2015 M6.5 and 18/11/2015 M5.0) can be found in [3]. Comparisons of records of the *SeismoBug*© MEMS accelerographs with those of adjacent high-accuracy *Guralp*© accelerographs are very satisfactory both in time and frequency domain (Figure 4, [3]). It was also observed that significant differences exist (both in time-history amplitudes and frequency content) between recordings at the station (LEF_DIM) at the basement of the Prefecture Building and those of the nearby (at approx. 70m) free-field one (LEF_DIMF), an observation that triggered further specific investigations ([5]).

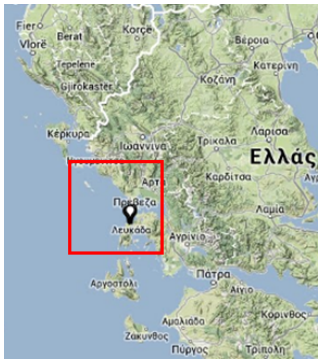

(a)

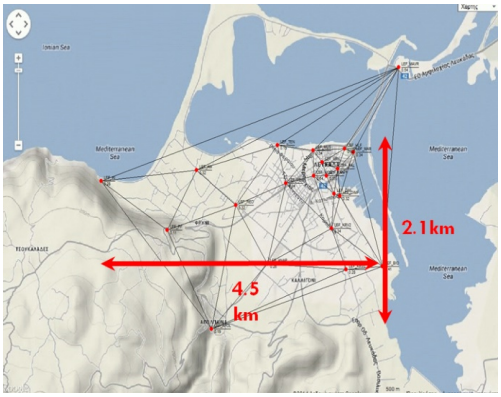

(b)

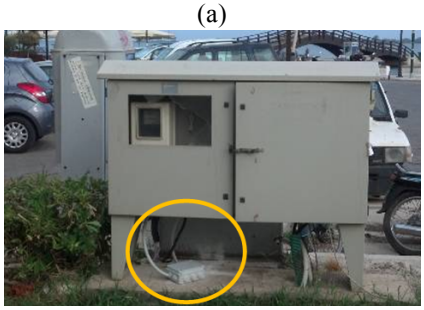

(c)

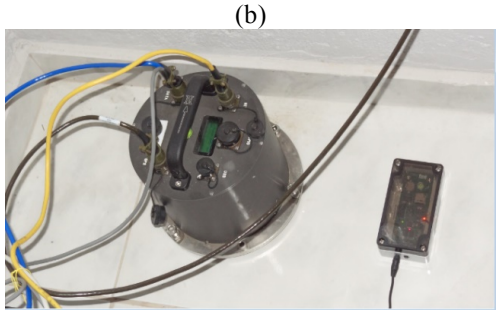

(d)

Figure 3. The ultra-dense network at the urban area of Lefkas (a) General location (b) Network grid (c) installation at free-field conditions (d) adjacent *SeismoBug*© (LEF_DIM) and *Guralp*© (LEF2) accelerographs (from [3])

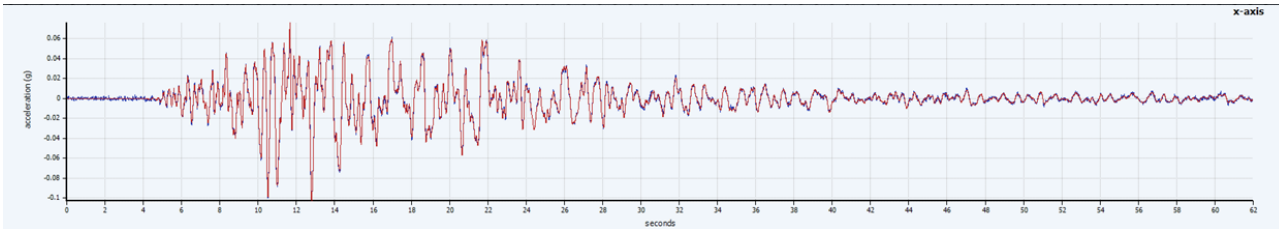

(a)

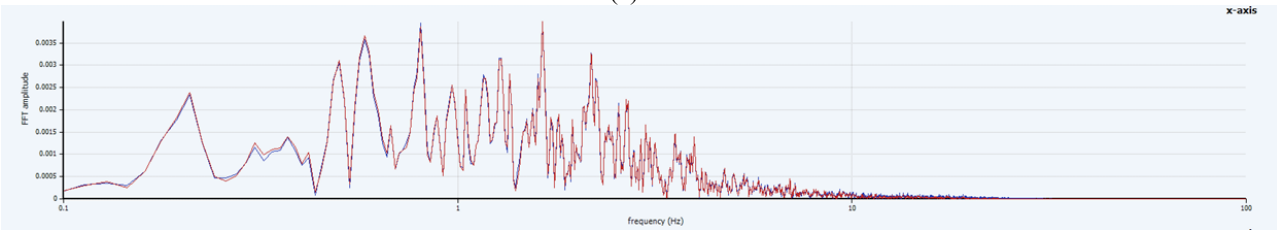

(b)

Figure 4. Comparison of a recorded event by the *SeismoBug*© (station LEF_DIM) (blue) and the adjacent *Guralp*© (station LEF2) sensor (red) in (a) the time and (b) the frequency domain

The collected data can be, among others, properly postprocessed with the custom-developed software to produce PGA distribution maps for each earthquake event recorded. One indicative map is presented in Figure 5 (Event 26/1/2014 M6.1, E-W direction). More detailed results for this and other events can be found in [2, 3].

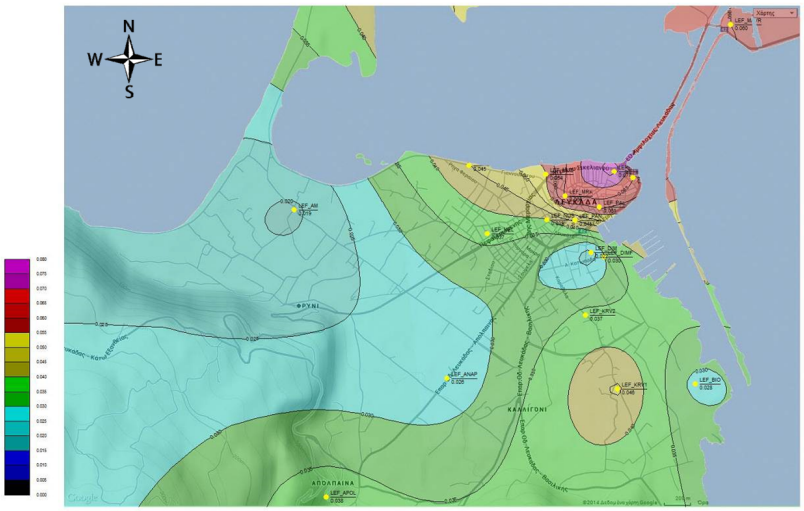

Figure 5. Event 26/1/2014 M6.1: PGA contours, E-W direction (from [2]).

5 CONCLUSIONS

The successful operation of the Lefkas ultra dense network has led to several important results and conclusions. Comparisons with high-accuracy instruments of the Hellenic National Strong Motion Network clearly demonstrate the ability of the developed device to record to a very satisfactory degree at least light intensity earthquake events (i.e. accelerations > 2 mg). Also, presented PGA variation maps based on the recordings of the network demonstrate a significant spatial variation for each event within the small-size area of the network, as well as significant differences of the PGA distribution patterns among earthquakes of different magnitude, azimuths and epicentral distances. Although it is well known that PGA is a parameter susceptible to large variations, it is nevertheless the one that is still currently used in the seismic codes for the design of buildings. Thus a question of the reliability of Seismic hazard maps adopted in the Seismic Codes arises from the fact that very few high-accuracy accelerographs are typically installed as stations of a National Strong Motion Network in each urban area due to high cost, and the actual intensity distribution cannot be reliably predicted. Hence, the proposed approach of developing ultra-dense networks based on low-cost sensors can certainly contribute towards an enhanced seismic resiliency of urban areas.

REFERENCES

[1] Papanikolaou V.K. and Karakostas C.Z., A low cost MEMS-based accelerograph. P*roceedings of Experimental Vibration Analysis for Civil Engineering Structures (EVACES'13)*, Ouro Preto, Brazil, 116-123, 28-30 October, 2013.

[2] Papanikolaou V.K. and Karakostas C.Z., Explicit shakemaps via low-cost instrumentation: The case of Lefkas city. *Proceedings of 2nd European Conference on Earthquake Engineering and Seismology (2ECEES),* Istanbul, Turkey, paper No 2171, 24-29 August 2014.

[3] Christos Z. Karakostas, Vassilis K. Papanikolaou, Nikolaos P. Theodoulidis "An Ultra-Dense Strong-Motion Urban Network Based On in-House Designed MEMS Accelerographs: The Case of Lefkas City, Greece" Proceedings of the 16th European Conference on earthquake Engineering (16ECEE), Thessaloniki, Greece, paper no 11191, June 18-21,2018.

[4] Karakostas C.Z. and Papanikolaou V.K., A low cost instrumentation approach for seismic hazard assessment in urban areas. *Proceedings of 9th International Conference on Risk Analysis and Hazard Mitigation (RISK2014)*, New Forest, UK, pp. 97-108, 4-6 June 2014

[5] Karakostas Ch., Kontogiannis G., Morfidis K., Rovithis E., Manolis G. and Theodoulidis N., Effect of soil-structure interaction on the seismic response of an instrumented building during the Cephalonia, Greece earthquake of 26-1-2014, *Proceedings of COMPDYN 2017, 6th ECCOMAS Thematic Conference on Computational Methods in Structural Dynamics and Earthquake Engineering,* M. Papadrakakis, M. Fragiadakis (eds.),Rhodes Island, Greece, 15–17 June 2017.

DIFFERENT LEVELS SEISMIC CAPACITY IDENTIFICATION METHOD OF REINFORCED CONCRETE FRAME BUILDINGS

Baijie ZHU[1], Lingxin ZHANG[2*]

[1] Assistant professor. Institute of Engineering Mechanics, China Earthquake Administration; Key Laboratory of Earthquake Engineering and Engineering Vibration of China Earthquake Administration, Harbin, China
e-mail: baijie_zhu@126.com

[2] Professor. Institute of Engineering Mechanics, China Earthquake Administration; Key Laboratory of Earthquake Engineering and Engineering Vibration of China Earthquake Administration, Harbin, China
e-mail: lingxin_zh@126.com (Corresponding author)

Keywords: Reinforced Concrete Frame Buildings, Seismic Design Levels, Seismic Capacity, Identification Method.

Abstract. *Identification of seismic capacity of existing reinforced concrete structures before earthquakes is the significant basis for effective earthquake disaster mitigation, which is also practically valuable to reduce the damage of this kind of structures in earthquake. In the framework of seismic capacity index method for reinforced concrete buildings, which is given the current national Standard for seismic appraisal of buildings (GB50023-2009), the seismic capacity coefficient method was proposed. However, there is no seismic capacity identification method for different levels of intensity corresponding to the Chinese code for seismic design of buildings. For this purpose, according to the seismic hazard curve formula of design acceleration Amax and earthquake influence coefficient α_{max} with the seismic hazard curve of intensity, combining a variety of ground motion parameters with the standard for seismic appraiser of building, seismic capacity identification method for different levels of intensity is proposed.*

1 INTRODUCTION

According to the Chinese Standard for Seismic Appraisal of Buildings (GB50023-2009) (hereafter referred to as "the Standard")[1], existing buildings with continuous seismic working life of 30 years, 40 years, or 50 years are defined as Category A, Category B, or Category C respectively. For RC frame structures, the seismic capacity identification for Category A-buildings should be divided into two grades. The first one is to check the structural system, materials, configurations, and local connections. The second one adopts the Compound Seismic Capacity Index Method (CSCIM), and the calculated index can estimate whether the seismic capacity is satisfied or not. The seismic capacity identification for Category B buildings either need to check the available capacity of components; or use the CSCIM. However, the former way only focuses on the components neglecting the whole structure, consequently, the CSCIM is more reasonable to all categories. The Code for Seismic Design of Buildings (GB50011-2010)[2], Chinese current code, presents three seismic capacity levels, which are not damaged under small earthquakes, repairable under moderate earthquakes, and not collapsed under large earthquakes. However, the CSCIM method is only applicable for the second level, instead of the other two. However, the seismic capacity index is calculated by earthquake influence coefficient

in "the Standard", regardless of the effect of buildings' continuous seismic service life, which means that ground motion parameters are constant for selection. A new three level seismic capacity identification method for existing RC frame structures is proposed in this study, based on ground motion parameters and the seismic intensity, which is on the basis of the CSCIM method with consideration of building continuous seismic service life and three seismic capacity levels.

2 SEISMIC CAPACITY INDEX METHOD

According to "the Standard", the building seismic capacity index should be calculated at least in two main axis directions respectively as follows:

$$\beta=\psi_1\psi_2\xi_y \tag{1}$$

Where β denotes the compound seismic capacity index which is unsatisfied if $\beta<1$, ψ_1 and ψ_2 denote the geometry and the local influence coefficient respectively, and ξ_y denotes the storey yield strength coefficient.

Further, ψ_1 can be obtained by the structural system, hoops of beam and column, axial compression ratio and so on. The value of ψ_1 will be more than one, if all configurations meet the Code for Seismic Design of Buildings(GB50011-2010) or Category A buildings conform to requirements of the Category B.

The storey yield strength coefficient can be calculated as follows:

$$\xi_y = V_y \Big/ V_e \tag{2}$$

Where V_y and V_e respectively denote the storey shear bearing capacity and the storey elastic earthquake shear force.

According to "the Standard", the storey elastic earthquake shear force can be calculated by the corresponding calculation formula is as follows:

$$F_{\mathrm{EK}} = \alpha_{\max} G_{\mathrm{eq}} \tag{3}$$

$$F_i = \frac{G_i H_i}{\sum_{j=1}^{n} G_j H_j} F_{\mathrm{EK}} \tag{4}$$

Where F_{EK} and F_{i} respectively denote the standard value of the total horizontal earthquake action of a structure and at the i^{th} mass, $\alpha_{\max}$ denotes the maximum of the horizontal seismic influence coefficient, G_{eq} and G_i respectively denote the total equivalent gravity load of a structure and the representative values of the gravity at the i^{th} mass, H_i denotes the calculated height of the i^{th} mass.

According to "the Standard", the storey shear capacity can be calculated as follows:

$$V_y = \sum V_{cy} + 0.7\sum V_{my} \tag{5}$$

Where V_y denotes available storey shear capacity, V_{cy} and V_{my} respectively denote sum of available storey shear capacity of frame column and of infill.

3 THREE-LEVEL GROUND MOTION PARAMETERS BASED ON THE INTENSITY FOR EXISTING BUILDINGS

According to the Code for Seismic Design of Buildings (GB50011-2010), the earthquakes are classified in the three levels as small, moderate, and large , which are respectively defined as the exceedance probability of the buildings suffering earthquake in 50 years being, and the corresponding value are 63%, 10% , and 2%-3%. The intensity corresponding to three

earthquake levels mentioned above are defined as Level 1 intensity, Level 2 intensity and Level 3 intensity in sequence.

3.1 Three-levels of seismic fortification objective for existing buildings

In order to realize the same seismic fortification objectives as the Code for Seismic Design of Buildings (GB50011-2010), the three-levels of seismic fortification objectives for existing buildings should adopt continuous seismic working life to calculate the exceedance probability, shown below:

Seismic capacity level	Continuous seismic working life of existing buildings		
Level 1(Not damaged under small earthquakes)	30	40	50
Level 2(Repairable under moderate earthquakes)	285	380	475
Level 3(Not collapsed under large earthquakes)	985-1485	1314-1980	1462-2475

Table 1. Return period of three-level earthquake for different continuous seismic working life (Unit: year).

Taking different continuous seismic working life of all categories existing buildings into consideration, results of seismic identification will be more reasonable and applicable.

3.2 Three-level parameters of ground motion based on intensity for different continuous seismic working life

The relationship between the exceedance probability and the intensity has been fit by results of seismic hazard analysis in Chinese cities and towns [4]. For random variables x, the relationship between probability distribution function $F(x)$ and probability of exceedance $P(X \geq x)$is:

$$F(x) = 1 - P(X \geq x) \tag{13}$$

And the distribution of seismic intensity is shown as follows:

$$F(i) = 1 - P(I \geq i) = \exp\left[-\left(\frac{\omega - i}{\omega - \varepsilon}\right)^{k}\right] \quad (i < \omega) \tag{14}$$

Where i denotes the seismic intensity, ω denotes the upper limit of intensity which can be taken as 12, ε denotes the Level 1 intensity, and k denotes the shape parameter.

Natural logarithm and common logarithm are respectively taken on both sides of the eq. (14), and i is given the value of the Level 2 intensity I_0. Consequently, the intensity curve of seismic hazard can be expressed as follows:

$$\lg\left\{-\ln\left[1 - P(I \geq i)\right]\right\} + 0.9773 = k \lg\left(\frac{\omega - i}{\omega - I_0}\right) \tag{15}$$

According to the Code for Seismic Design of Buildings (GB50011-2010), horizontal seismic influence coefficient $\alpha_{\max}$ and seismic acceleration $A_{\max}$ can be calculated as follows:

$$\lg \alpha_{\max} = 0.3i - 2.75 \tag{16}$$

$$\lg A_{\max} = 0.3i - 2.1 \tag{17}$$

Furthermore, the expression of intensity curve of seismic hazard about horizontal seismic influence coefficient and seismic acceleration is:

$$\lg\left\{-\ln\left[1 - P(I \geq i)\right]\right\} + 0.9773 = k \lg\left(\frac{0.85 - \lg \alpha_{\max}}{0.85 - \lg \alpha_{\max}^{10}}\right) \tag{18}$$

$$\lg\left\{-\ln\left[1-P\left(I\geq i\right)\right]\right\}+0.9773=k\lg\left(\frac{1.5-\lg A_{\max}}{1.5-\lg A_{\max}^{10}}\right) \tag{19}$$

Where $\alpha_{\max}^{10}$ and $A_{\max}^{10}$ respectively denote the value of $\alpha_{\max}$ and $A_{\max}$ in the moderate earthquakes.

From the above, seismic intensity i with a 10% exceedance probability in 50 years, horizontal seismic influence coefficient $\alpha_{\max}$, and seismic acceleration $A_{\max}$ can be obtained by the equation (15), (18), and (19), by using the I_0, $\alpha_{\max}^{10}$, $A_{\max}^{10}$, and the shape parameter k that is shown as Table 2.

Fortification intensity	6	7	8	9
Shape parameter k	9.79	8.33	6.87	5.40

Table 2. The shape parameter values of current Code

The exceedance probability of different levels can be converted via equal (20) as in 50 years [4].

$$P=1-\left(1-P^{'}\right)^{t/50} \tag{20}$$

Where t denotes continuous seismic working life, $P^{'}$ denotes exceedance probability of continuous seismic working life corresponding to three seismic capacity levels, P denotes the relative exceedance probability which is in 50 years

By taking the relative exceedance probability into equation (18) and (19), horizontal seismic influence coefficient $\alpha_{\max}$ and seismic acceleration $A_{\max}$ for three seismic capacity levels with continuous working life t years can be calculated as Table 3 [3].

Continuous working life	Seismic capacity level	Fortification intensity			
		6	7	8	9
30	Level 1(Not damaged under small earthquakes)	0.029	0.060	0.115	0.227
	Level 2(Repairable under moderate earthquakes)	0.090	0.185	0.364	0.734
	Level 3(Not collapsed under large earthquakes)	0.207	0.415	0.755	1.168
40	Level 1(Not damaged under small earthquakes)	0.034	0.070	0.136	0.272
	Level 2(Repairable under moderate earthquakes)	0.102	0.210	0.411	0.825
	Level 3(Not collapsed under large earthquakes)	0.230	0.457	0.828	1.283
50	Level 1(Not damaged under small earthquakes)	0.040	0.080	0.160	0.320
	Level 2(Repairable under moderate earthquakes)	0.112	0.230	0.450	0.900
	Level 3(Not collapsed under large earthquakes)	0.250	0.500	0.900	1.400

Table 3. Horizontal seismic influence coefficient $\alpha_{\max}$ for different continuous working life (unit: year)

4 CONCLUSIONS

According to the seismic hazard curve formula of design acceleration Amax and earthquake influence coefficient αmax with the seismic hazard curve of intensity, combining a serious of ground motion parameters with the Chinese Standard for Seismic Appraisal of Buildings (GB50023-2009), seismic capacity identification method for different levels of intensity is proposed. Considering of the earthquake uncertainty and randomness, whether structures satisfy the design requirements on different levels of intensity is easy to identify. It can be predicted whether the building is "not damaged under small earthquakes, repairable under moderate earthquakes, not collapsed under large earthquakes".

Continuous working life	Seismic capacity level	Fortification intensity			
		6	7	8	9
30	Level 1(Not damaged under small earthquakes)	13	26	51	101
	Level 2(Repairable under moderate earthquakes)	40	80	162	326
	Level 3(Not collapsed under large earthquakes)	93	181	336	519
40	Level 1(Not damaged under small earthquakes)	15	30	60	120
	Level 2(Repairable under moderate earthquakes)	45	91	183	367
	Level 3(Not collapsed under large earthquakes)	103	200	368	570
50	Level 1(Not damaged under small earthquakes)	18	35	70	140
	Level 2(Repairable under moderate earthquakes)	50	100	200	400
	Level 3(Not collapsed under large earthquakes)	/	220	400	620

Table 4. Seismic acceleration $A_{\max}$ for different continuous working life (unit: cm/s^2)

REFERENCES

[1] GB50023-2009 Standard for seismic appraisal of buildings [S]. Beijing: China Architecture & Building Press, 2009(in Chinese)

[2] GB50011-2010 Code for seismic design of buildings [S]. Beijing: China Architecture & Building Press, 2010(in Chinese)

[3] Bai X. S. Experimental research on seismic appraisal method of existing reinforced concrete frame structures [D], Beijing: China Academy of Building Research, 2012(in Chinese)

[4] Xie L. L., Ma Y. H., Zhai C. H. Performance-Based Seismic Design and Design Ground Motion [M], Science Press, 2009. (in Chinese)

A BUILDING-SPECIFIC BI-DIRECTIONAL DYNAMIC LOADING PROTOCOL FOR EXPERIMENTS OF NON-STRUCTURAL COMPONENTS

Zhe Qu[1], Yuteng Cao[1], Xiaodong Ji[2]

[1] Key Laboratory of Earthquake Engineering and Engineering Vibration, Institute of Engineering Mechanics, CEA, Hebei 065201, China, e-mail: quz@iem.ac.cn, cwwhustiem@163.com

[2] Department of Civil Engineering, Tsinghua University, Beijing 100084, China, e-mail: jixd@mail.tsinghua.edu.cn

Abstract. *Experimental research on the seismic performance of non-structural components in China is still very limited, especially for those sensitive to multiple engineering demanding parameters. Inspired by the Non-structural Component Simulator at the University at Buffalo (UB-NCS), a similar simulator is being developed at the Institute of Engineering Mechanics (IEM) at Beijing, China, which aims at providing a general-purpose test bed that simulates the simultaneous motions of the floor and ceiling of a full-scale room of various occupancies hosted in different types of buildings. Unlike the UB-NCS which utilizes dynamic actuators for loading, the IEM-NCS will be based on an 5m by 5m shake table and incorporates sub-structure shake table testing technique to enable the simulation of floor motions that exceed the capacity of the table. To fully exploit the flexibility of the simulator, the dynamic loading protocol previously developed for UB-NCS is modified primarily in the following aspects: (1) the random vibration process for determining the height-wise floor acceleration and inter-story drift distribution is replaced by a nonlinear time-history analysis of the building of concern subjected to a suite of selected earthquake ground motions; (2) the a-function in the UB-NCS protocol is modified to match floor response spectra; (3) a bi-directional loading rule is introduced taking advantage of the shake table.*

Keywords: acceleration-sensative, displacement-sensative, shake table test, floor response spectrum, bi-directional loading.

1 INTRODUCTION

As past studies have revealed, many non-structural components are dependent on multiple engineering demand parameters. To make things more complicated, different non-structural components may interact with each other. A convenient way of simulating the complicated behavior of nonstructural components in the lab is to carry out shake table test of full-scale building models [e.g., Soroushian et al., 2012]. But this kind of tests can be either too expensive to afford or too small to simulate the nonstructural behavior in realistic large-scale buildings. The nonstructural component simulator at the University at Buffalo provides an interesting alternative solution. The facility is consisted of two layers of floor slabs each of which is driven by a pair of very slender actuators to simulate the real-time motion of the floor in a prototype building [Mosqueda et al., 2009].

Inspired by the simulator at Buffalo, we are developing a similar nonstructural simulator taking advantage of the shake table at the Beijing campus of IEM. An immediate benefit of using a shake table is the wider frequency band and the convenience to impose bi-directional or even tri-directional loading. A substructure will provide a floor and a ceiling slab for a full-scale room and the motions of two neighboring floors of a building will be simulated by substructure shake table testing technique (Figure 1).

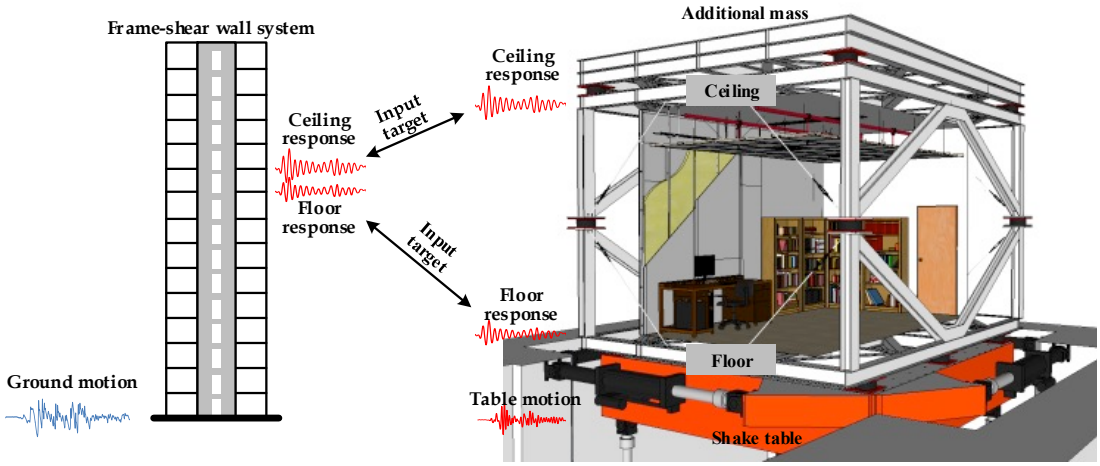

Figure 1. IEM-NCS concept

To fully exploit the flexibility of the to-be-developd simulator at IEM, the dynamic loading protocol previously developed for UB-NCS [Retamales et al., 2011] is reviewed and modified. In the rest of this paper, following a brief description of the UB-NCS protocol, the major modifications are introduced.

2 THE UB-NCS PROTOCOL AND ITS REVISIONS

The target loading time history of the UB-NCS protocol is described by two functions in Equations 1 and 2, which contain five time-domain functions. It is basically a series of sinusoids of gradually changing frequencies from high to low and then from low to high again. The *a*-function can be used to adjust the shape of the response spectrum of the loading time history and the exponential function in Equation 2 controls the amplitude of the inter-story drift. In addition, there are also two amplitude factors, one is called FRS factor in the Buffalo protocol and is refered to as $A(h/H)$ function hereinafter, which describes the maximum acceleration distribution along height of the building. Another $d(h/H)$ function describes the maximum inter-story drift along height of the building.

$$x_{\text{Bottom}}\left(t,\frac{h}{H},S_{\text{DS}},S_{\text{D1}}\right)=\alpha\left(t,\frac{h}{H},S_{\text{DS}},S_{\text{D1}}\right)f(t)^{\beta}\cos\left(\varphi(t)\right)w(t)A\left(\frac{h}{H}\right) \tag{1}$$

$$x_{\text{Top}}\left(t,\frac{h}{H},S_{\text{DS}},S_{\text{D1}}\right)=x_{\text{Bottom}}\left(t,\frac{h}{H},S_{\text{DS}},S_{\text{D1}}\right)+\boldsymbol{\Delta}\left(t,\frac{h}{H},S_{\text{D1}}\right) \tag{2a}$$

$$\boldsymbol{\Delta}\left(t,\frac{h}{H},S_{\text{D1}}\right)=h\frac{S_{\text{D1}}}{0.5g}e^{-\left(\frac{t-t_{\text{d}}}{\sigma}\right)^{2}}\delta\left(\frac{h}{H}\right)cos\left(\varphi(t)\right)w(t) \tag{2b}$$

where x_{bottom} and x_{top} are the target displacement time histories of the floor and the ceiling, respectively; t is time, h/H is the relative height of the non-structural component in the building; S_{DS} and S_{D1} are the design spectral acceleration at short period and 1 second, respectively. β=-1.25 is a calibration factor; t_d is the half duration of the testing protocol.

2.1 Heightwise distributions of peak floor responses

The first modification made to serve the purpose of IEM-NCS is to make the two heightwise functions, A and d, building-specific. In these cases, the nonlinear seismic responses, rather than the linear elastic ones in the UB-NCS procedures, need to be considered. Therefore, a more straightforward approach is suggested, in which the amplitude factors are determined through nonlinear time history analysis of the building of concern subjected to a suite of ground motions that match the design spectrum. The nonlinear flexural-shear lumped mass model proposed by Xiong et al. [2016] is used.

2.2 Buiding-specific floor response spectra

Vukobratovic and Fajfar [2015] proposed a method of determining approximate floor response spectra without conducting time-consuming time history analysis. Take a 141.8m-tall 42-story reinforced concrete core tube-frame building for example. The floor response spectra at the mid-height of the buiding according to FEMA 450, UB-NCS protocol and Vukobratovic and Fajfar's method are compared in Figure 2, where T_s is the period of the secondary structure, that is, the non-structural component. The periods of the first two modes of the building, T_{p1} and T_{p2}, are respectively 2.7s and 0.85s. As compared to the Vukobratovic and Fajfar spectrum, the period-independent FRS in FEMA 450 substantially underestimates the floor response around T_{p1}, while overestimates it in short-period range.

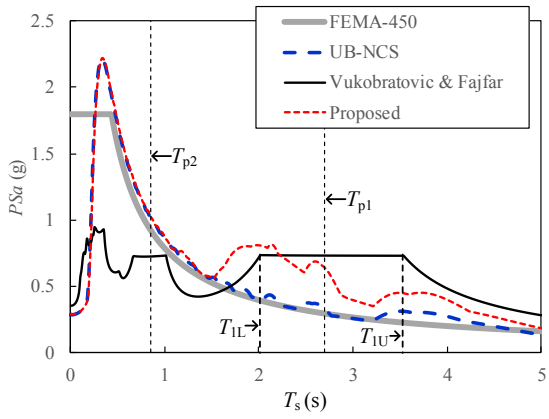

Figure *2*. Floor response spectrum

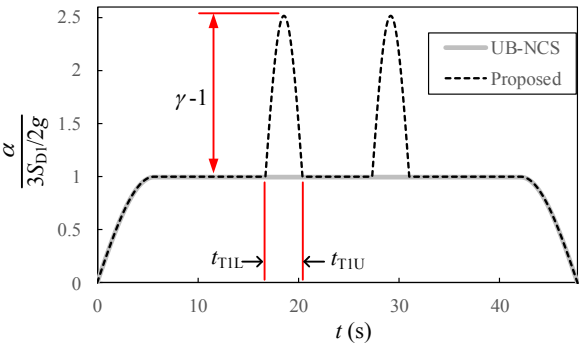

Figure *3*. Revised a-function

A half-cycle sinusoid is superimposed to each half of the original symmetric a-function (Equation 3 and Figure 3) within the period of time from t_{T1L} and t_{T1U}, which are the time instances corresponding to the starting and ending periods of the plateau, T_{1L} and T_{1U}, respectively, of the Vukobratovic and Fajfar's FRS around T_{p1}. The frequency- to time-domain transformation is made possible by the f function. The amplitude of the additional sinusoid is determined by the ratio of the pseudo spectral acceleration at T_{p1} by Vukobratovic and Fajfar and by FEMA 450, which is denoted as g. The pseudo acceleration spectrum of the resultant loading protocol for the mid-floor of the aforementioned 42-story building is compared with that of the original loading protocol in Figure 2.

$$\alpha = \frac{3S_{D1}}{2g}\left[1 + (\gamma - 1)\sin\left(\pi \frac{t - t_{T1L}}{t_{T1U} - t_{T1L}}\right)\right] \text{ for } t_{T1L} \le t \le t_{T1U} \quad (3)$$

2.3 Bidirectional loading

As already mentioned, the use of substructure shake table testing is inherently capable of loading bi-directionally. However, the motions in the two directions will always be in the same phase if

the aforementioned loading protocol is followed, unless a phase difference, *f*, between the motions in the two directions is introduced (Equation 4).

To assist the selection of an appropriate phase difference, the flatness, *F*, and the eccentricity, *e*, are defined to characterize the shape of the orbit of an earthquake ground motion. Take any orbit in Figure 3 for example. By the farthest point on the orbit from the origin, one can define a new coordinate system with a primary axis and a secondary axis. By finding a second point that is farthest to the primary axis, an ellipse can be uniquely defined. The semi-major and semi-minor axes of the ellipse are denoted as a and b, respectively. Furthermore, we denote the projection distance of the orbit on the major axis as D_1 and on the minor axis as D_2. The flatness and eccentricity of the orbit of any ground motion are then defined in Equations 5 and 6, respectively. The flatness describes how an orbit is similar in amplitudes in two orthogonal directions, whereas the eccentricity describes how the orbit is symmetric around the original position.

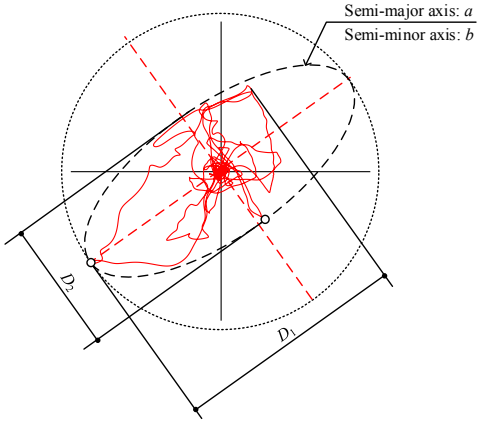

Figure 3. Charateristics of shape of ground motion orbit

$$y_{\text{Bottom}}\left(t,\frac{h}{H},S_{\text{DS}},S_{\text{D1}}\right)=\alpha\left(t,\frac{h}{H},S_{\text{DS}},S_{\text{D1}}\right)f(t)^{\beta}\cos(\varphi(t)+\phi)\,w(t)A\left(\frac{h}{H}\right) \quad (4)$$

where y_{Bottom} is the target displacement time history of the floor in the direction orthorgonal to the x-direction.

$$F=b/a \quad (5)$$

$$\varepsilon=\left(\frac{2a-D_1}{2a}+\frac{2b-D_2}{2b}\right)/2 \quad (6)$$

A suite of 80 ground motions are selected by matching the Chinese design spectrum [GB 50011-2010, 2010] and their flatnesses and eccentricities are calculated. The scattering is very large, while the average flatness and eccentricity, F_{m} and e_{m}, are approximately 0.6 and 0.12, respectively. These are very close to the flatness and eccentricity of an orbit if the phase difference is taken as $f=p/3$. Therefore, a phase difference of $p/3$ would be a good choice.

3 CONCLUSIONS

An IEM-NCS is being developed for simulating seismic behavior of various types of nonstructural components in various types of buildings and their interactions. The following modifications are made on UB-NCS protocol to fully exploit the capacity of of IEM-NCS:

(1) Drift and acceleration amplitudes become building-specific by a procedure incorporating nonlinear time history anslysis;

(2) a-function is revised to match building-specific floor response spectra;

(3) A phase difference, f, is introduced between the horizontal loading of two orthorganal directions to enable bi-directional loading.

REFERENCES

FEMA 450. [2003] *NEHRP Recommended Provisions for Seismic Regulations for New Buildings and Other Structures* Federal Emergency Management Agency, USA.

GB 50011-2010. [2010] *Code of seismic design of buildings*. Beijing: China Architecture & Building Press (in Chinese).

Miranda, E. and S. Taghavi. [2005] Approximate floor acceleration demands in multistory buildings. I: Formulation. *ASCE Journal of structural engineering,* **131**(2): p. 203-211.

Mosqueda, G., Retamales, R., Filiatrault, A., et al. [2009] Testing facility for experimental evaluation of non□structural components under full□scale floor motions. *The Structural Design of Tall and Special Buildings*, Vol. 18, No. 4, pp. 387-404.

Retamales, R., Mosqueda, G., Filiatrault, A., et al. [2011] Testing protocol for experimental seismic qualification of distributed nonstructural systems. *Earthquake Spectra*, Vol. 27, No. 3, pp. 835-856.

Soroushian, S., Ryan, K.L., Maragakis, M., et al. [2012] "NEES/E-defense tests: seismic performance of ceiling/sprinkler piping nonstructural systems in base isolated and fixed base building", *Proceedings of the 15th World Conference on Earthquake Engineering (15WCEE)*, Lisbon, Portugal.

Vukobratović V, Fajfar P. [2015] A method for the direct determination of approximate floor response spectra for SDOF inelastic structures. *Bulletin of Earthquake Engineering*, 13(5):1405–1424.

Xiong C, Lu X.Z, Guan H, Xu Z. [2016] A nonlinear computational model for regional seismic simulation of tall buildings. *Bulletin of Earthquake Engineering*, 14:1047–1069.

INFLUENCE OF THE "STRUCTURAL FLEXIBILITY" OF MONUMENTS AT THE DAMAGE DISTRIBUTION DURING STRONG EARTHQUAKES

Salonikios N. Thomas[1], Theodoulidis Nikos[1], Morfidis E. Konstantinos[1], Zacharopoulou Georgia[2]

[1]Researchers, Earthquake Planning and Protection Organization (EPPO-ITSAK)
Terma Dasylliou, 55535, Thessaloniki, Hellenic Republic
e-mail: salonikios@itsak.gr

[2]Dr Civil & Structural Engineer, MA in Conservation Studies, Ephorate of Antiquities of Thessaloniki, Ministry of Culture and Sports, Eptapyrgio, Thessaloniki, Hellenic Republic
e-mail: gzachar.heritage@gmail.com

Keywords: Earthquake Damage, Seismic retrofit, Monuments, Damage Mitigation, Numerical Modeling, Ambient Noise, Ground Motion Simulation.

1. THE SEISMIC EVENT

The city of Thessaloniki in northern Greece was the first urban metropolitan area in Greece which was hit by a strong EQ in modern times and after the first national seismic code put in force. The EQ with magnitude M6.5 occurred on 20 June 1978, 20:03GMT at an epicentral distance of 30km to the east of downtown and demonstrated the vulnerability of a modern city. An eight-storey reinforced concrete building collapsed in the city center, causing 37 deaths out of 47 in total due to the main shock ground shaking. Overall, about 4000 buildings suffered serious, 13000 intermediate and 49000 only slight damage. Several monuments in the historical center of the city suffered various degree of damage as well. The location of the metropolitan area of Thessaloniki and the causative fault are shown in Fig. 1a. That EQ could not be considered as a near field event for the city of Thessaloniki, spatial variation of damage distribution has been mainly attributed to site effects given that local geologic conditions in the city vary considerably. The city of Thessaloniki (Greece) has been damaged several times in the past due to strong EQs around its vicinity. One of the most destructive EQs occurred in June 22, 1759 (M6.6) when the majority of the residents left the city for about two years. During the June 20, 1978 EQ, the observed macroseismic Modified Mercali intensity in the city varied between IV and VIII. The unique accelerograph installed in the city historic center recorded a peak ground horizontal acceleration 0.15g. Horizontal acceleration response spectra, for critical damping D=0.05, showed a maximum value of ~0.5g in the period range 0.3-0.5sec, and vertical acceleration response spectra of ~0.45g in the period range 0.15-0.2sec. In addition, for horizontal acceleration spectral values a second peak of ~0.25g appeared in intermediate period range 0.8-1.0sec. That is, strong ground motion due to mainshock of June 20, 1978, exhibited high spectral accelerations in a broadband period range, capable of exciting a variety of structures with different dynamic properties.

2. TWO SELECTED MONUMENTS

2.1 Acheiropoietos basilica

The basilica is 51.90 m long, 30.80 m wide and 14 m high at the side external walls, and 22 m high at the top of the roof of the central aisle. Even though the ground-plan of the monument has remained unaltered through the ages, its upper-structure was subsequently remodeled. Based on the architectural analysis of the monument, it occurs that Acheiropoietos was originally erected as a western-Roman-type basilica, without galleries, during the last decade of the 5th or the first decade of the 6th century. The tall clerestory of the first phase basilica was probably severely cracked and statically devastated during the disastrous series of EQs that shook Thessaloniki during the third probably decade of the 7th century. The basilica was afterwards restored as a three-aisled Basilica of the so-called Helleni(sti)c type with galleries above the lateral aisles and the narthex. During the first half of the 9th c. structural interventions took place, probably to restore the impact that the 813-820 EQs had on the edifice. Consolidation works also occurred on the upper-structure of the building during the last quarter of the 15th c. when the basilica –which was already turned into a mosque in 1430- lost its 7th c. clerestory. However, the most severe devastation of the building, documented so far, is probably due to the series of EQs that occurred during the summer and the fall of 1759. The alterations that took place in the following period, so as to rehabilitate the building were radical: most of the openings including the tribelon were closed with masonry, the colonnades of the lateral upper galleries were altered into brick-built rows of piers –that in the case of the southern part enclosed the marble columns- while the few remains of the western gallery, which was probably totally ruined due to the partial collapse of the minaret onto it, were demolished. These interventions to the static system of the basilica were removed during the early 20th restoration phase, with the aim to restore the Christian characteristics of the monument. However, even this last restoration-rehabilitation of the monument during 1909-12 (under Ottoman rule) and 1912-14 (under Greek authority) did not manage to raise the weakness of the basilica in the N-S axis; due to the 1978 EQ, the flexible untrimmed timber floors and the timber roofs of the galleries held but did not prevent the columns from conducting autonomously. That was registered as divergence of the longitudinal walls and colonnades from the vertical axis, caused mainly by their marginal shifting. After the 1978 EQ that aggravated the pre-existing static sensitivity of the structure, the basilica presented multiple masonry disorganizations, caused by intense compressive or tensile strain. An extensive network of pre-existing cracks due to further deterioration of previous EQ deformations –ranging from hairline to those of several centimeters wide and/or through masonry cracks- were mostly stimulated on the arches and windowsills of the northern ground level masonry and on the semi-dome of the sanctuary apse. Severe structural dislocation and outwards movement of the walls were recorded on the intersection corners of the external masonries – on top of the NE (≈15cm), NW (≈9cm) and SE (≈55cm) corner of the monument- whilst the middle of the north wall has curved inwards because of the different construction (historical and/or material) phases. Outwards movements of the west (≈10cm) and the east wall (≈14cm) have also been measured. Masonry disorganizations were localized on the higher perimetrical walls attributable to the thrust of the timber trusses of the central aisle's roof. As expected, the –one phase- reconstructed south wall presented a remarkably improved damage pattern. Generally speaking, both north and south colonnade were deformed outwards at the E (max 6cm and 14cm, correspondingly) and W corners and inwards in the middle. It is worth mentioning that both the declination of the southern colonnade and the northern external masonry from the vertical axis were not completely fixed by the restoration interventions. The remaining deformations were accurately measured in 1999. For the perimeter walls at the north side, displacements at the out direction (at the east and west ends of the wall) were found, while displacements at the inner direction were

measured at the intermediate points. Regarding the colonnades, displacements mainly at the west direction and partially at the north and south directions were detected. The absence of displacements at the eastern direction is attributed to the way that the sanctuary is constructed. It is observed that there are large openings at the entrance to the sanctuary and there is no vertical support at the walls over that location. For this reason the distribution of displacements indicate that the sanctuary walls push the colonnades(Fig.2a, 2b).

This response is a result of the in plane deformation and of rotation of the east walls, through elongation of the outer fiber, from the base points and along height. These displacements are attributed to the seismic excitation of the basilica due to 1978 EQ and possibly to previous EQs.

Fig. 1. Left: South – East view of the basilica (Raptis 2016) Right: Inside view of the basilica, (Raptis 2016).

2.2 Bey hamam, an Ottoman public bath

Ottoman buildings of a public character –of a religious (cami, medrese, tekke, türbe etc) or secular (hamams, imaret, bedestens, caravanserais etc) and military use (fortresses, castles, towers etc)- were the first constructions in a recently conquered area. The "Bey hamam" (or "Paradise baths") was built in 1444 i.e. just after the conquest of Thessaloniki by Mourat II, in 1430. Roman and byzantine baths are the precursors of this building type. It is a double bath with two distinctive functional parts (male, female), where the male one dominates in size and decoration.

Hamam's typical sequence of rooms directly corresponds to the rigid order of their main functional areas, namely disrobing room (sogumanlik or camekân), tepid section (soğukluk or iliklik), hot section (sicaklik), private corner cells (halvet) and finally the water reservoir.

The ground floor of the Bey hamam has remained unaltered through the ages, as well as its facades. The monument is 43.26 m long, 28.84 m wide and max 12.98 m high at the dome of the men part, and max 10.10 m high at the dome of the women part. Research on the potential standardization -of their floor plans, sections and facades- demonstrated that a certain geometric construction emvatis is actually present in each functional area of a bath. As a result, the successive square or rectangular functional spaces are mainly organized in such a way as to obtain both spatial, and structural (bearing structure) autonomy. The sections and moreover the facades present a greater variation than those detected in the floor plans, but still the structural conception is traceable within a clearly organized synthesis. Among the most characteristic structural and metrological features of the Bey hamam are i) the diffusion of domes' loads through octagons (disrobing room in men part and tepid section in both women and men parts), ii) the construction of equal domes in the tepid section in both women and men parts, iii) the unequal domes in hot sections and their perimeter spaces, iv) the net height is equal to the diameter of the relevant dome in disrobing and tepid section and twice or three times in hot

sections and perimeter spaces and v) double arches are selected between the spaces of the hot section rendering each space structurally autonomous. The sophisticated design of the bath is apparent; only the absolute necessary bearing components are physically constructed, while the "empty" spaces –e.g. created by the octagon walls and others- are inspirationally decorated and used.

The bath is laid on the upper layer of soft soil (alluvium deposits). The foundation level was found 3.50m below the surface of the surrounding soil. For this reason, the restrain of walls was selected at 0.70m under the lower floor of the bath. The alluvium deposits layer is extended to 30-40 meters under the monument. Next, a marga layer of 100m thick follows. During the visual inspections, differential sedimentations were not observed. This is attributed to the expected low stresses at the foundation level of the structure, since it is a one story structure. A smart network of stone shaped channels (hypocausts) produced and circulated hot air below the stone floor of the bath's tepid and hot sections. Also a series of pipes, through which the hot air passes, warm the walls. These channels do not influence the response of the structure to vertical and seismic loads.

Fig.2. The disrobing room (entrance hall, cold section) of the men part. Hot section and private corner cells of the men part

The masonry walls were constructed by well-shaped stones, clay bricks and lime based mortar. Four series by height of timber ties reinforce the bearing masonries. As told, the whole structure is divided into two main parts; the male and the female longwise to the bath. The men section is larger and its entrance is located at the southwestern corner at Egnatia Street. The entrance hall (disrobing room) is surrounded by octagonal masonry walls and is covered by a spherical dome. There is also a timber attic with special rooms for dressing and undressing. Following and in parallel with Egnatia Street, there is the octagonal tepid section. Continuing in the same direction there are the hot section with eight private corner cells shown on figure 3b, (bath type A). The quadrilateral disrobing room (entrance hall, cold section) of the women part is at the northwestern corner of the structure. Similarly, there is an entrance hall with a concrete attic −which replaced the original timber attic, after WWII. Then, there is the octagonal tepid section followed by the hot section and four private corner cells (bath type C). At the east end, there is the water reservoir –also constructed by masonry walls- heated by a fireplace. All domes are hemispherical constructed by fired bricks laid on lime based mortar and covered by clay tiles. The connection points of the vertical walls with horizontal domes seem to be in very good condition.

After the 1978 EQ, the bath presented local domes and masonries disorganizations, caused by intense compressive or tensile strain. The cracks were stimulated at the larger distinctive sections

(entrance halls) both in men and women parts and on men hot section. The most severe cracks are highlighted by red color. The cracks are more apparent in damage patterns at the west facade (entrance halls) of the women and men parts. A widespread network of hairline cracks –and also some centimeters wide- were mostly appeared on the arches and windowsills of the each section. No severe unsafe outwards movement of the walls or structural dislocation was recorded on the middle of the external masonries or their intersection corners.

3. FINDINGS AND CONCLUSIONS

The analytical model of Acheropoietos was solved for the record of Thessaloniki Earthquake. The stresses shown in Fig. 3 resulted from the same analysis step for synchronous application of the components of the 1978 Thessaloniki Earthquake. The east and west walls of the basilica were significantly stressed. The damages in the actual structure largely affected these walls, thus indicating that the model largely approaches the response of the basilica to the 1978 Earthquake. The equivalent seismic coefficient for these analyses is derived from the division of the base shear in each direction by the axial forces at the base restraints that were obtained after the solution of the structure to vertical loads. For 5% damping, the equivalent seismic coefficient is 25.4% along the X'X direction and 14.8% along the Y'Y direction. The corresponding coefficients for 20% damping are 16.4% and 12.1%. This result means that a reduction of up to 1.5 times the seismic loads was achieved in the case of the development of 20% equivalent damping. The maximum drift ratios obtained in the time-history elastic analysis for both 5% and 20% damping are shown in Table 5. The combination of the developed drift ratios and Figure 7a leads to the assumption that the eigenperiods of the basilica were increased to 0.60 s along the Y'Y direction and 0.41 s along the X'X direction from the initial values of T_{YY}= T_{YY}*0.7=0.60 s * 0.7=0.42 s and T_{oXX}= T_{XX}*0.45=0.41 s * 0.45=0.18 s.

Max drift for	Wall Orientation (joint #)			
"ζ":	S_X/E_Y (4134)	S_X/W_Y (4094)	N_X/W_Y (1009)	N_X/E_Y (1049)
5%	1.12‰/0.38‰	1.34‰/0.52‰	1.39‰/0.52‰	1.09‰/0.39‰
20%	0.61‰/0.28‰	0.72‰/0.33‰	0.72‰/0.33‰	0.62‰/0.27‰

Table 1: Maximum drift ratios for the perimeter walls of the basilica during the time-history linear analysis.

The above analyses demonstrate that the main eigenproperties of the examined monument were similar to the resonant frequencies of the Thessaloniki earthquake response spectrum. For this reason, the walls of the basilica that are oriented in the X'X direction were subjected to higher drift ratios, whereas the walls that were oriented in the Y'Y direction were subjected to lower drift ratios. The latter was possible due to the significantly higher eigenperiods of these walls, which increased from 0.42 s to 0.60 s after the formation of cracks. Along the X'X direction, the walls of the basilica were subjected to higher drift ratios because the eigenperiod of the temple along this direction was located in the resonance space of the earthquake. In both directions, the drift ratios of the walls were significantly reduced after the formation of the cracks and thus after consideration of 20% damping.

The historic center of Thessaloniki - in which many UNESCO monuments subjected to June 20, 1978 EQ are located - constitutes an invaluable real scale laboratory. Two Thessaloniki monuments with quite different structural systems - a Byzantine basilica monument included in the World Heritage List of UNESCO with a flexible structural system and an Ottoman public bath with a stiff structural system- were comparatively studied. The present research focuses on the study of the section stresses on the walls of masonry monuments when they are subjected to seismic loading.

The study is based on architectural and pathology drawings of the monuments (EFAPOTH archive) in combination with the EQ recorded unique time history. The basic assumption is that when masonry monuments are modeled by the use of finite elements and are subjected to real earthquake time histories, severe damages resulted, although the real monuments present lower level of damages. The indicative generally accepted conclusion is that damage on monuments estimated through analytical calculation is usually overestimated. Particularly, when horizontal stresses, S11, due to seismic action are combined with stresses due to permanent vertical loads the resulted damages are extended. According to these figures and analyses, the recorded and calculated damages are safely interpreted, as their locations coincide. The damage area on the real structure is less wide in relation to the corresponding area on the model.

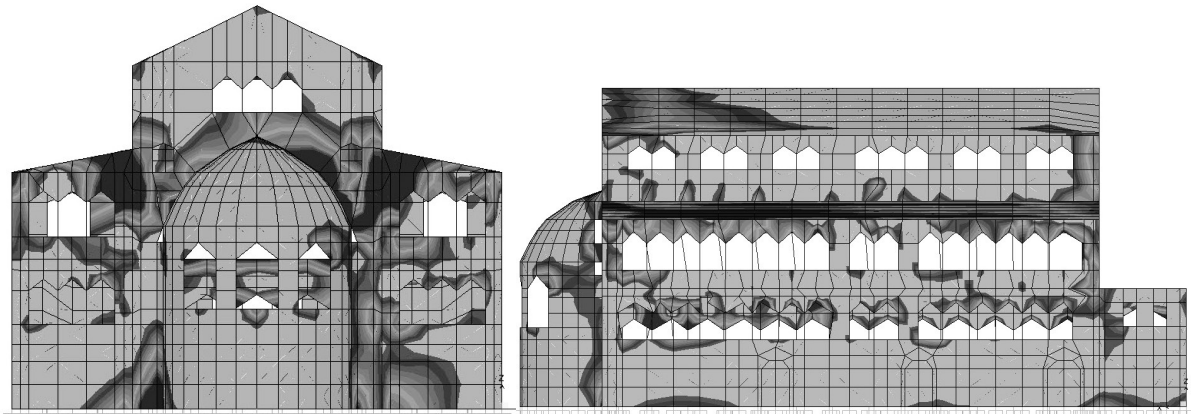

Figure 3. Areas with maximum tension at the north wall (similar stress distribution for the south wall).

A similar damage history was extracted by the more flexible structural system of Acheiropoietos basilica.

The horizontal tension stresses develop lower values than the corresponding stresses of the Ottoman bath; however they are spread at much more elements along the length of the internal and perimeter walls. As expected, after the addition of horizontal stresses that resulted from the vertical and seismic loadings in the model, the stress excess was also very high. In the framework of the present research targets, justifications are derived towards bridging the gap between the (i) evaluation seismic loads – structural model response and (ii) exact time history – response of the structural system of the monument. Usually in case (ii), the response is milder in relation to the analysis for the same parameters, in case (i). This is most probably justified, among others, by the considered material properties and mainly by the available damping of the structural system as is described below:

a) There is a micromovement and microcracking process that is activated during the construction stages of the monument. The resulted horizontal tension stresses during the erection of the walls are zeroed due to micro-movements in horizontal direction. The calculation of horizontal tension stresses of the complete monument model, loaded at once, results to horizontal tension stresses with unrealistic high values. When these section stresses are combined with the corresponding stresses due to seismic loading the resulted differences are increased.

b) The material viscous damping, of stone masonry walls that were built with mortar at two outer fibers and irregular construction at the intermediate should be significantly higher than 5% that is usually suggested by code provisions. This is essentially attributed to i) the gradual slow masonry construction methodology, ii) the common reinforcement of masonries by horizontal timber ties and iii) the favorable lime based mortar properties, i.e. considerable ductility imparting enhanced static and dynamic behavior and significant self-healing capacity of cracks.

c) During the earthquake the width of the resulted cracks propagate from low to higher values at the maximum loading cycle, increasing thus the seismic energy absorption.

The above statements drive to the conclusion that there are consistent reasons to consider higher damping for the stone and/or brick masonry walls of monuments, resulting this way to the application of rational seismic loads for the monuments overall performance evaluation.

It is anticipated that the future research towards deeper understanding of the favorable structural behavior of historic flexible or stiff structural systems in terms of tensile strength, fracture energy and ductility - based on traditional masonry construction with soft lime based mortars compared to modern masonry with stiff and brittle mortars - will minimize intervention in monuments and properly mitigate their seismic risk.

Through the aforementioned research results the general conclusion that in monuments with high flexibility the damages are distributed to many structural elements. In monuments with stiffer structural system the damages are concentrated to less (limited) structural elements.

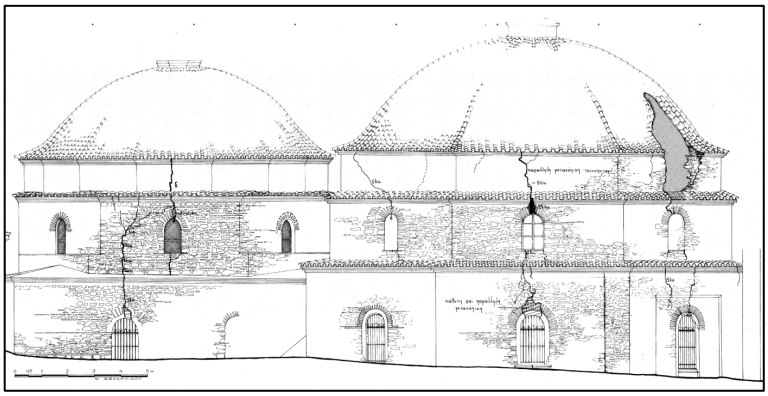

Fig. 4. Damage patterns at the west facades (entrance halls) of the women (left) and men (right) parts

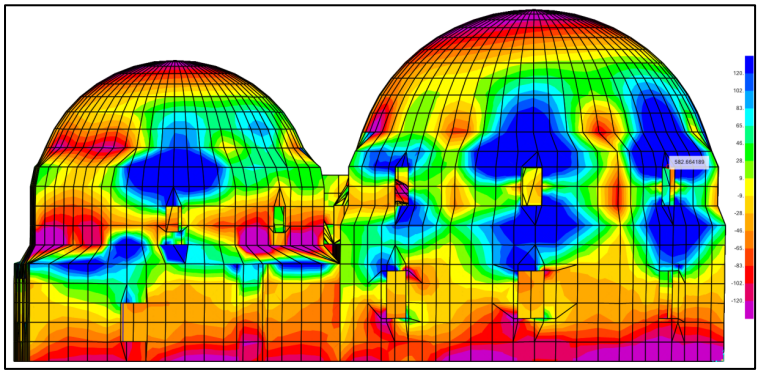

Fig 5. Horizontal stresses S11 as resulted from the combination of the time history analysis at time step 8.475sec and vertical loads.

REFERENCES

[1] Salonikios Thomas N., Konstantinos E. Morfidis "Seismic evaluation of masonry monuments through the utilization of in-situ measurements – case study on a Byzantine basilica". Mediterranean Archaeology and and Archaeometry International Journal, Vol. 18, No 1, pp. 93-112, 2018, https://doi.org/10.5281/zenodo.1069529.

[2] Salonikios Thomas, Nikolaos Theodoulidis, Konstantinos Morfidis, Georgia Zacharopoulou, Konstantinos Raptis, "Efficiency investigation of structural interventions based on in situ ambient vibration measurements on Acheiropoietos Early Byzantine basilica, Thessaloniki,

Greece", Journal of Civil Structural Health Monitoring, Springer, Vol. 8, No 1, January 2018. https://doi.org/10.1007/s13349-017-0262-3.

[3] Thomas Nikolas Salonikios, Kostantinos Morfidis, Nikolas Theodoulidis, Zacharopoulou Georgia, Raptis Constantinos (2018). Historical dilapidations at Acheiropoietos Basilica – Analytical Approach of Failure Mechanism. Religious monumental masonry structures in seismic areas: assessment, retrofit, numerical and experimental evaluation, 16ECEE, Paper # 11882.

MECHANICAL BEHAVIOR OF ASSEMBLED STEEL DAMPERS WITH OPTIMIZED SHAPES

Lingxin ZHANG[1], Baijie ZHU[2*]

[1] Professor. Institute of Engineering Mechanics, China Earthquake Administration; Key Laboratory of Earthquake Engineering and Engineering Vibration of China Earthquake Administration, Harbin, China
e-mail: lingxin_zh@126.com

[2] Assistant professor. Institute of Engineering Mechanics, China Earthquake Administration; Key Laboratory of Earthquake Engineering and Engineering Vibration of China Earthquake Administration, Harbin, China
e-mail: baijie_zhu@126.com (Corresponding author)

Keywords: Steel Shear Panel Damper; Yield Stress Contour Line; Shape Optimization; Assembled Damper; Mechanical Properties.

Abstract. *A metallic shear damper is developed with the shape optimized by stress contour lines to mitigate the stress concentration, reduce the effect of hot welds, and improve the efficiency of energy consumption. The stress contour line is defined according to the J2 plasticity theory, where the micro units yield simultaneously. To demonstrate the effectiveness of the proposed shape-optimization method and the correctness of design formulas, seven damper specimens were fabricated and tested quasi-statically, including six optimized dampers and one with a rectangle shape as a comparison. Physical tests demonstrate that the proposed metallic shear damper has a good low-cycle fatigue capability and a stable energy-dissipation capacity. The stiffness and strength design equations predicted the specimen performance very well.*

1 INTRODUCTION

In order to improve the seismic performance of buildings, Kelly et al. [1] has put forward the steel shear panel damper (SSPD) in 1972. Basing on more studies [2-4] focused on the deployment and the design of that, a new type of SSPD is proposed in this paper, which has an optimized shape by stress contour lines. The shape is determined by the simultaneous yielding on the stress contour line considering different loading patterns. All components of the damper are assembled by use of high-strength bolts so that it can be easily installed and replaced. The design equations for the stiffness and strength are developed for the engineering application. Finally, the effectiveness of the shape-optimized damper and the correctness of the design formulas are demonstrated through the cyclic loading of seven specimens. The influence of the vertical axial load on the lateral bearing force is also examined.

2 CONFIGURATION OF ASSEMBLED STEEL SHEAR PANEL DAMPERS

The proposed shape-optimized steel shear panel damper (SOSSPD) consists of one energy dissipater, four connectors, two buckling restrainers, some high strength bolts and one stopper, as shown in Fig.1. The weld work has been significantly reduced and welding heat-affect particularly on the energy dissipater can be ignored. The bolt connection renders the damper a capability of quick replaced after damaged. The energy dissipater deforms laterally in the plane, and its shape is defined by the effectiveness height h, the effectiveness width b and the profile

function $y(x)$. Note that four corners are chamfered to reduce the stress concentration. Four L-shaped connectors clamp the energy dissipater tightly through the high-strength friction-type bolts, and are connected to the main structural components also by another group of high-strength bolts. Two pieces of buckling restrainers are employed to confine the energy dissipater from out-of-plane buckling. Five high-strength bolts are used to connect the two pieces of buckling restrainers.

Under the shear force, the damper is supposed to deform in the plane and the entire area could yield simultaneously. However, the stress is often concentrated at the four corners where both shear and bending forces are maximum. This would significantly reduce the efficiency to dissipate energy. For more complex cases where the axial load exists, the concentration may be more complex. To this end, the yield line of the panel can be defined as Eq. (1) according to the J2 theory, where the axial force N is considered as the participation factor α by Eq. (2):

$$4t^2 f_y^2 y^4(x) - (3+\alpha^2)V^2 y^2(x) - 6|\alpha|V^2 xy(x) - 9V^2 x^2 = 0 \quad (1)$$

$$N = \alpha V \quad (2)$$

where the thickness of the panel is defined as t; the designed yield force is V; and the material yield strength is f_y.

Once the profile shape function of energy dissipater is determined by the stress contour line, its elastic stiffness will be further derived for the design purpose as the series combination of the shear stiffness and the bending stiffness, as Eq. (3).

$$K = \frac{1}{\frac{3}{2E}\int_{-\frac{h}{2}}^{\frac{h}{2}} \frac{x^2}{ty^3(x)}dx + \frac{1}{tG}\int_{-\frac{h}{2}}^{\frac{h}{2}} \frac{dx}{2y(x)}} \quad (3)$$

where E is the young's modulus, and G is the shear modulus.

Fig. 1 Configuration of SOSSPD

3 QUASI-STATIC TESTS FOR DMPERS

To demonstrate the effectiveness of the optimized shape on the mitigation of plastic strain concentration, quasi-static tests are carried out on seven specimens. The accuracy of the design formula for the yield strength and initial stiffness is further examined.

3.1 Specimens parameters

Three groups of dampers are designed with different heights (250mm, 450mm, 650mm). The design shear forces for all dampers are 260kN. Different axial force participation factors, i.e., 0, 0.25, 0.5, and 0.75 are considered. The width of each optimized damper is determined by the corresponding shape function.

Specimen	SOSSPD-1	SOSSPD-2	SOSSPD-2	SOSSPD-2	SOSSPD-2	SSPD-2	SOSSPD-3
α	0	0	0.25	0.5	0.75	0	0
t	6	6	6	6	6	6	6
h	250	450	450	450	450	450	650
b	344	437	453	469	486	437	514
N	0	0	65	130	195	0	0
Optimization	Yes	Yes	Yes	Yes	Yes	Non	Yes

Table 1 Parameters of analyzed dampers (Units: kN, mm)

3.2 Test setup

A test frame, as shown in Fig. 2, is used to test the specimens, which consists of four columns and three beams to form a steady loading frame. Each specimen is installed between the bottom beam and the loading beam. The bottom beam is securely fixed on the strong reaction floor, while the loading beam is connected to a parallelogram system through which the rotation of the loading beam is restrained while the translational movements remain free. One end of the loading beam is connected to the horizontal actuator, which is displacement-controlled and used for the shear loading on the damper specimen. The vertical actuator is connected at the mid points of the loading beam, which is force-controlled and balances the gravity of the loading beam. It is also used to exert the axial load on the specimens when considering a constant design axial force.

The same loading protocol as shown in Fig.3 is used, and the load is applied until the horizontal force decreases to 85% of the maximum. The loading speed is no more than 5 mm/min. The horizontal and vertical loading forces are measured through the actuator load cells. Two displacement transducers are set in the horizontal, one at the bottom and the other on the top of the specimen. Both are attached directly to the energy dissipater of each damper. The relative displacement of the two transducers is used as the displacement control target of the horizontal actuator.

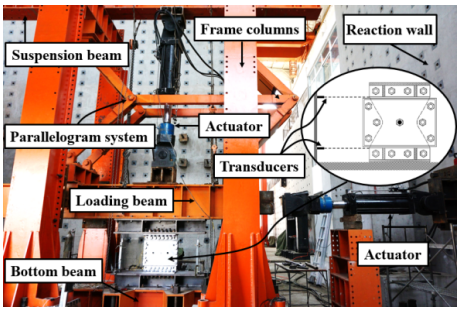

Fig. 2 Test setup

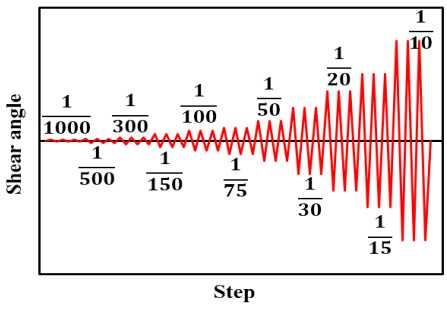

Fig. 3 Loading protocol

3.3 Discussion of test results

The hysteretic curves of seven specimens are plotted in Fig. 4. Because of the initial imperfection of the installed dampers, the actually applied axial forces were 25kN, 50kN and 75kN, for the third to fifth specimen, respectively. Good energy dissipation capacity is observed for all dampers. As Fig. 6 shows, there are pinching on SOSSPD-1, SOSSPD-2 ($\alpha = 0$), SOSSPD-2 ($\alpha = 0.25$), SSPD-2 and SOSSPD-3 when bearing nearly half the ultimate shear force. The out-of-plane deformation is not well restrained on these specimens. After enhancing the buckling restrainers, the hysteretic curves of SOSSPD-2 ($\alpha = 0.5$) and SOSSPD-2 ($\alpha = 0.75$) are much plump. The shear angle of SOSPD-2 achieved 1/15, while the non-optimized dampers SSPD-2 lost 15% of maximum bearing force at 1/20 shear angle, indicating a better low

cycle fatigue performance than the non-optimized one. The shear angle of SOSSPD-2 ($\alpha = 0.75$) is smaller than the other optimized dampers, demonstrating the large axial force has a negative effect.

Mechanical properties	Specimen	SOSSPD-1	SOSSPD-2	SOSSPD-2	SOSSPD-2	SOSSPD-2	SSPD-2	SOSSPD-3
	Design α	0	0	0.25	0.5	0.75	0	0
	Applied N	0	0	25	50	75	0	0
	Actual α	0	0	0.05	0.10	0.15	0	0
Initial stiffness kN/mm	Test	421.2	240.8	226.4	251.2	262.5	342.3	152.6
	Calculated	412.5	223.6	239.4	256.8	274.2	325.2	149.2
	Error	+2.1%	+0.8%	+0.5%	-0.2%	-0.4%	+5.3%	+2.2%
Yield force kN	Test	252.5	254.2	279.8	285.7	300.6	291.5	250.5
	Calculated	260.0	260.0	260.0	260.0	260.0	288.6	260.0
	Error	-0.3%	-2.2%	+7.6%	+9.8%	+15.6%	+1.0%	-3.7%

Table 2 Stiffness and strength comparison between test and design formulas

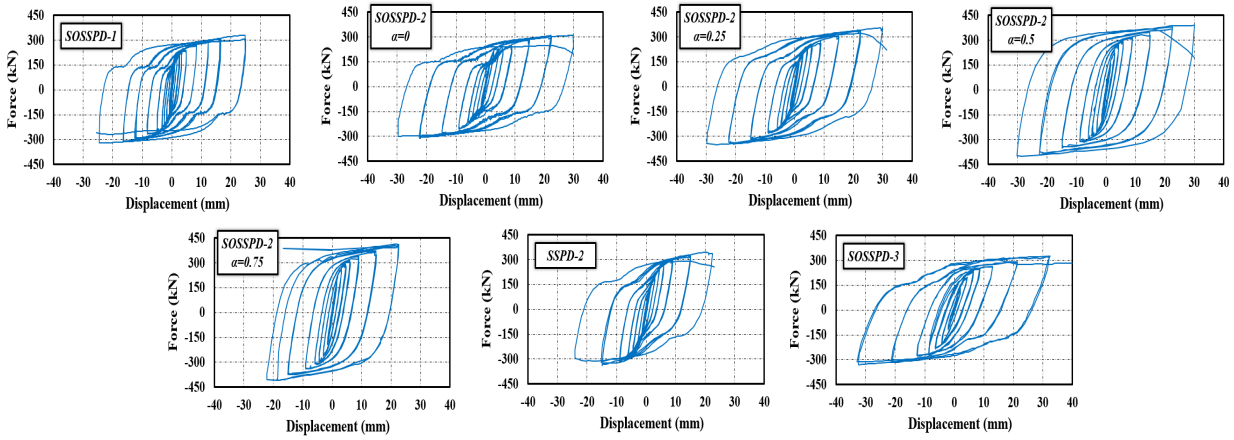

Fig. 4 Hysteresis curves

The measured initial stiffness matches the calculated values very well as shown in Table 2 with small error from -0.4% to +5.3%. The yield forces were obtained by the graphical method introduced by [5], The design equations for yield force all predicted the measured values very well except for specimen applied with axial force. Because the axial loading became smaller, the specimen could sustain a larger shear force.

As Fig. 5 (e), the non-optimized SSPD-2 suffered a premature failure at the corners of the dissipater where the crack occurred, and significant plasticity concentration was observed. The crack finally penetrated through the closest bolt hole, so that the energy dissipater could not be tightly clamped, thus resulting in the complete failure of the damper. And a little lateral buckling happened on the corner area shown in Fig. 5 (d), and grids of corners bended obviously which is different from the center section where the grid were nearly unchanged. The specimen SOSSPD-2 ($\alpha = 0.5$) is the representative of dampers with optimized shape shown in Fig. 5 (a). It is finally completely destroyed by diagonal cracks at mid-section, and the scratch lines along the shear direction were almost unchanged, while the vertical lines on the whole surface have been bent obviously as shown in Fig. 5 (b), which indicating the shear failure. And the oxidation layer of steel surface gradually fell off and spread around as shown in Fig. 5 (c). This implies a good low cycle fatigue property, a good energy dissipation and a secure connection performance.

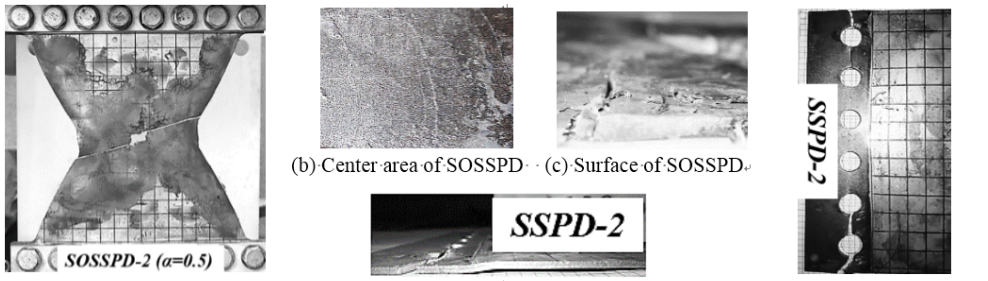

(a) Failure of SOSSPD-2 (b) Center area of SOSSPD (c) Surface of SOSSPD (d) Clamped area of SSPD (e) Bolt hole crack of SSPD

Fig. 5 Local damage of dampers

4 CONCLUSIONS

A metallic shear damper with optimized shape has been developed and studied numerically and experimentally. Major findings are as follows:

(1) The design formulas for the elastic stiffness agree well with the simulation and test results. Both can be used in engineering applications.

(2) The shape optimized dampers have better mechanical behavior than that without optimization, and the ultimate shear deformation is much larger than the one without optimization because of the low concentration of plastic strains.

(3) The damper is assembled by high-strength bolts which would save time for installation, and reduce economic costs obviously.

REFERENCES

[1] Kelly J M, Skinner R I, Heine A J. Mechanisms of energy absorption in special devices for use in earthquake resistant structures. Bulletin of N. Z. Society for Earthquake Engineering, 1972; 5(3): 63-88.

[2] Liu Y, Aoki T, Shimoda M. Strain distribution measurement of a shear panel damper developed for bridge structure. J Struct 2013; 1-11.

[3] Liu Y, Shimoda M. Shape optimization of shear panel damper for improving the deformation ability under cyclic loading. Structural and Multidisciplinary Optimization 2013; 1-9.

[4] Deng K, Pan P. Experimental study of steel shear panel dampers with varying cross-sections. Engineering Mechanics 2016; 99(8): 187-193.

[5] Xu L, Nie X, Fan J. Cyclic behavior of low-yield-point steel shear panel dampers. Engineering Structures 2016; 391-404.

A MULTIPHASE YIELDING STEEL BRACE WITH TAILORED MATERIAL PROPERTIES

Konstantinos A. Skalomenos[1], **Masahiro Kurata**[1] **and Minehiro Nishiyama**[2]

[1] Disaster Prevention Research Institute, Kyoto University
skalomenos.konstantinos.7z@kyoto-u.ac.jp
kurata.masahiro.5c@kyoto-u.ac.jp

[2] Department of Architecture and Architectural Engineering, Kyoto University
mn@archi.kyoto-u.ac.jp

Keywords: Steel brace, Induction heating, Sectional Strength Variation, High-strength, Eccentricity

Abstract. *Induction heat (IH) treatment is an efficient material technology to increase several times the strength of a selected part of steel elements. This paper presents an experimental investigation on the material properties of IH-treated steel elements and a novel application to steel braces. Compared to the conventional steel, the IH-treated steel provides with two-to-three times higher yield stress and tensile strength. The proposed steel brace is a steel tube with a specified partial strength enhancement along its cross-section. One-half of the section is treated by IH, while the other one-half of the section maintains the material properties of conventional steel. The conventional steel part yields earlier and dissipates energy, whereas the IH steel part remains elastic until large deformations. An intentional eccentricity is introduced along the brace length to magnify the contrast of material properties and take in the maximum their advantages. The effective combination of the partial strength IH enhancement and eccentricity provides the brace with a beneficial multiphase yielding response that can meet rationally multiple performance objectives in seismic design. The brace can offer a reduced initial stiffness up to 60% maintaining a similar ultimate strength with the conventional design, exhibit a high tensile post-yielding stiffness nearly up to 20% of the initial stiffness and stably dissipate energy during cyclic loading up to 2.0% story drift by delaying the onset of local buckling in the middle. This story drift is two time larger than that of the corresponding conventional brace design.*

1 INTRODUCTION

In the last decades, several experimental and analytical studies have been carried out on the inelastic seismic responses of steel bracing members [1,2]. Steel bracing members constitute the main seismic-resistant member in steel braced frame structures. The seismic design of concentrically braced steel frames (CBFs) requires high strength and stiffness to meet serviceability requirements during frequent earthquakes, and a ductile behavior to prevent the collapse in strong earthquakes [3]. However, the information obtained from the previous research programs and the experience gained from past earthquakes have revealed some drawbacks in the seismic behavior of steel braces. Steel braces provide with limited post-yielding stiffness to structures that may result in a sudden increase of floor deformation and a soft-story failure mechanism at large deformation [4]. Although steel braces efficiently absorb seismic energy through yielding, they lose rapidly compressive strength when they buckle. Overall buckling is followed by a local buckling at mid-length of the brace, which promotes

early fracture, thus limiting the structure ductility. The treatment of the negative traits of steel braces is a critical issue and can be the basis for developing new-type high-performance bracing members [5] that can reduce seismic damages derived from their inelastic behavior as well as comply more sufficiently with the multiple performance objectives of the current seismic design methodologies [6].

2 BRACE CONCEPT

The proposed brace design utilizes an IH-treated circular hollow structural steel section (HSS), as shown in Fig. 1(a). One-half of the brace section has a two-to-three times higher strength than the other half which maintains the material properties of conventional steel. This significant strength variation in the cross-section is achieved by the IH-treatment technology. The IH-treated steel part has about 2.6 times higher yield stress than the conventional steel part. In the proposed concept, the conventional steel part yields when a relatively small axial force is applied. The conventional part of the brace yields earlier and dissipates the seismic energy, whereas the IH steel part remains elastic and is expected to act as a source of elasticity and restoring force beyond the yielding of the conventional steel counterpart.

An intentional eccentricity is introduced along the brace length, as shown in Fig. 1(a) [7]. As a result, the strain distribution along the cross-section is asymmetric and the contrast of the material properties of the IH and conventional steel is magnified. The conventional steel part is subjected to larger strain demands and yields earlier than usually, whereas the IH steel part remains elastic until very large deformation. The dual action of the partial strength enhancement and eccentricity realizes a unique hysteresis behavior of the developed brace, as shown in Fig. 1(b). Under tension, the brace exhibits a trilinear behavior providing with a high post-yielding stiffness. In compression, an almost bilinear behavior is observed. The brace transits into the post-buckling behavior smoothly without a severe drop of compression force as it is observed in conventional steel braces. Furthermore, due to the overall bending behavior and the existence of the IH steel part that serves as an elastic, stresses and strains are distributed more uniformly along the brace length. Local deformation in the middle delays until high compression deformations. As a result, the fracture capacity of the member can increase and an enhanced ductility can be reached.

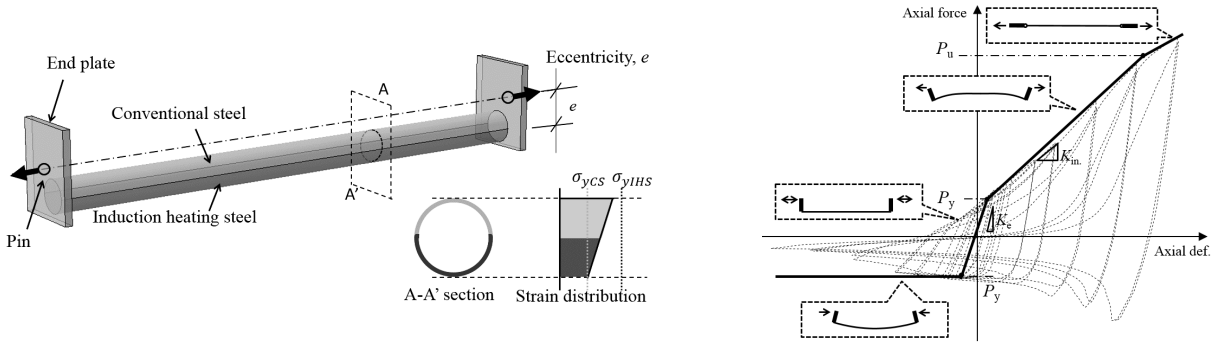

(a) (b)

Fig. 1. Introduction of IH-brace: (a) Configuration; (b) Hysteretic behavior

3 BRACE MANUFACTURING

The IH-treatment technology uses the induction heating as a very efficient non-contact way to heat up only a selected part of the steel member. As introduced in Fig. 1, only the one-half of the cross-section is heat treated. Fig. 2 shows the process of the IH treatment. In this study, IH is applied to a compact circular HSS with a diameter (D = 114.3 mm) and thickness (t_b = 3.5 mm), namely STK400 (made of steel material equivalent to A36 in the United States for hollow sections). The nominal carbon content in STK400 is smaller than or equal to 0.25%.

The circular HSS is placed horizontally and simply supported at its ends. An induction coil heats up over 1000 ^{o}C the one half of the section passing through the entire length (Fig. 2(a)). The heated part is rapidly cooled by water (quenching). The treated part obtains the new material properties (Fig. 2(b)). One meter of the steel HSS can be hardened within four minutes. Due to the recent progress in manufacturing by Netsuren Corporation, it is now possible to prepare large size IH-treated steel structural members with a precise control in an automatic manner. Among the advantages of the IH technology, the following are commonly recognized: (a) energy efficiency; (b) speed; (c) safety; (d) cleanliness; (e) accuracy; and (f) repetition. Fig. 2(d) shows the surface condition of the IH-treated steel part.

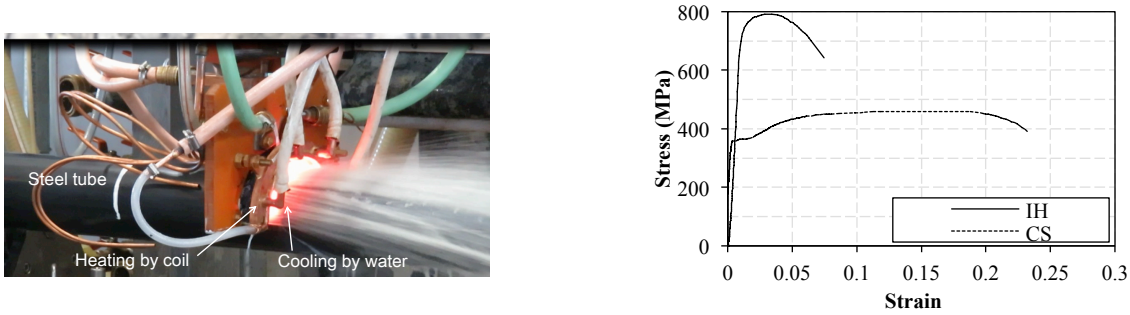

(a) (b) Material property of IH steel

Fig. 2. Brace manufacturing and new material properties: (a) Induction heating and quenching process; and (b) IH against conventional steel.

4 EXPERIMENTAL INVESTIGATION

Two brace specimens were tested under cyclic loading. One brace based on the conventional design (CBB) and one based on the proposed design (IH-brace). The steel tubes had a ratio D/t = 32.7 with slenderness ratio λ = 54.4. An eccentricity equal to 60 mm was introduced for the proposed brace; the e:r ratio was equal to 1.53. The lateral loading history consisted of several drift levels (0.1~4.0%) with two cycles imposed at each level.

Figure 3 shows the results of CBB specimen. The CBB specimen exhibited a nearly bilinear behavior in tension providing a post-yielding stiffness of 1.0% to the elastic stiffness. Overall buckling as shown in Fig. 3(b) occurred during the compression cycle of 0.5% story drift, followed by sudden reduction in the compression strength. Local buckling observed at the second compression cycle of 1.0% story drift in the brace middle (Fig. 3(c)) followed by fracture during the second tension cycle of 2.0% story drift.

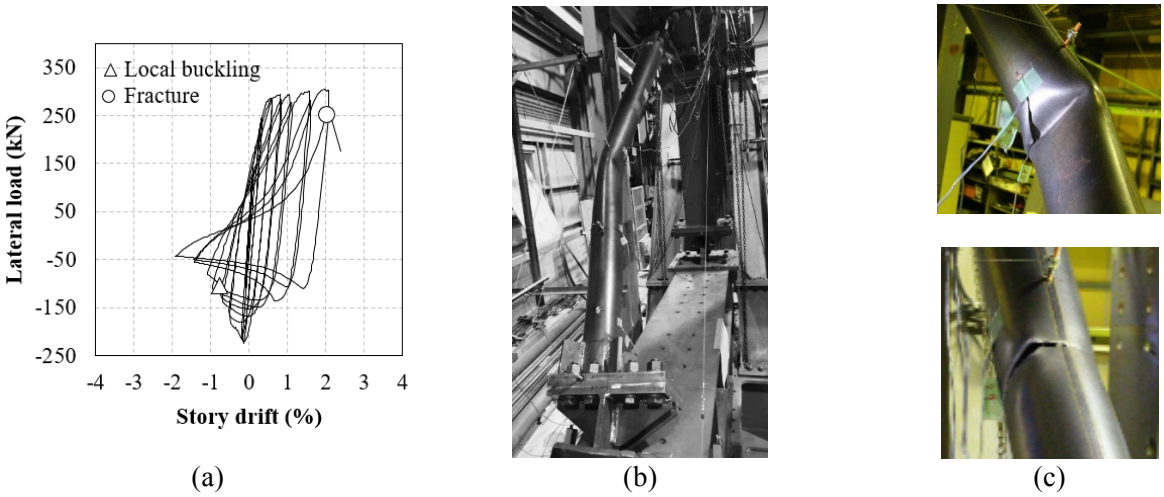

(a) (b) (c)

Fig. 3 Cyclic behavior of conventional steel brace (CBB): (a) hysteresis behavior; (b) overall buckling; and (c) local buckling at the mid-length.

Being subject to bending moment and axial load, IH-brace inherently provides with lower stiffness and yielding strength than the conventional brace. In the IH-brace shown in Fig. 4, the elastic stiffness was 60% lower than CBB. The IH part remained elastic until 1.5% story drift while the conventional steel part yielded during the first tension cycle of 0.25% story drift. Due to the elastic behavior of IH steel part beyond the yielding of conventional steel counterpart, the IH-brace provided a larger post-yielding stiffness nearly at 20% of the initial stiffness. In compression, the brace smoothly entered the post-buckling region without a significant reduction of the compressive strength. After that, the reduction of the compressive strength remained lower than the 20% of the maximum compressive strength. The specimen exhibited a uniform overall bending due to the almost elastic behavior of the IH steel part and presence of eccentricity. The combination of both design features prevented the brace mid-length from local buckling up to relatively large story drift in seismic design (Fig. 4(c)). During the second compression cycle of 2.0% story drift, the onset of local buckling was observed. Compared to the CBB specimen, local buckling in IH-brace occurred in a story drift two times larger. Fig. 4(b) shows a representative photo of the overall deformation of the specimen in the first compression cycle of 2.0% story drift.

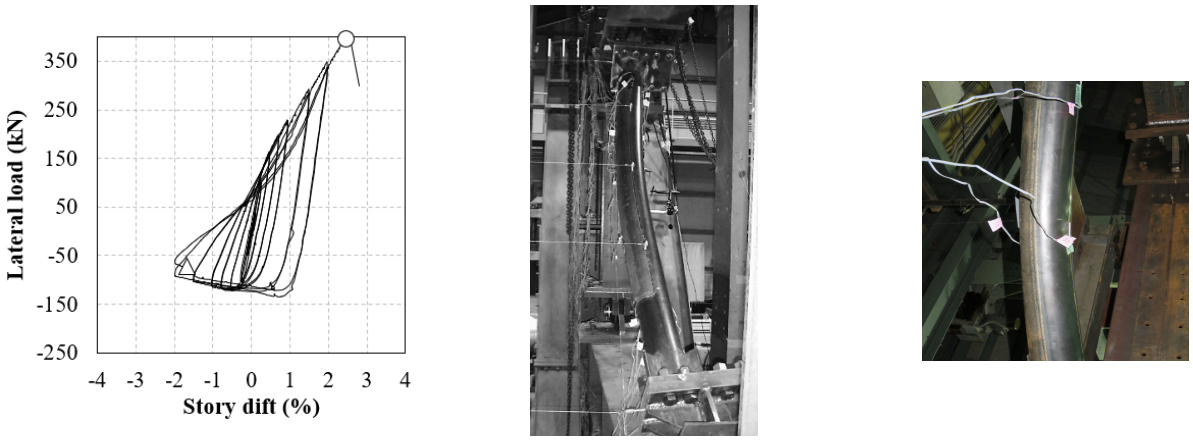

(a) (b) (c)

Fig. 4 Cyclic behavior of induction heat (IH) treated steel brace (IH-brace): (a) hysteresis behavior; (b) overall bending; and (c) deformation in the brace mid-length

5 CONCLUSIONS

An experimental study to investigate the seismic behavior of a new steel brace using the induction heating (IH) technology was conducted. The test results showed that the proposed steel brace can overcome the negative traits of conventional steel braces, such as the large inherent strength and stiffness, low post-yielding stiffness and limited ductility. Compared to the conventional design, IH-brace provided up to a 60% lower elastic stiffness maintaining a similar tensile strength, reached a higher tension post-yielding stiffness equal to 20 to 30% of the elastic stiffness, while no strength deterioration was observed up to 2.0% story drift. The post-yielding stiffness depends on both eccentricity and IH-to-conventional yielding stress ratio, and the fracture ductility can be further enhanced.

REFERENCES

[1] R. Tremblay, Inelastic seismic response of steel bracing members. *Journal of Construction Steel Research*, **58(5-8)**, 665–701, 2002.

[2] B.V. Fell, A.M. Kanvinde, G.G. Deirlein, A.T. Myers, Experimental investigation of inelastic cyclic buckling and fracture of steel brace. *Journal of Structural Engineering of ASCE,* **135(1)**, 19–32, 2009.

[3] J. Jin, S. Sherif El-Tawil, Inelastic Cyclic Model for Steel Braces. *Journal of Engineering Mechanics*, **129(5)**, 548–557, 2002.

[4] S. Kiggins, C.M. Uang, Reducing residual drift of buckling-restrained braced frames as a dual system. *Engineering Structures*, **28 (11)**, 1525–1532, 2006.

[5] M.G. Gray, C. Christopoulos, J.A. Packer, Design and Full-Scale Testing of a Cast Steel Yielding Brace System in a Braced Frame. *Journal of Structural Engineering of ASCE*, **143(4)**, 04016210, 2017.

[6] American Society of Civil Engineering (ASCE). Seismic Evaluation and Retrofit of Existing Buildings, ASCE/SEI 41-13, ASCE, Reston, Virginia: 2014.

[7] K. A. Skalomenos, H. Inamasu, H. Shimada, M. Nakashima, Development of a Steel Brace with Intentional Eccentricity and Experimental Validation. *Journal of Structural Engineering*, **143(8)**, 04017072, 2017.

NOTES